NASA Technical Memorandum 88277

Application of Fracture Mechanics and Half-Cycle Method to the Prediction of Fatigue Life of B-52 Aircraft Pylon Components

W.L. Ko, A.L. Carter, W.W. Totton, and J.M. Ficke
Ames Research Center, Dryden Flight Research Facility, Edwards, California

1989

National Aeronautics and
Space Administration
Ames Research Center
Dryden Flight Research Facility
Edwards, California 93523-5000

CONTENTS

SUMMARY 1

INTRODUCTION 1

NOMENCLATURE 1

SYMBOLS 2

FRACTURE MECHANICS 4

PROOF LOAD TESTS 5

REMAINING FLIGHTS 5

HALF-CYCLE THEORY 6

STRESS POINTS 7

CALCULATIONS OF CRACK SIZES 8

FLIGHT DATA 9

CALCULATIONS OF LOAD SPECTRA 9

CRACK GROWTH CALCULATIONS 10
- Direct Method . . . 10
- Indirect Method . . . 10
- Missing Data Extrapolations . . . 11

RESULTS 11

CONCLUSION 12

TABLES 13

FIGURES 16

APPENDIX A—EQUATIONS FOR B-52 PYLON HOOK LOADS 38
- Figures . . . 40

APPENDIX B—PYLON LOADS AT B-52 WING ATTACHMENT POINTS AND THE ASSOCIATED STRESS POINTS 43
- Maneuver 1. . . . 44
- Maneuver 2. . . . 44
- Maneuver 3. . . . 45
- Maneuver 4. . . . 45
- Maneuver 5. . . . 45
- Stress Points . . . 46
- Figure . . . 47

APPENDIX C—COMPUTER PROGRAMS USED IN THE CALCULATIONS OF σ_i AND CRACK GROWTH 48
Crack Growth Calculation Overview 48
Background 48
Problems 48
Procedure 48
SRBHOOK Program 50
THIN Program 52
CONCAT Program 55
CCLAMP Program
(Compute crack length at maximum points) 57
CPLOT Program 65
Figures 73

REFERENCES 75

SUMMARY

Stress intensity levels at various parts of the NASA B-52 carrier aircraft pylon were examined for the case when the pylon store was the space shuttle solid rocket booster drop test vehicle. Eight critical stress points were selected for the pylon fatigue analysis. Using fracture mechanics and the half-cycle theory (directly or indirectly) for the calculations of fatigue-crack growth, the remaining fatigue life (number of flights left) was estimated for each critical part. It was found that the two rear hooks had relatively short fatigue life and that the front hook had the shortest fatigue life of all the parts analyzed. The rest of the pylon parts were found to be noncritical because of their extremely long fatigue life associated with the low operational stress levels.

INTRODUCTION

The NASA B-52 carrier aircraft has been used to carry various types of test vehicles for high-altitude drop tests. Test vehicles carried by the B-52 aircraft in the past include X-15, HL-10, highly maneuverable aircraft technology (HiMAT), and drones for aerodynamic and structural testing aircraft (DAST), and the space shuttle solid rocket booster drop test vehicle (SRB–DTV). The test vehicle was attached to the B-52 pylon (airborne launch system) by one front hook and two rear hooks (see fig. 1, in which the store is the SRB–DTV). The B-52 pylon (fig. 2) is almost 30 years old and has been subjected to considerable structural fatigue. Recently, the two rear hooks of the pylon fractured during the towing of the B-52 aircraft carrying the SRB–DTV on a relatively smooth taxiway. During towing, the hook loads were far below the design limit loads. Careful observation of the fracture surfaces of the two failed rear hooks revealed that "micro" surface cracks existed at the rounded inner boundaries of the two failed rear hooks (Ko and Schuster, 1985). This incident raised the serious concern about the remaining fatigue life of the front hook and critical parts of the pylon and also the available fatigue life of the new rear hooks (made of high-performance material and of better design). Before resuming the new series of SRB–DTV drop tests, it was necessary to conduct proof tests of the pylon by loading it up to specified limit loads to establish confidence in the pylon structural integrity. The main purpose of proof tests is as follows. During the proof tests, if some pylon components should fail, then those components are to be replaced. If all the pylon parts survive the proof tests, then fracture mechanics can be applied to estimate the fatigue life (or number of flights left) for each of the critical parts of the pylon based on proof test data and data obtained from the SRB–DTV test flights following the proof tests. This report shows the application of fracture mechanics and the half-cycle method to calculate the remaining fatigue life (number of flights left) for each critical component of the pylon carrying the SRB–DTV as a store.

NOMENCLATURE

CCLAMP	compute crack length at maximum points
CC LH	computed crack lengths
EOS	end of segment
EPSL	epsilon
FLIDAB	flight database
HMS	subroutine; h, min, sec
NASTRAN	NASA structural analysis
PCM	pulse code modulation
SMAX	sigma maximum

SMIN	sigma minimum
SRB–DTV	space shuttle solid rocket booster drop test vehicle

SYMBOLS

A	crack location parameter
A_B	pylon–wing attachment bolt cross-sectional area
a	crack length of edge crack, half crack length of through-thickness crack, or depth of surface crack
a_c^P	initial fictitious crack length (or depth) established by the proof tests
a_{Vj}^P	initial fictitious crack depth established by the proof tests for the pylon-wing attachment bolts
a_c^o	limit crack length (or depth) associated with the operational load level
a_ℓ	crack size (length or depth) after the ℓth flight of random stress cyclings
C	material constant in Walker crack growth rate equation
c	half-length of surface crack
D_{CL}	left drag load
D_{CR}	right drag load
D_j	pylon–wing attachment point drag loads
E	complete elliptic function of the second kind
F_ℓ	number of flights left after the ℓth flight
f	fraction of limit stress (or limit load)
g	gravitational acceleration
I_P	SRB–DTV pitching moment of inertia
I_R	SRB–DTV rolling moment of inertia
I_Y	SRB–DTV yawing moment of inertia, $I_Y \approx I_P$
i	integer associated with half-cycles, or associated with different regions of crack growth curve
j	integer associated with half cycles
K_I	Mode I stress intensity factor
K_{I_c}	Mode I critical stress intensity factor
K_j	function of hook loads and pylon accelerations
K_{max}	Mode I stress intensity factor associated with σ_{max}, K_{max}, = $AM_K\sigma_{max}\sqrt{\pi a/Q}$
k	modulus of elliptic function
ℓ	integer associated with flights
M_K	flaw magnification factor
M_y	aerodynamic pitching moment acting on SRB–DTV, in.-lb, positive nose up
M_z	aerodynamic yawing moment acting on SRB–DTV, in.-lb, positive nose right
m	Walker exponent associated with K_{max}
N	number of stress cycles available for operations

N_ℓ	number of stress cycles used during ℓth flight
n	Walker exponent associated with stress ratio R
P_x	aerodynamic drag force acting on SRB–DTV, lb, positive aft
P_y	aerodynamic sideforce acting on SRB–DTV, lb, positive right
P_z	aerodynamic lift force acting on SRB–DTV, lb, positive up
$\dot{p}$	roll inertia load factor, $\dot{p} = -\ddot{\theta}_x/g$
Q	surface flaw shape and plasticity factor
$\dot{q}$	pitch inertia load factor, $\dot{q} = -\ddot{\theta}_y/g$
$\bar{q}$	dynamic pressure
R_{a_i}, R_{b_i}, R_{c_i}, R_{d_i}, R_{e_i}, R_{f_i}	coefficients of hook load equation for hook load R_i
R	stress ratio, $R = \sigma_{min}/\sigma_{max}$
$\dot{r}$	yaw inertia load factor, $\dot{r} = -\ddot{\theta}_z/g$
S_A	front side load
S_{CL}	rear side load
S_j	pylon–wing attachment point side loads
S_{k_i}, S_{ℓ_i}, S_{m_i}, S_{n_i}, S_{p_i}, S_{q_i}, S_{r_i}, S_i	coefficients of stress equation for σ_i
T	time
t	plate thickness
V_A	front hook vertical load
V_{BL}	left rear hook vertical load
V_{BR}	right rear hook vertical load
V_{CL}	left drag shaft vertical load
V_{CR}	right drag shaft vertical load
V_j	pylon–wing attachment point vertical loads
W	weight of SRB–DTV
x, y, z	rectangular Cartesian coordinates
$\bar{x}$	location of aerodynamic center of pressure on x axis for SRB–DTV
α	slope of crack growth curve (or crack growth rate)
α_{FUS}	fuselage angle of attack
β	yaw angle
Δa_ℓ	amount of crack growth during the ℓth flight
δa_i	crack growth increment caused by one cycle of constant-amplitude stress cycling under loading magnitude of ΔK_i and R_i
ΔK	Mode I stress intensity range, $\Delta K = AM_K(\sigma_{max} - \sigma_{min}), \sqrt{\pi a/Q}$
η_x	$= -\ddot{x}/g$, inertia load factor in the x direction at SRB–DTV center of gravity

η_y	$= -\ddot{y}/g$, inertia load factor in the y direction at SRB–DTV center of gravity
η_z	$= -\ddot{z}/g$, inertia load factor in the z direction at SRB–DTV center of gravity
$\bar{\eta}_x$	dimensionless acceleration in the x direction at pylon center of gravity
$\bar{\eta}_y$	dimensionless acceleration in the y direction at pylon center of gravity
$\bar{\eta}_z$	dimensionless acceleration in the z direction at pylon center of gravity
θ_x	angular displacement about the x axis (roll angle)
θ_y	angular displacement about the y axis (pitch angle)
θ_z	angular displacement about the z axis (yaw angle)
θ	angular coordinate of critical points σ_4 and σ_6
σ_∞	remote uniaxial tensile stress
σ_∞^P	uniaxial tensile stress induced by the proof load
σ_∞^o	uniaxial tensile stress associated with the operational load level
σ_{Vj}	uniaxial tensile stress at pylon–wing attachment point induced by the proof loads
σ_Y	yield stress
σ_U	tensile strength
σ_{max}	maximum stress of the stress cycle
σ_{min}	minimum stress of the stress cycle
σ_i	tensile stress at stress point i
σ_i^*	limit value of σ_i established by proof tests
τ	ultimate shear strength
ϕ	angular coordinate for semielliptical surface crack
$[\ ]_\ell$	quantity associated with the ℓth SRB–DTV test flight
$[\dot{\ }], [\ddot{\ }]$	time derivatives

FRACTURE MECHANICS

The upper part of figure 3 shows the most common types of cracks: through-thickness crack, surface crack, and edge crack. According to fracture mechanics, the stress intensity factor K_I for the Mode I deformation (tension mode) associated with any type of crack can be expressed as

$$K_I = AM_K\sigma_\infty\sqrt{\frac{\pi a}{Q}} \tag{1}$$

where

- A is the crack location parameter ($A = 1$ for the through-thickness crack, $A = 1.12$ for both the surface and the edge cracks (see fig. 3)),
- M_K is the flaw magnification factor (for a very shallow crack, $M_K = 1$; as the depth of the crack reaches the back surface of the plate, $M_K = 1.6$ (see fig. 3)),
- σ_∞ is remote uniaxial tensile stress,
- a is half crack length for the through-thickness crack, or length of the edge crack, or

depth of the surface crack (see fig. 3), and

Q is surface flaw shape and plasticity factor,

$$Q = [E(k)]^2 - 0.212 \left[\frac{\sigma_\infty}{\sigma_Y}\right]^2 \tag{2}$$

where σ_Y is the yield stress and $E(k)$ is the complete elliptic function of the second kind defined as

$$E(k) = \int_0^{\pi/2} \sqrt{1 - k^2 \sin^2 \phi}\, d\phi \tag{3}$$

where the angle ϕ is defined in figure 3 and the modulus k of the elliptic function is defined by

$$k^2 = 1 - \left[\frac{a}{c}\right]^2 \tag{4}$$

where c is the half-length of the surface crack (see top center of fig. 3). The lower part of figure 3 shows the plots of $a/2c$ as a function of Q for different values of σ_∞/σ_Y and the plot of M_K as a function of a/t, where t is the plate thickness.

PROOF LOAD TESTS

The purpose of proof load tests is to load the entire aircraft structure (or its components) up to certain proof load levels to test structural integrity and to establish initial fictitious crack sizes for critical structural components for fatigue life analysis. The proof load levels are usually slightly lower than the design limit load conditions associated with different maneuvers. If a previously undetected crack in a certain component exists and is larger than the critical crack size, that component will certainly fail during the proof load tests and will be replaced. Thus, a catastrophic accident during flight could be avoided. If the entire structure survives the proof load tests, then the critical point of the structural component has been subjected to a proof stress σ_∞^P induced by the proof loads. If K_{I_c} is the critical stress intensity factor (or material fracture toughness) of the structural component material, the maximum crack length a_c^P the structural component can carry under the proof loads without failure (or rapid crack extension) may be calculated from equation (1) by setting $K_I = K_{I_c}$ and $\sigma_\infty = \sigma_\infty^P$. In reality, cracks may not develop during the proof tests; however, it will be assumed that a fictitious crack of length a_c^P has been created at the critical point of the structural component during the proof load tests. During actual operations, the structural component will be subjected to much lower stress levels than the proof stress level σ_∞^P. If σ_∞^o is the peak operational stress level (highest peak of the stress cycles), then according to equation (1) the structural component can carry a fictitious crack of size a_c^o, which is much larger than a_c^P. The value a_c^o thus determined will be considered as the limit crack size toward which the initial crack a_c^P is allowed to grow after repeated operations. The crack size difference, $a_c^o - a_c^P$, will then be the available crack size increase permitted for the structural component in repeated operations. The left side of figure 4 shows the plot of crack length, a, as a function of normalized stress σ_∞/σ_U, where σ_U is the failure stress of the material. The lower the operational stress level, the more the available crack size increase is allowed for the structural component. The right side of figure 4 shows the corresponding plot of the crack length, a, as a function of number of constant stress cycles N.

REMAINING FLIGHTS

If the structural component is cycled under constant stress amplitude (idealized case for the purpose of discussion) for N_1 cycles during the first flight with the associated crack growth of Δa_1, then the number of remaining flights

F_1 may be estimated approximately from (see fig. 4)

$$F_1 = \frac{a_c^o - a_c^P}{\Delta a_1} = \frac{N}{N_1} \tag{5}$$

Equation (5) is based on the assumption that the crack growths for all subsequent flights will be equal to Δa_1 of the first flight. In reality, the crack growth rate will steadily increase with the number of flights accumulated, and the actual remaining flights will be less than the value F_1 predicted by equation (5) if the number of remaining flights is large (that is, $F_1 \gg 1$). For a moderate range of F_1, equation (5) should give a sufficiently accurate prediction of the number of remaining flights. The amount of crack growth Δa_1 in equation (5) may be calculated from the following Walker equation (Forman and others (1967), Walker (1970), and Schijve (1979)) for fatigue-crack growth rate under constant-amplitude stress cyclings:

$$\frac{da}{dN} = C(K_{max})^m(1 - R)^n = C(\Delta K)^m(1 - R)^{n-m} \tag{6}$$

where C, m, and n are material constants and K_{max}, ΔK, and R are respectively the stress intensity factors associated with σ_{max}, the stress intensity range, and the stress ratio, given by

$$K_{max} = AM_K\sigma_{max}\sqrt{\frac{\pi a}{Q}} = \Delta K(1 - R)^{-1} \tag{7}$$

$$\Delta K = AM_K(\sigma_{max} - \sigma_{min})\frac{\pi a}{Q} \tag{8}$$

$$R = \frac{\sigma_{min}}{\sigma_{max}} \tag{9}$$

where σ_{max} and σ_{min} are respectively the maximum and minimum stresses of the constant-amplitude stress cycles.

In reality, the stress cycles at the critical points of the structural components are not constant-amplitude stress cycles. To apply equations (6) to (9) to the variable-amplitude stress cycles, certain methods must be developed. In this report, a half-cycle theory (Starkey and Marco (1957), Incarbone (1963), and Smith (1965)) is used to calculate the fatigue-crack growth rate for variable-amplitude stress cycles.

HALF-CYCLE THEORY

The upper part of figure 5 shows an example of random stress cycles (variable-amplitude loading history). The stress history curve is the combination of a series of increasing and decreasing load half-cycles of different loading magnitude (ΔK, R), as shown in the lower part of figure 5. The half-cycle (or half-wave) theory (Starkey and Marco (1957), Incarbone (1963), and Smith (1965)) states that the damage (or crack growth) caused by each half-cycle of either increasing or decreasing load is assumed to be equal to half the damage caused by a complete cycle of the same loading magnitude (ΔK, R). This means that the damage caused by the complete cycle could be equally divided between the two phases of increasing and decreasing loads. The loading sequence can thus be resolved into half-cycle groups of increasing and decreasing loads (lower part of fig. 5). Each half-cycle (either increasing or decreasing load) can then be considered as a half-cycle of the constant-amplitude cyclings under the same loading magnitude (ΔK, R) and can be computed separately in time sequence to estimate the corresponding damage. The half-cycle theory thus permits accurate evaluation of the load spectrum from a recorded load time history. If a_ℓ ($\ell = 1, 2, 3, \ldots$) is the final crack length after N_ℓ ($\ell = 1, 2, 3, \ldots$) random stress cyclings in the ℓth flight, then according to the half-cycle theory, a_ℓ may be calculated from

$$a = a_{\ell-1} + \sum_{i=1}^{2N_\ell}\frac{\delta a_i}{2} = a_{\ell-1} + \Delta a_\ell \quad (\ell = 1, 2, 3, \ldots) \tag{10}$$

with

$$\Delta a_\ell = \sum_{i=1}^{2N_\ell} \frac{\delta a_i}{2} \quad \text{and} \quad a_{\ell-1} = a_c^P \tag{11}$$

where $\delta a_i/2$ is the crack growth increment induced by the ith half-cycle under the loading magnitude ΔK_i and R_i, and which is assumed to be equal to the crack growth increment induced by a half-cycle of the constant-amplitude stress cycling fatigue test under the same loading magnitude $(\Delta K_i, R_i)$. Thus, by using equations (6) to (9), $\delta a_i/2$ may be calculated from

$$\frac{\delta a_i}{2} = \frac{1}{2}\left[\frac{da}{dN}\right]_i = \frac{C}{2}\left[(K_{max})_i\right]^m (1 - R_i)^n = \frac{C}{2}(\Delta K_i)^m (1 - R_i)^{n-m} \tag{12}$$

The crack length, a, associated with ΔK_i (see eq. (7)) will be the summation of initial crack size a_c^P and all the crack growth increments created by all the previous half-cycles. Namely,

$$a = a_c^P + \sum_{j=1}^{i-1} \frac{\delta a_j}{2} \quad (i \geq 2) \tag{13}$$

Similar to the constant-amplitude stress cyclings (see eq. (5)), the number of remaining flights F_1 predicted using the random stress cyclings of the first flight will be

$$F_1 = \frac{a_c^o - a_c^P}{\Delta a_1} = \frac{a_c^o - a_c^P}{\sum_{i=1}^{2N_1} \frac{\delta a_i}{2}} = \frac{a_c^o - a_c^P}{a_1 - a_c^P} \tag{14}$$

Similarly, after the ℓth flight, the number of remaining flights F_ℓ calculated from the flight data of the ℓth flight will be

$$F_\ell = \frac{a_c^o - a_{\ell-1}}{\Delta a_\ell} = \frac{a_c^o - a_{\ell-1}}{\sum_{i=1}^{2N_\ell} \frac{\delta a_i}{2}} = \frac{a_c^o - a_{\ell-1}}{a_\ell - a_{\ell-1}} \tag{15}$$

Figure 6 graphically illustrates how to evaluate the crack growth increment $\delta a_i/2$ associated with the ith half-cycle of the random stress cyclings by using the plots of ΔK_i as a function of da/dN for different values of R.

STRESS POINTS

From the stress analyses of the B-52 pylon hooks (Ko and Schuster, 1985) and pylon parts (North American Aviation, Inc., 1963), eight stress points (stresses σ_1 to σ_8) were selected for the pylon fatigue analysis. Each of the stress points is located at a critical point of each of the eight parts. Table 1 lists the names of the eight pylon parts and the associated material and fatigue properties of the parts. The stress points σ_1, σ_2, and σ_3 are respectively located at the critical points of the inner circular boundaries of the front hook, left rear hook, and right rear hook (figs. 7 and 8). The stress point σ_4 is located at the critical point of the boundary of the left drag shaft (fig. 9). The stress point σ_5 is located at the critical point of the right drag shaft (fig. 10). The stress points σ_6 and σ_7 are respectively located at the critical points of the left drag pin (fig. 9) and right drag pin (fig. 10). Finally, the stress point σ_8 is located at the lower edge (fig. 11) of the right drag shaft lower support.

Based on the NASA structural analysis computer program (NASTRAN) stress analyses of the three B-52 pylon hooks (σ_1, σ_2, and σ_3; (Ko and Schuster, 1985)), the proof tests of the left drag shaft (σ_4) and the stress analyses of

the B-52 pylon parts (σ_5 to σ_8; (North American Aviation Inc., 1963)), the eight stresses σ_1 to σ_8 (in kips, or 10^3 lb/in.^{2}) can be expressed in terms of the hook loads (in pounds) as follows:

$$\sigma_1 = 7.3522 \times 10^{-3} V_A \tag{16}$$

$$\sigma_2 = 5.8442 \times 10^{-3} V_{BL} \tag{17}$$

$$\sigma_3 = 5.8442 \times 10^{-3} V_{BR} \tag{18}$$

$$\sigma_4 = (6.3481 - 5.4514 \times 10^{-5} D_{CL}) \times 10^{-3} D_{CL} \cos\theta - (9.9653 + 3.4363 \times 10^{-4} S_{CL}) \times 10^{-3} S_{CL} \sin\theta \tag{19}$$

where the angular coordinate θ of critical point is given by

$$\theta = \tan^{-1} \left| \frac{S_{CL}}{D_{CL}} \right|_{\text{proof}} = \tan^{-1} \frac{8210}{32080} = 14.36°$$

$$\sigma_5 = 2.1868 \times 10^{-3} D_{CR} \tag{20}$$

$$\sigma_6 = 7.1420 \times 10^{-3} (D_{CL} \cos\theta - S_{CL} \sin\theta) \tag{21}$$

$$\sigma_7 = 7.3055 \times 10^{-3} D_{CR} \tag{22}$$

$$\sigma_8 = 4.2141 \times 10^{-3} D_{CR} \tag{23}$$

where the front hook vertical load V_A, the left rear hook vertical load V_{BL}, the right rear hook vertical load V_{BR}, the rear side load S_{CL}, the left drag load D_{CL}, and the right drag load D_{CR}, may be (1) obtained from strain gage measured data if the strain gage instrumentations are available for measuring the hook loads or (2) calculated from the hook load equations given in appendix A using accelerometers and aerodynamic data if the strain gage data are not available. The stress points at the pylon–wing attachment bolts and several other pylon parts were also investigated; however, those stress points turned out to be noncritical, and therefore they are not included in the pylon fatigue analysis. Appendix B shows the calculations of the pylon–wing attachment bolt tensile loads and the initial surface crack sizes associated with the attachment bolt stress points.

CALCULATIONS OF CRACK SIZES

Table 2 shows different combinations of the maximum hook loads used in the proof tests. To obtain the highest possible values of the stresses σ_i ($i = 1, 2, \ldots, 8$) for the fatigue analysis, the highest values of the maximum hook loads or the highest values of the combined applied loads (for σ_4 and σ_6 only) were used. The values of σ_i ($i = 1, 2, \ldots, 8$) thus obtained were used to calculate the initial fictitious crack size a_c^P and the operational limit crack size a_c^o for each stress point using the following equations (eq. (1) rewritten):

$$a_c^P = \frac{Q}{\pi} \left[\frac{K_{I_c}}{A M_K \sigma_i^*} \right]^2 \quad (i = 1, 2, \ldots, 8) \tag{24}$$

$$a_c^o = \frac{Q}{\pi} \left[\frac{K_{I_c}}{A M_K f \sigma_i^*} \right]^2 \quad (i = 1, 2, \ldots, 8) \tag{25}$$

where f is the fraction of the limit stress σ_i^* (that is, $f\sigma_i^*$ is the peak operational stress) and the critical stress intensity factors K_{I_c} for all the stress points are given in table 1.

In the calculations of a_c^P and a_c^o (see eqs. (24) and (25)), all the surface cracks will be considered to be semi-elliptical in shape, with aspect ratio $a/2c = 1/4$. This value is based on the worst case of the failed old rear hooks.

For the value $a/2c = 1/4$, the lower left plot of figure 3 gives the surface flaw shape factor of $Q = 1.25$ taking $\sigma_\infty/\sigma_Y = 1$ because most of the limit stresses σ_i^* ($i = 1, 2, \ldots, 8$) calculated from equations (16) to (23) exceeded the corresponding yield points of the parts materials. Only for the stress point σ_8, Q was taken to be $Q = 1$ because the crack was a two-dimensional edge crack. Also, the value of the flaw magnification factor M_K was set to unity ($M_K = 1$) for all the stress points because the depths of the cracks were very small compared with the characteristic dimensions (such as thickness, diameter, and depth of the pylon parts under consideration). Table 3 shows the calculated initial fictitious crack size a_c^P established from the proof tests, the amount of crack growth per flight, and the number of flights left calculated from the ℓth flight data for the eight stress points. As mentioned previously, the limit crack size a_c^o for the actual operation is based on the peak stress recorded during the flight. Since the operational peak stress varies each flight, the number of flights left calculated from the ℓth flight data may be larger or smaller than those predicted for the earlier flights (such as σ_1 and σ_3).

FLIGHT DATA

A total of eight successful (that is, with SRB–DTV launching) SRB–DTV flight tests were conducted. One additional flight, which occurred between flights 4 and 6, was an aborted flight without the launching of the SRB–DTV. During the entire SRB–DTV flight-test program, there were only three channels available for recording the strain gage outputs. For flights 1 to 7 (including the aborted flight), the three available channels were used to measure V_A, V_{BL}, and V_{BR} (D_{CL}, D_{CR}, and S_{CL} were not measured). At the end of flight 7, the left drag shaft was removed from the B-52 pylon for proof test and for the installation of strain gages for measuring D_{CL} and S_{CL}. For flights 8 and 9, the two channels used for measuring V_{BL} and V_{BR} were switched to measure D_{CL} and S_{CL} (V_{BL} and V_{BR} were not measured). The value of D_{CR} was not measured during the flight-test program. Accelerometer data (accelerations in x, y, and z directions) were available for the entire test program. However, the accelerometer outputs were poor and unreliable and therefore could not be used to calculate accurate hook loads. An alternative method (called the indirect method, using strain gage measured hook loads from other flights) for calculating the crack growths without using accelerometer data is described later in this report.

CALCULATIONS OF LOAD SPECTRA

To perform the crack growth analysis, the loading histories for the eight stress points must first be calculated. Using the strain gage measured values of V_A, V_{BL}, and V_{BR} (for flight 1) and D_{CL} and S_{CL} (for flight 9), the eight stresses σ_i ($i = 1, 2, \ldots, 8$) may be calculated from equations (16) to (23). Figures 12 to 19 show portions of the loading histories calculated for the eight stress points during taxiing for flight 1 (σ_1 to σ_3) and for flight 9 (σ_4 to σ_8). These stress history curves (load spectra) were filtered down to 5 Hz to eliminate the small-amplitude, high-frequency cycles, which are not important in the present fatigue analysis. Notice from figures 12 to 19 that the load spectra for all the stress points are random. It must be mentioned that in the calculations of σ_5, σ_7, and σ_8 (see figs. 16, 18, and 19 and eqs. (20), (22), and (23)), the strain gage measured values of D_{CL} for flight 9 were used instead of D_{CR} values which were not measured during the entire SRB–DTV flight-test program. Since the values of D_{CL} and D_{CR} are quite close and their perturbation parts are mutually out of phase by a half cycle (see eqs. (A-23) and (A-24) in app. A), using the D_{CL} strain gage data for calculating σ_5, σ_7, and σ_8 should give reasonably accurate results for the crack growth analysis.

Appendix C discusses in detail the computer programs used to calculate σ_i ($i = 1, 2, \ldots, 8$) from the strain gage measured hook loads or from the accelerometer output (if the data are good) using the hook loads equations presented in appendix A.

CRACK GROWTH CALCULATIONS

Direct Method

For certain flights, if the load spectra for certain stress points can be calculated directly from the strain gage measured hook loads, the half-cycle method may be used "directly" to calculate the crack growths for these stress points. By resolving the calculated load spectra (see figs. 12 to 14) into a series of half-cycles with different loading magnitudes ($\Delta K, R$) and applying the half-cycle theory mentioned previously, the crack growth increments per half-cycle could be calculated in time sequence and summed to give the total crack growth per flight for each stress point. Finally, equation (14) or (15) may be used to calculate the number of remaining flights associated with each stress point. It must be emphasized that in using the half-cycle theory, every half-cycle in the load spectrum is calculated without neglecting insignificant low-amplitude half-cycles. Thus, the half-cycle method gives accurate evaluations of the crack growth. Based on the status of the flight data (strain gage measured hook loads) mentioned previously, the direct method for calculating crack growth may be used for the eight stress points in the following way:

σ_1 ..... flight 1 to flight 9
σ_2, σ_3 ..... flight 1 to flight 7
σ_4 to σ_8 ..... flights 8 and 9 (after the left drag shaft proof tests and the strain gage instrumentation)

Indirect Method

The indirect method for calculating the crack growths for several stress points must be used for some flights:

σ_2, σ_3 ..... flights 8 and 9
σ_4 to σ_8 ..... flight 1 to flight 7

The crack growth curve for each stress point for a typical flight may be divided into four major regions with different slopes (crack growth rates) and different time durations:

1. taxiing,
2. takeoff run,
3. airborne, cruise power, and
4. cruising.

The upper curve of figure 20 shows the crack growth curve calculated for, say, σ_4 using the strain gage data of flight 9 and using a_c^P as the initial crack size (the initial crack size for flight 1). From this curve, the four averaged slopes α_i ($i = 1, 2, 3, 4$) for the four regions can be determined. Using the α_i thus obtained and the known durations T_i ($i = 1, 2, 3, 4$) for the four regions of flight 1, it is possible to construct a crack growth curve for flight 1, (lower curve of fig. 20). Thus, the estimated crack growth at stress point σ_i for flight 1 may be calculated from

$$\Delta a_1 = \sum_{i=1}^{4} \alpha_i T_i \tag{26}$$

For calculating the amount of crack growth at stress point σ_4 for flight 2, one has to go back to the strain gage data of flight 9, recalculate the crack growth curve, and determine the new set of slopes α_i. This time, the initial crack size of $a_c^P + \Delta a_1$ must be used. This process can be used up to flight 7. Calculations of crack growths for the stress points σ_5 to σ_8 may be carried out in a similar manner. In applying the indirect method for the calculations of crack growths at stress points σ_2 and σ_3 for flights 8 and 9, the master slopes α_i (crack growth rates) established from the strain gage data of flight 7 were used.

Missing Data Extrapolations

During the flights, short intervals of strain gage data were lost as a result of noise, interference, and the interruption by parts of the B-52 aircraft in the line-of-sight signal path from the transmitter on the payload to the ground receiver. To account for those missing data in a particular maneuver region (such as taxiing, takeoff run, airborne and cruise power, or cruising), "forward" extrapolation of the crack growth curve with respect to time was performed using the average crack growth rate α_i (or slope) from the previous maneuver transition point (or check point). Figure 21 illustrates this missing data extrapolation.

For certain flights, the initial taxiing data were not recovered. For such a case, the "backward" extrapolation of the crack growth curve had to be performed. As shown in the upper part of figure 22, the crack growth curve was first calculated starting from point B to point B' (the next check point, or maneuver transition point) using the proof crack size a_c^P. Then the averaged slope α_1 of the crack growth curve lying between points B and B' was established. Using the slope α_1 thus established, the amount of crack growth Δa that occurred during time T_1 of the initial missing data region could be calculated from

$$\Delta a = \alpha_1 T_1 \tag{27}$$

After Δa was calculated, point B was then shifted upward to location B'' by an amount Δa (that is, the crack size for point B is increased to $a_c^P + \Delta a$; see lower part of fig. 22), and then the final calculations of the crack growth curve proceeded from point B''.

Appendix C discusses in detail the computer programs used in the calculation of fatigue-crack growths using the half-cycle method directly and indirectly.

RESULTS

Figures 23 to 30 show the crack growth curves calculated for the eight stress points σ_i ($i = 1, 2, \ldots, 8$) for flight 1. The crack growth curves for other flights are quite similar and therefore are not shown. Figures 23 to 25 (curves for stress points σ_1 to σ_3) were calculated by using the direct method; figures 26 to 30 were constructed by using the indirect method. The maneuver transition points are indicated in those figures. In figures 23 to 25, the data dropout regions are also shown. For the front and the two rear hooks (σ_1, σ_2, σ_3, figs. 23 to 25) the crack growth rate is most rapid during the initial stage of taxiing and the takeoff run and becomes very slow during cruising because of relatively low-amplitude stress cyclings. However, for the rest of the stress points (σ_4 to σ_8, figs. 26 to 30) the crack growth rate is very low during taxiing because of negligible drag and becomes larger during takeoff and cruising because of increased drag. Table 3 summarizes the results of the crack growth analysis of the eight pylon parts calculated for each SRB–DTV test flight. For practical applications, the calculated values of F_ℓ should be reduced by using a safety factor in the range of 2 to 4 to account for uncertainties. Notice in table 3 that the value of F_ℓ does not decrease monotonically with accumulated flights. The reason for this is that the duration and flight conditions for each flight are different (different Δa_ℓ), and therefore the value of F_ℓ predicted at the end of the ℓth flight could be smaller or larger than the value $F_{\ell-1}$ predicted at the end of $(\ell-1)$th flight, depending on the size of crack growth Δa_ℓ during the ℓth flight. Figure 31 shows plots of the number of flights left F_1 as functions of percent limit loads for the eight stress points for the first flight. The arrows in the figure indicate the locations of the peak operational load levels. Notice that the left and right drag shafts (σ_4, σ_5), the left and right drag pins (σ_6, σ_7), and the right drag shaft support (σ_8) have long fatigue life left after the completion of the SRB–DTV flight tests because of low operational stress levels. These parts (σ_4 to σ_8) turned out to be noncritical because the operational crack sizes a_c^o exceeded the characteristic dimensions of the corresponding parts (see table 3). Fatigue lives for the three hooks (σ_1, σ_2, σ_3) after the final flight are relatively short. The front hook (σ_1) has the shortest fatigue life because of relatively high operational stress levels, and it is therefore the most critical part of the pylon. Figure 32 shows plots

of amounts of crack growth with the increase in flight number for the front hook (the most critical part) and the two rear hooks (critical parts) during the entire SRB–DTV test program.

CONCLUSION

Eight stress points, located respectively at eight critical points of the B-52 pylon parts, were selected for the pylon fatigue life analysis. Using fracture mechanics and the half-cycle theory (directly and indirectly) for the calculation of fatigue-crack growth, the remaining fatigue life (or number of flights left) was estimated for each of the pylon critical parts. The results showed that the left and right drag shafts (stress points σ_4, σ_5), and drag pins (stress points σ_6, σ_7), and the right drag shaft lower support (stress point σ_8), have long fatigue life because of low operational stress levels and can be considered as noncritical parts. Also, the fatigue lives of the three hooks (stress points σ_1, σ_2, σ_3) are relatively short. The front hook (stress point σ_1) has the shortest fatigue life compared with other pylon parts because of relatively high operational stress level, and it is therefore the most critical part of the pylon.

National Aeronautics and Space Administration
Ames Research Center
Dryden Flight Research Facility
Edwards, California
July 25, 1986

Table 1. Material properties for critical parts (stress points).

Stress point	Part name	Part number	Material	σ_u, ksi	σ_Y, ksi
σ_1	Front hook	2581-630620	Inconel 718 alloy	175	145
σ_2	New left rear hook	---	AMAX MP35N alloy	250	235
σ_3	New right rear hook	---	AMAX MP35N alloy	250	235
σ_4	Left drag shaft	2581-630706	4340 steel	180 to 200	225
σ_5	Right drag shaft	2581-630707	4340 steel	160 to 180	163
σ_6	Left drag pin	2581-630718	AMAX MP35N alloy	250	235
σ_7	Right drag pin	2581-630716	AMAX MP35N alloy	250	235
σ_8	Right drag shaft lower support	2581-630711	4340 steel	160 to 180	163

Stress point	Part name	τ, ksi	C, $\frac{\text{in.}}{\text{cycle}}(\text{ksi}\sqrt{\text{in.}})^{-m}$	m	n	K_{I_c}, ksi $\sqrt{\text{in.}}$
σ_1	Front hook	135	9.220×10^{-12}	3.60	2.16	125
σ_2	New left rear hook	141	2.944×10^{-11}	3.24	1.69	124
σ_3	New right rear hook	141	2.944×10^{-11}	3.24	1.69	124
σ_4	Left drag shaft	156	1.043×10^{-9}	2.70	2.27	105
σ_5	Right drag shaft	108	1.043×10^{-9}	2.70	2.27	105
σ_6	Left drag pin	141	2.944×10^{-11}	3.24	1.69	124
σ_7	Right drag pin	141	2.944×10^{-11}	3.24	1.69	124
σ_8	Right hand drag lower support	108	1.043×10^{-9}	2.70	2.27	105

Table 2. Proof test hook loads.

Maneuver identification number	Hook load, lb						
	V_A	V_{BL}	V_{BR}	S_A	S_{CL}	D_{CL}	D_{CR}
1	35,019	28,708	31,437	1,684	5,369	25,660	26,113
2	35,603	36,754	36,088	0	0	0	0
3	27,416	32,859	42,756	3,995	−10,099	0	0
4	27,415	42,871	32,744	3,995	10,099	0	0
5	29,728	31,806	30,991	0	−8,210	32,080	30,060
	Maximum proof load						
	36,520	44,110	44,230	3,590	10,100	31,900	30,030
						−9,650	−9,660

Table 3. Summary of crack growth analysis.

Stress point		Proof load test	Flight duration, min: 49.48	64.70	67.55	52.83	99.43
			Flight number: 1	2	3	4	5
σ_1	a_ℓ	0.0990	0.1008295	0.1021277	0.1044369	0.1062016	0.1120766
	a_c^o		0.3333052	0.3333052	0.2835354	0.2835354	0.2059647
	Δa_ℓ		0.0018295	0.0012982	0.0023092	0.0017646	0.0058250
	$a_c^o - a_\ell$		0.2324758	0.2309243	0.1790985	0.1773338	0.0938881
	F_ℓ		128	179	78	101	17
	Percent limit load		54.50	51.31	59.09	55.77	69.33
σ_2	a_ℓ	0.0734	0.0739887	0.0746227	0.0753477	0.0760176	0.0776691
	a_c^o		0.2076090	0.2057364	0.2057364	0.1856398	0.1776967
	Δa_ℓ		0.0005887	0.0006340	0.0007250	0.0006699	0.0016515
	$a_c^o - a_\ell$		0.1336203	0.1311137	0.1302389	0.1096222	0.1000276
	F_ℓ		227	207	180	164	61
	Percent limit load		59.46	59.73	59.47	62.88	64.27
σ_3	a_ℓ	0.0730	0.0737705	0.0742656	0.0751271	0.0758267	0.0775514
	a_c^o		0.2037274	0.2037274	0.1930696	0.1930696	0.1930696
	Δa_ℓ		0.0007705	0.0004951	0.0008615	0.0006996	0.0017247
	$a_c^o - a_\ell$		0.1299569	0.1294618	0.1179425	0.1174803	0.1155182
	F_ℓ		169	263	137	168	78
	Percent limit load		59.86	54.19	61.49	60.68	58.79
σ_4	a_ℓ	0.1410	0.1412347	0.1415575	0.1416992	0.1419603	0.1424520
	a_c^o		3.4865426	3.4865426	3.4865426	3.4865426	3.4865426
	Δa_ℓ		0.0002347	0.0003228	0.0001417	0.0002610	0.0004917
	$a_c^o - a_\ell$		3.3453079	3.3449851	3.3448434	3.3445823	3.3440906
	F_ℓ		14,255	10,362	23,608	12,813	6,802
	Percent limit load		20.11	20.11	20.11	20.11	20.11
σ_5	a_ℓ	0.3815	0.3816163	0.3817765	0.3818368	0.3819657	0.3822081
	a_c^o		14.0298566	14.0298566	14.0298566	14.0298566	14.0298566
	Δa_ℓ		0.0001163	0.0001602	0.0000604	0.0001289	0.0002424
	$a_c^o - a_\ell$		13.6482403	13.6480801	13.6480198	13.6478909	13.6476485
	F_ℓ		117,418	85,211	226,097	105,904	56,317
	Percent limit load		16.49	16.49	16.49	16.49	16.49
σ_6	a_ℓ	0.0872	0.0872515	0.0873233	0.0873520	0.0874094	0.0875180
	a_c^o		3.7446171	3.7446171	3.7446171	3.7446171	3.7446171
	Δa_ℓ		0.0000515	0.0000719	0.0000286	0.0000574	0.0001086
	$a_c^o - a_\ell$		3.6573656	3.6572938	3.6572651	3.6572077	3.6570991
	F_ℓ		70,992	50,872	127,739	63,628	33,669
	Percent limit load		15.26	15.26	15.26	15.26	15.26
σ_7	a_ℓ	0.1010	0.1010611	0.1011467	0.1011772	0.1012458	0.1013746
	a_c^o		3.7143264	3.7143264	3.7143264	3.7143264	3.7143264
	Δa_ℓ		0.0000611	0.0000855	0.0000305	0.0000683	0.0001291
	$a_c^o - a_\ell$		3.6132653	3.6131797	3.6131492	3.6130806	3.6129518
	F_ℓ		59,105	42,259	118,442	52,942	27,980
	Percent limit load		16.49	16.49	16.49	16.49	16.49
σ_8	a_ℓ	0.1750	0.1751166	0.1752773	0.1753379	0.1754673	0.1757108
	a_c^o		6.4201312	6.4201312	6.4201312	6.4201312	6.4201312
	Δa_ℓ		0.0001166	0.0001607	0.0000606	0.0001294	0.0002435
	$a_c^o - a_\ell$		6.2450146	6.2448539	6.2447933	6.2446639	6.2444204
	F_ℓ		53,609	38,884	103,134	48,282	25,660
	Percent limit load		16.51	16.51	16.51	16.51	16.51

Table 3. Concluded.

Stress point		Proof load test	Flight duration, min: 95.55	58.55	44.23	67.65
			Flight number: 6	7	8	9
σ_1	a_ℓ	0.0990	0.1154196	0.1186624	0.1207648	0.1267761
	a_c^o		0.2059647	0.2059647	0.2059647	0.2059647
	Δa_ℓ		0.0033930	0.0032429	0.0021024	0.0060133
	$a_c^o - a_\ell$		0.0905455	0.0873023	0.0851999	0.0791886
	F_ℓ		27	27	41	14
	Percent limit load		54.09	55.42	53.49	66.72
σ_2	a_ℓ	0.0734	0.0790510	0.0799232	0.0806427	0.0816830
	a_c^o		0.1776967	0.1440195	0.1440195	0.1440195
	Δa_ℓ		0.0013819	0.0008722	0.0007195	0.0010403
	$a_c^o - a_\ell$		0.0986457	0.0640983	0.0633768	0.0623365
	F_ℓ		72	74	89	60
	Percent limit load		63.12	71.39	71.39	71.39
σ_3	a_ℓ	0.0730	0.0790016	0.0799302	0.0807175	0.0818549
	a_c^o		0.1930696	0.1779445	0.1779445	0.1779445
	Δa_ℓ		0.0014502	0.0009286	0.0007873	0.0011374
	$a_c^o - a_\ell$		0.1140680	0.0980143	0.0972270	0.0960896
	F_ℓ		79	106	124	85
	Percent limit load		59.73	64.05	64.05	64.05
σ_4	a_ℓ	0.1410	0.1428617	0.1431225	0.1412063	0.1415535
	a_c^o		3.4865426	3.4865426	3.4865426	3.4865426
	Δa_ℓ		0.0004097	0.0002609	0.0002063	0.0003473
	$a_c^o - a_\ell$		3.3436809	3.3434201	3.3453363	3.3449891
	F_ℓ		8,162	12,817	16,220	9,633
	Percent limit load		20.11	20.11	20.11	20.11
σ_5	a_ℓ	0.3815	0.3824089	0.3825361	0.3826368	0.3828103
	a_c^o		14.0298566	14.0298566	14.0298566	14.0298566
	Δa_ℓ		0.0002008	0.0001272	0.0001007	0.0001735
	$a_c^o - a_\ell$		13.6474477	13.6473205	13.647220	13.6470463
	F_ℓ		67,990	107,295	135,614	78,668
	Percent limit load		16.49	16.49	16.49	16.49
σ_6	a_ℓ	0.0872	0.0876037	0.0876603	0.0872441	0.0873218
	a_c^o		3.7446171	3.7446171	3.7446171	3.7446171
	Δa_ℓ		0.0000857	0.0000566	0.0000441	0.0000778
	$a_c^o - a_\ell$		3.6570134	3.6569568	3.6569127	3.6568349
	F_ℓ		42,634	64,571	82,938	47,002
	Percent limit load		15.26	15.26	15.26	15.26
σ_7	a_ℓ	0.1010	0.1014763	0.1015435	0.1015959	0.1016893
	a_c^o		3.7143264	3.7143264	3.7143264	3.7143264
	Δa_ℓ		0.0001018	0.0000672	0.0000524	0.0000934
	$a_c^o - a_\ell$		3.6128501	3.6127829	3.6127305	3.6126371
	F_ℓ		35,508	53,779	69,005	38,684
	Percent limit load		16.49	16.49	16.49	16.49
σ_8	a_ℓ	0.1750	0.1759127	0.1760407	0.1761420	0.1763168
	a_c^o		6.4201312	6.4201312	6.4201312	6.4201312
	Δa_ℓ		0.0002019	0.0001280	0.0001013	0.0001748
	$a_c^o - a_\ell$		6.2442185	6.2440905	6.2439892	6.2438144
	F_ℓ		30,948	48,797	61,675	35,742
	Percent limit load		16.51	16.51	16.51	16.51

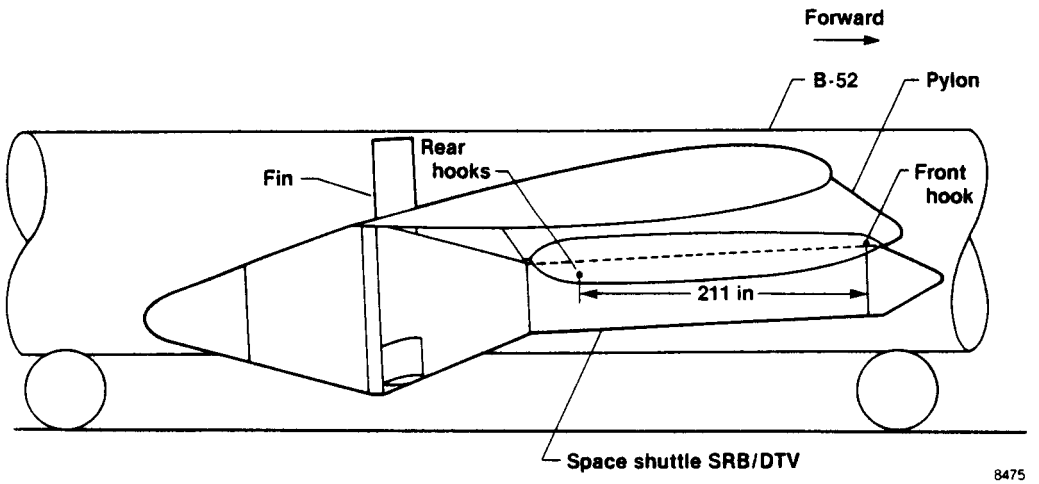

Figure 1. Geometry of space shuttle solid rocket booster drop test vehicle (SRB–DTV) attached to B-52 pylon. View, looking inboard at right side of B-52 and SRB–DTV.

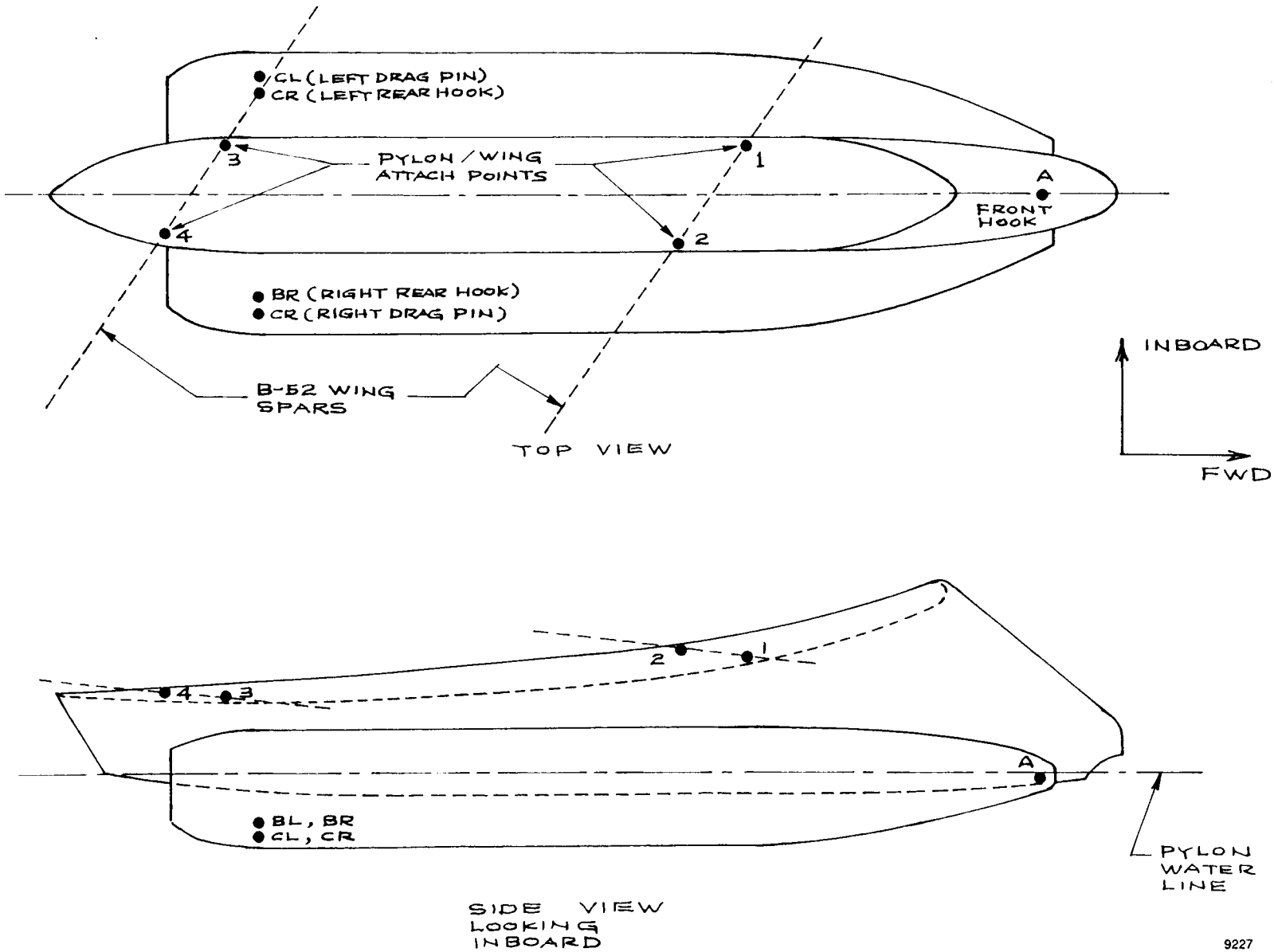

Figure 2. Geometry of B-52 pylon.

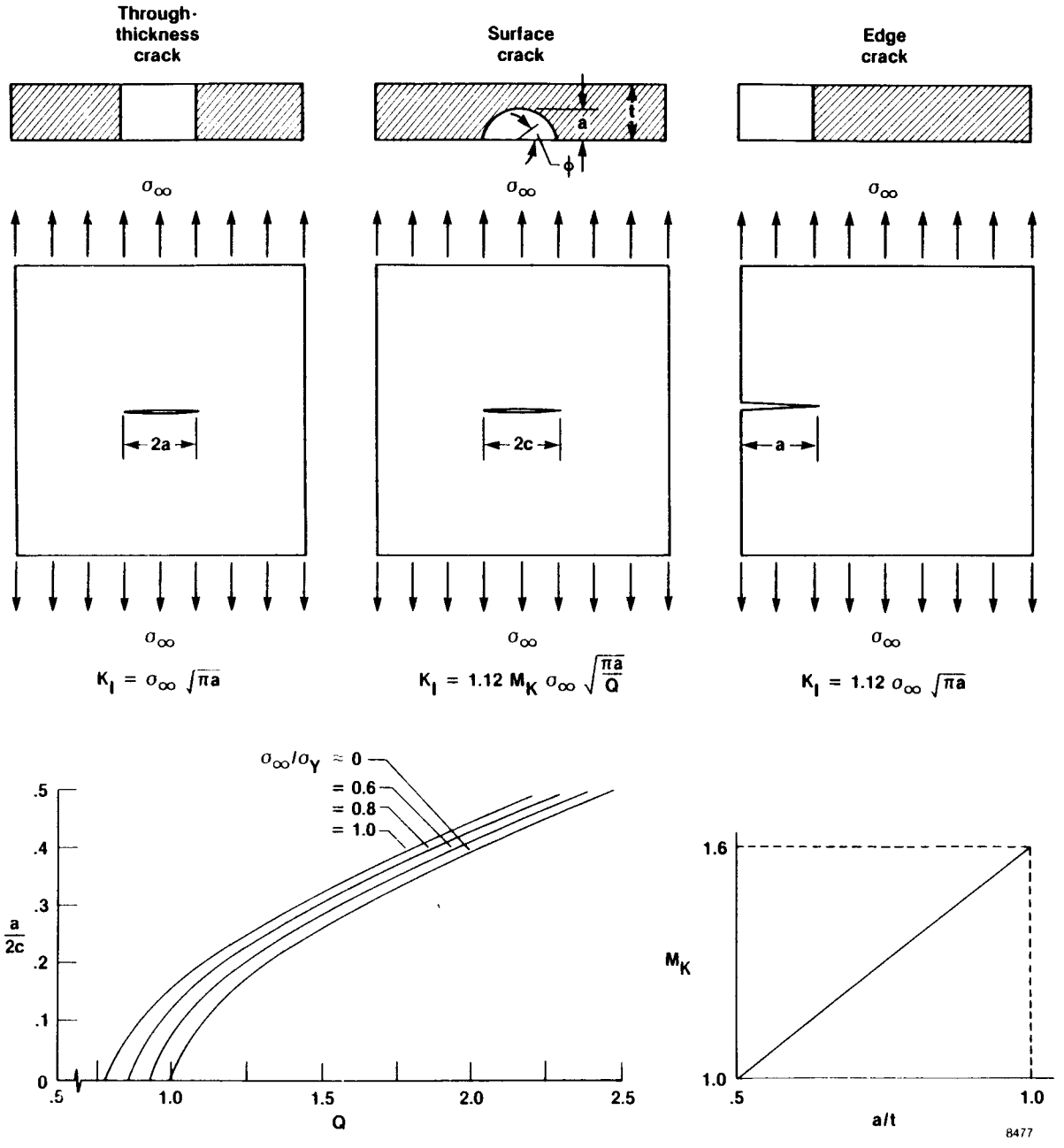

Figure 3. Three types of cracks and the plots of surface flaw shape factor and the flaw magnification factor.

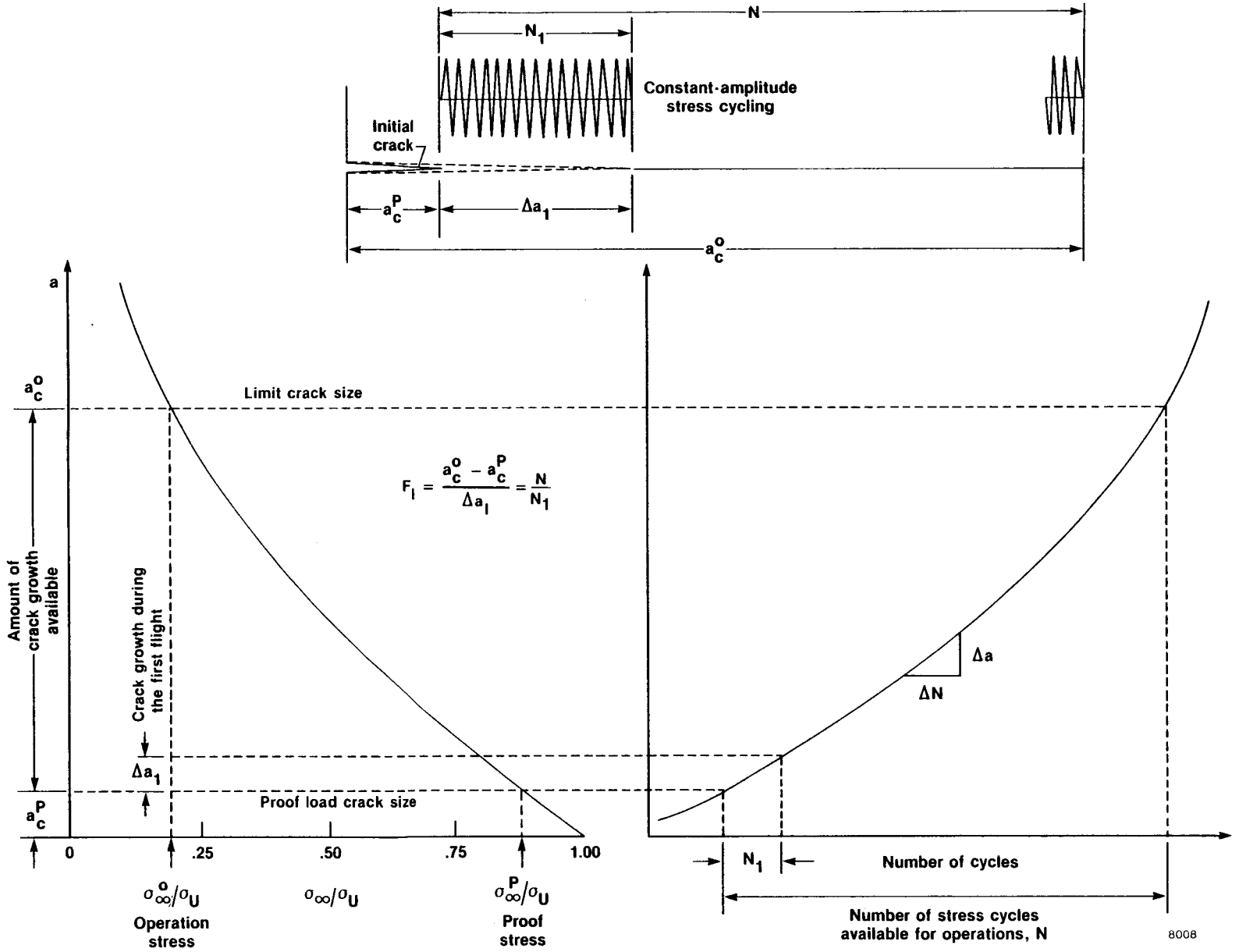

Figure 4. Crack length as a function of applied stress and number of cycles.

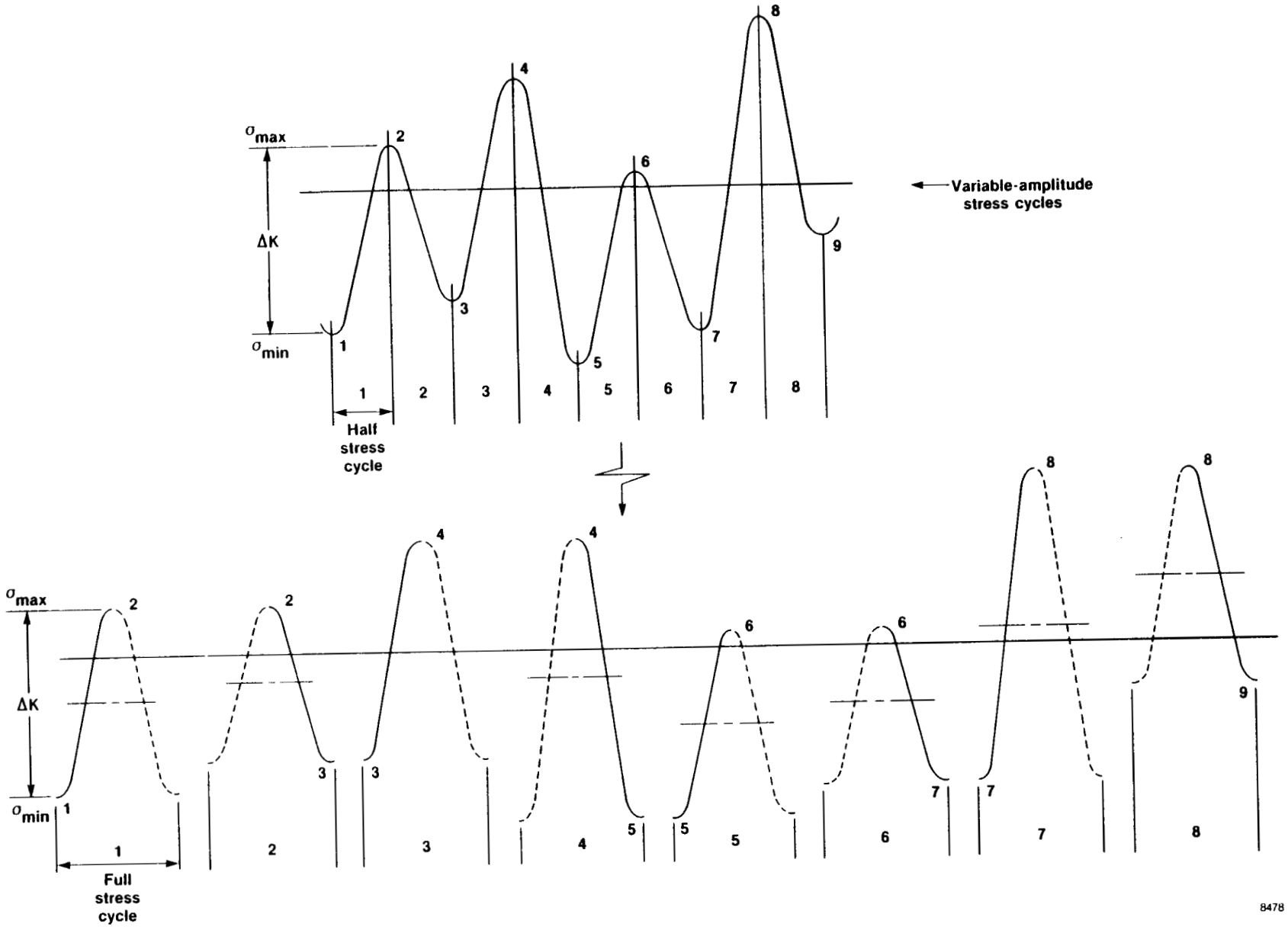

Figure 5. Resolution of random stress cycles into half stress cycles of different stress ranges.

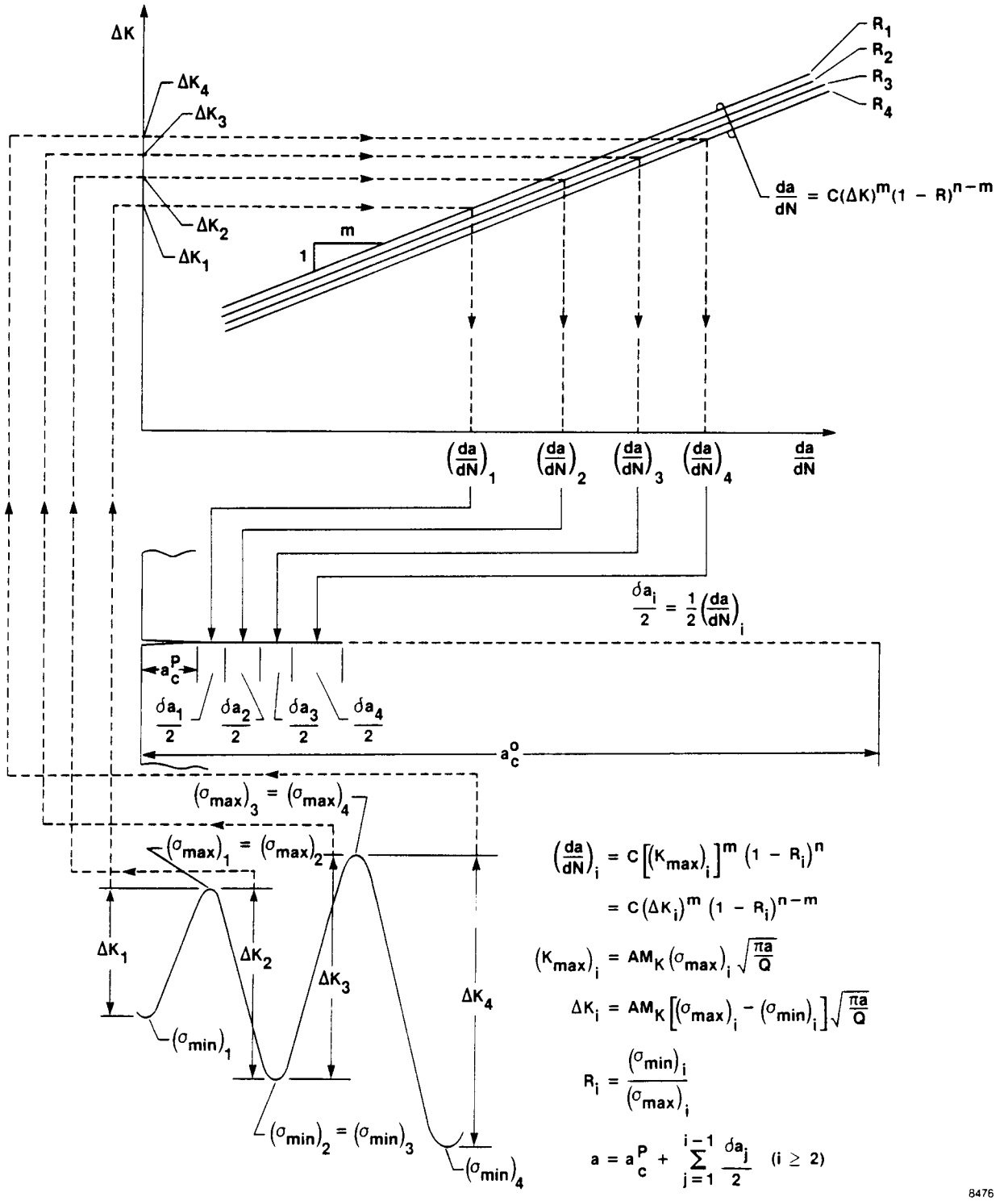

Figure 6. Graphic evaluation of crack increments for random stress cycles using half cycle method.

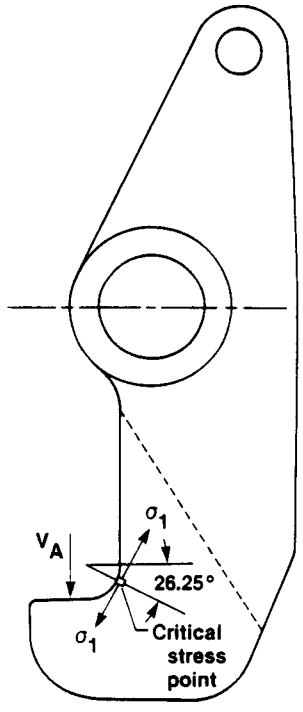

Figure 7. Front hook and the location of critical stress point σ_1.

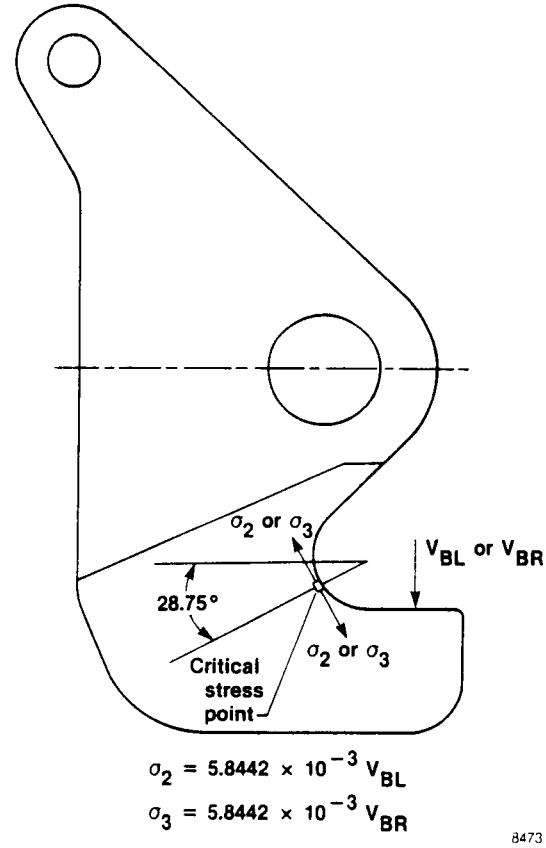

Figure 8. Rear hook (left or right) and the location of critical stress point (σ_2 or σ_3).

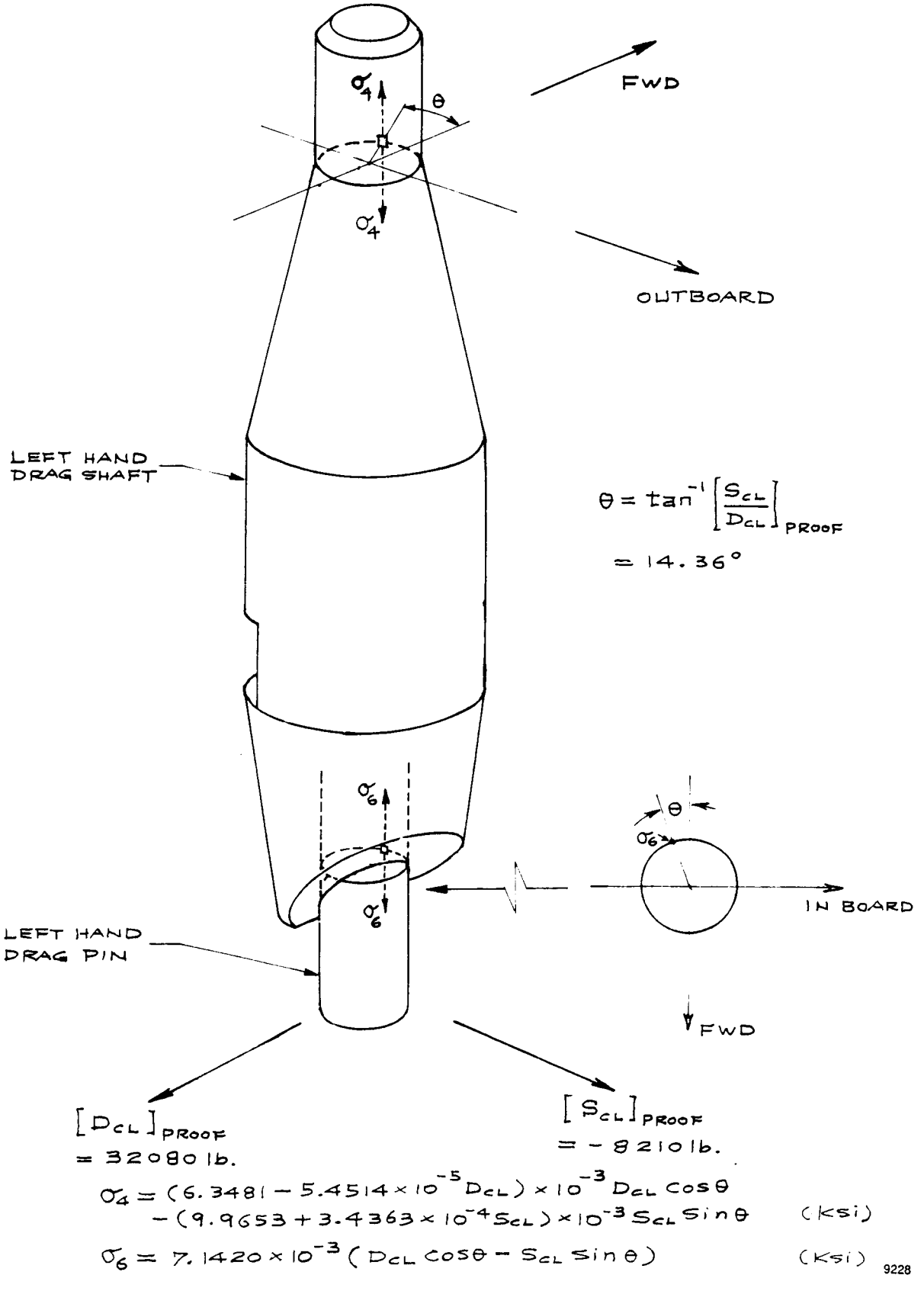

Figure 9. Left hand drag shaft and drag pin and the location of critical stress points σ_4 and σ_6.

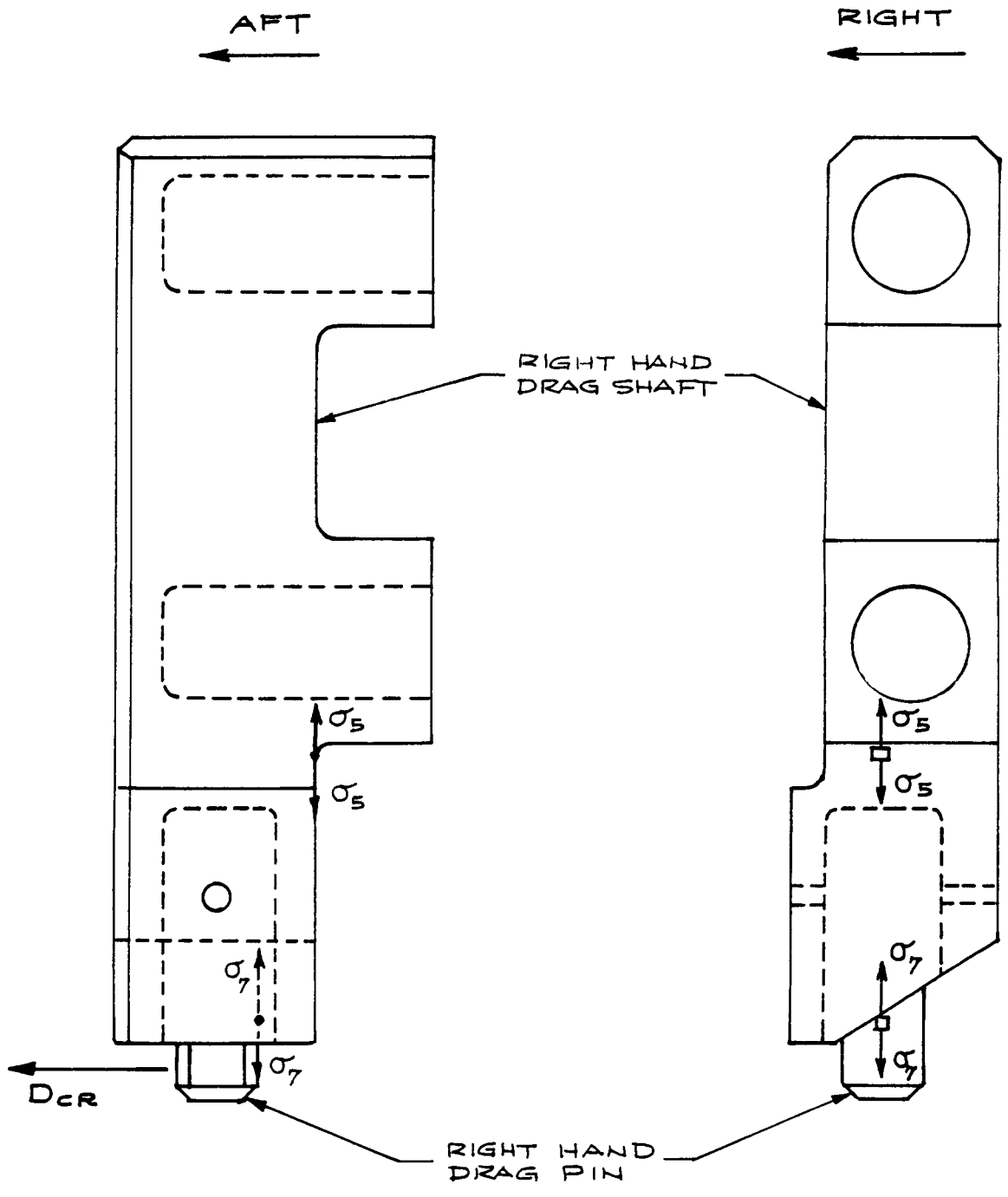

$$\sigma_5 = 2.1868 \times 10^{-3} D_{CR} \quad (ksi)$$

$$\sigma_7 = 7.3055 \times 10^{-3} D_{CR} \quad (ksi)$$

9229

Figure 10. Right hand drag shaft and drag pin and the location of critical stress points σ_5 and σ_7.

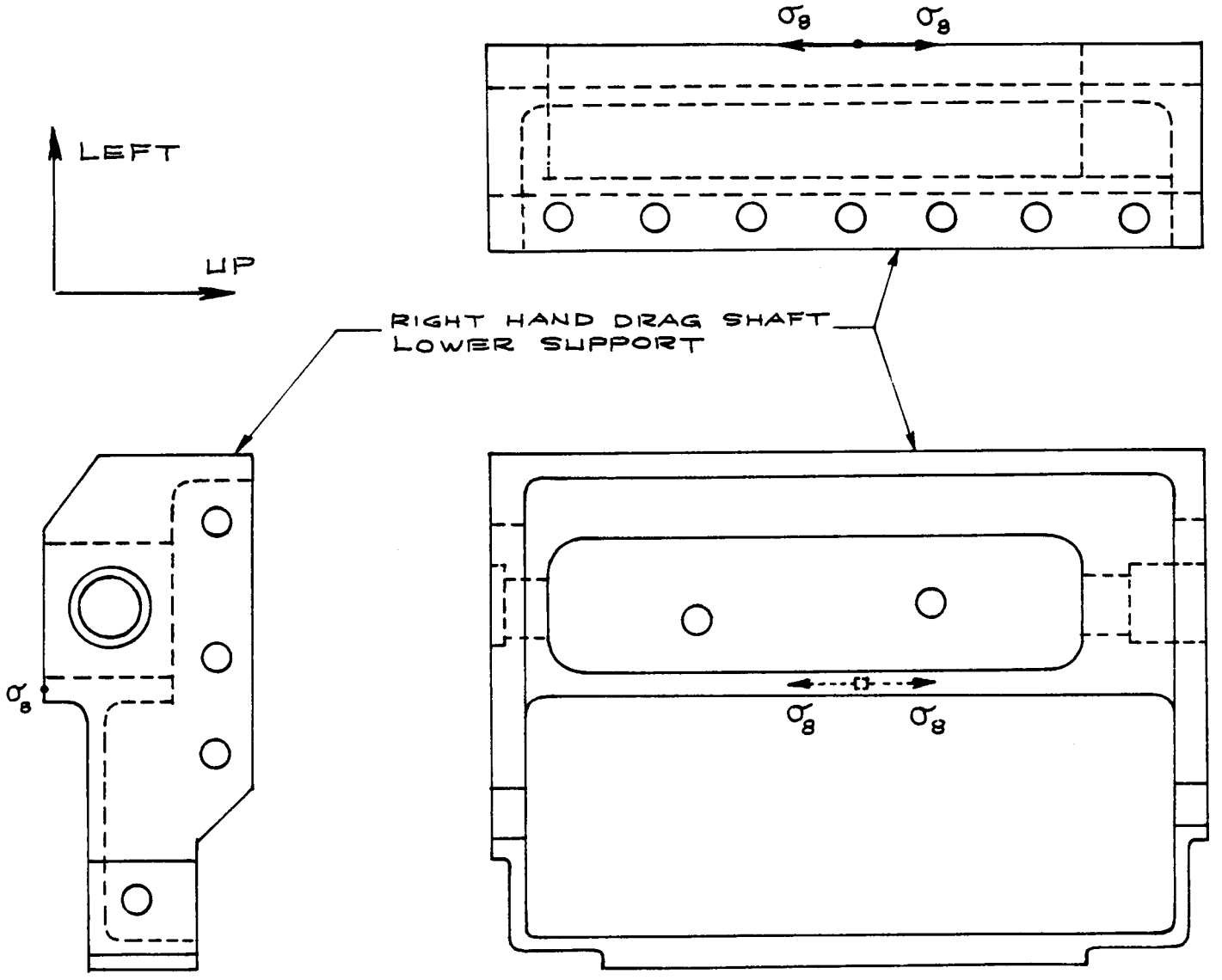

$$\sigma_8 = 4.2141 \times 10^{-3} D_{CR} \quad (ksi)$$

9230

Figure 11. Right hand drag shaft lower support and the location of critical stress point σ_8.

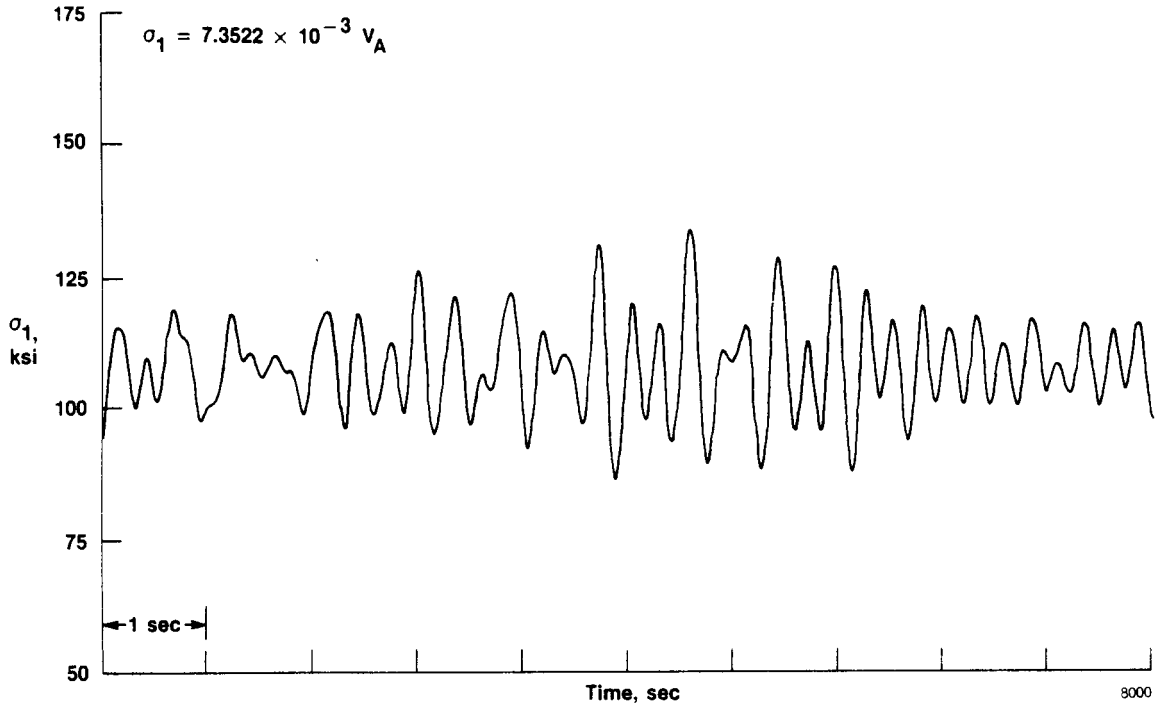

Figure 12. Stress cycles for critical stress point σ_1 at front hook V_A.

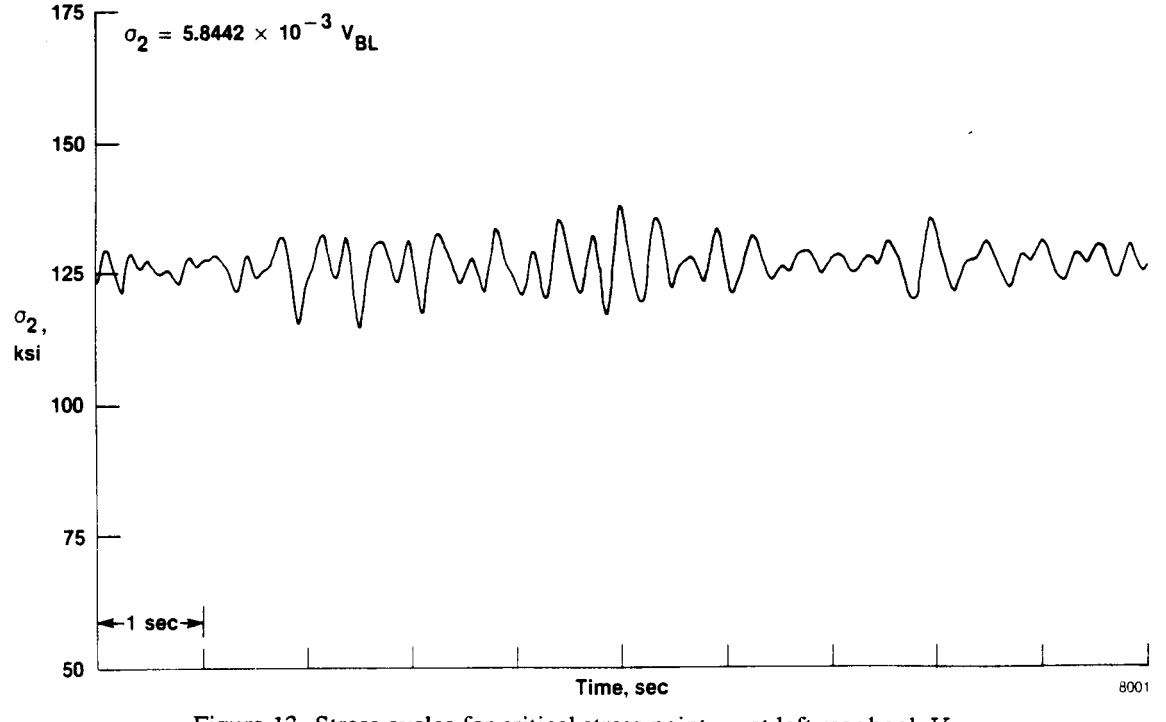

Figure 13. Stress cycles for critical stress point σ_2 at left rear hook V_{BL}.

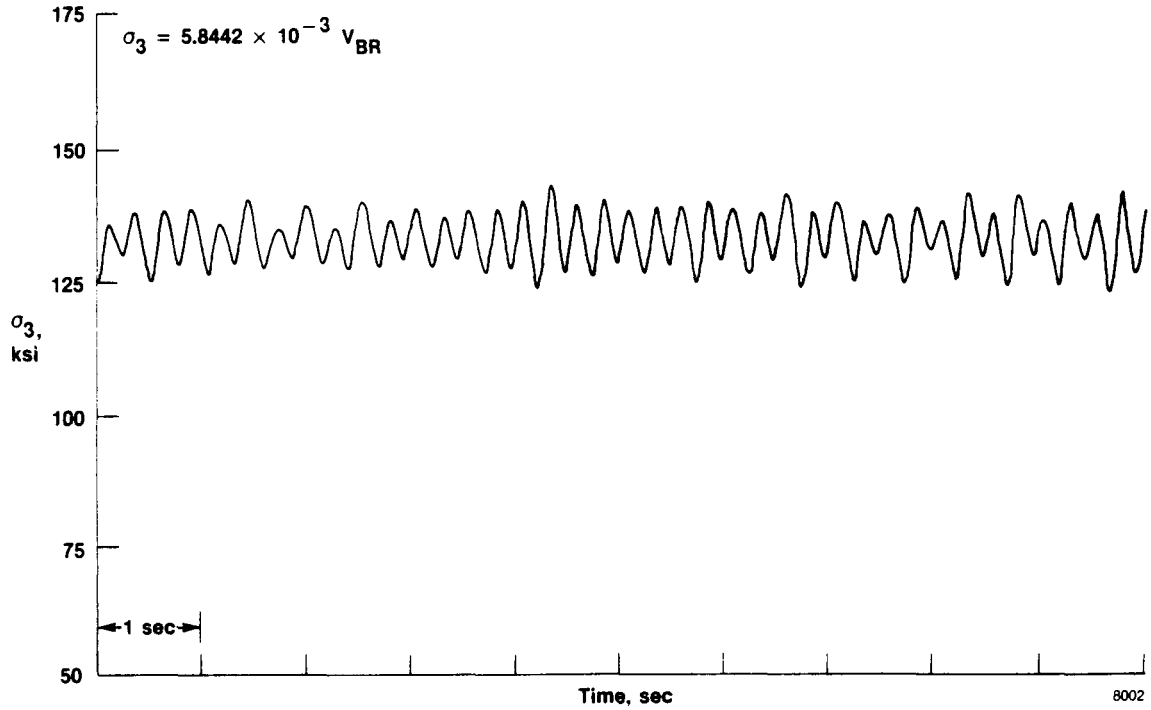

Figure 14. Stress cycles for critical stress point σ_3 at right rear hook V_{BR}.

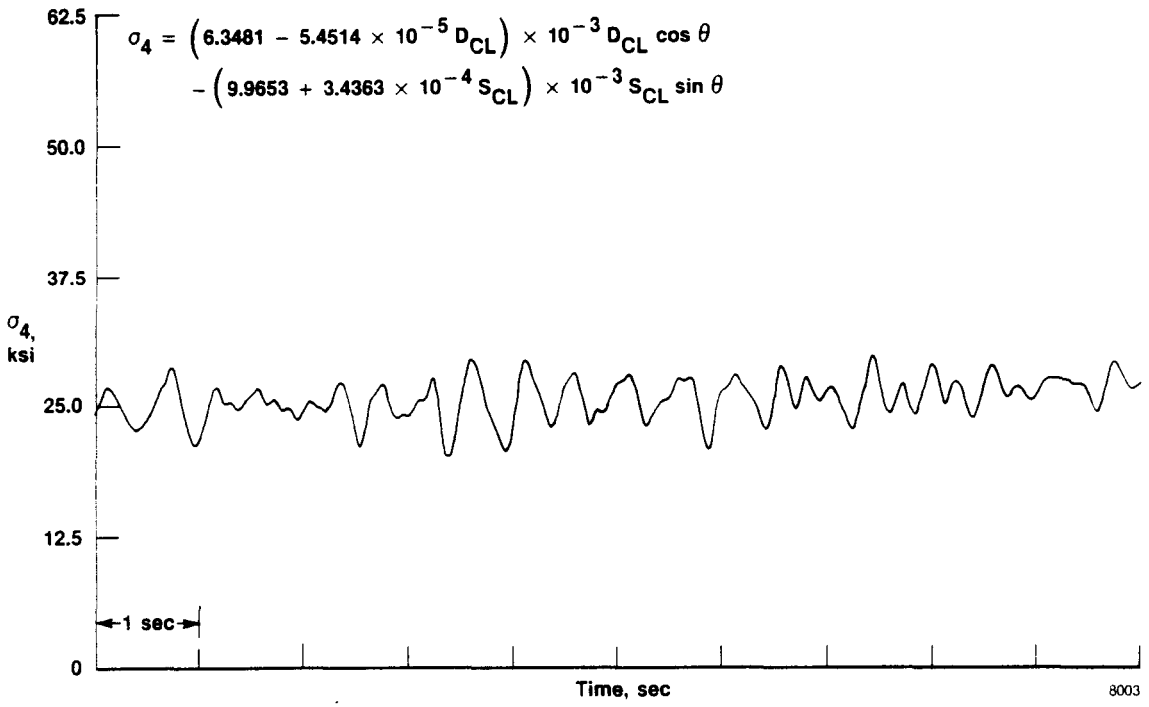

Figure 15. Stress cycles for critical stress point σ_4 at left-hand drag shaft, flight 9.

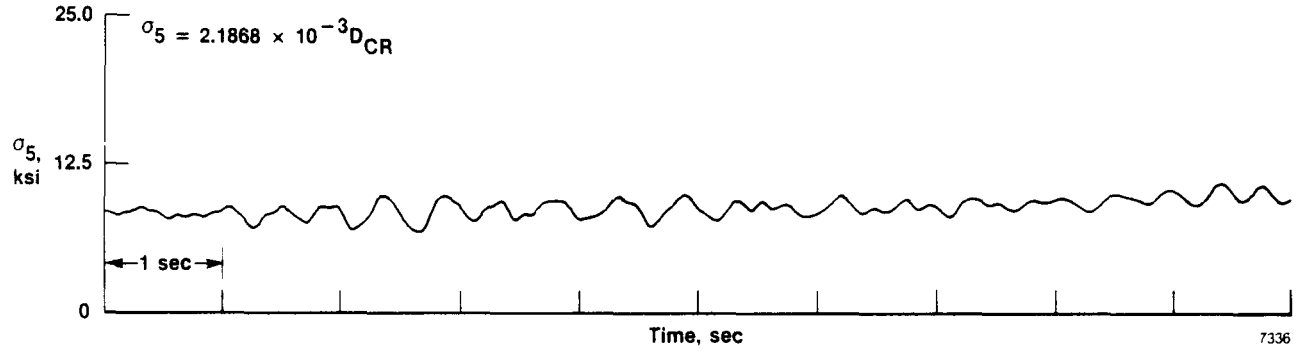

Figure 16. Stress cycles for critical stress point σ_5 at right-hand drag shaft, flight 9.

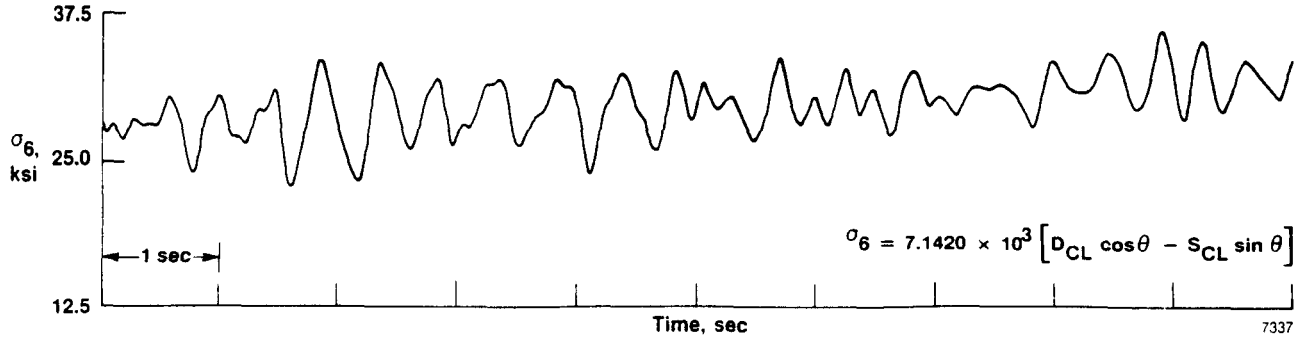

Figure 17. Stress cycles for critical stress point σ_6 at left-hand drag pin, flight 9.

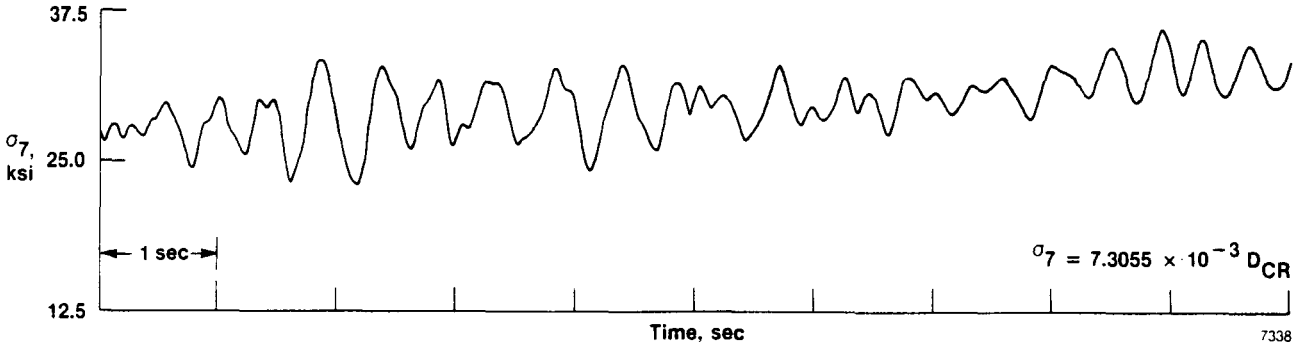

Figure 18. Stress cycles for critical stress point σ_7 at right-hand drag pin, flight 9.

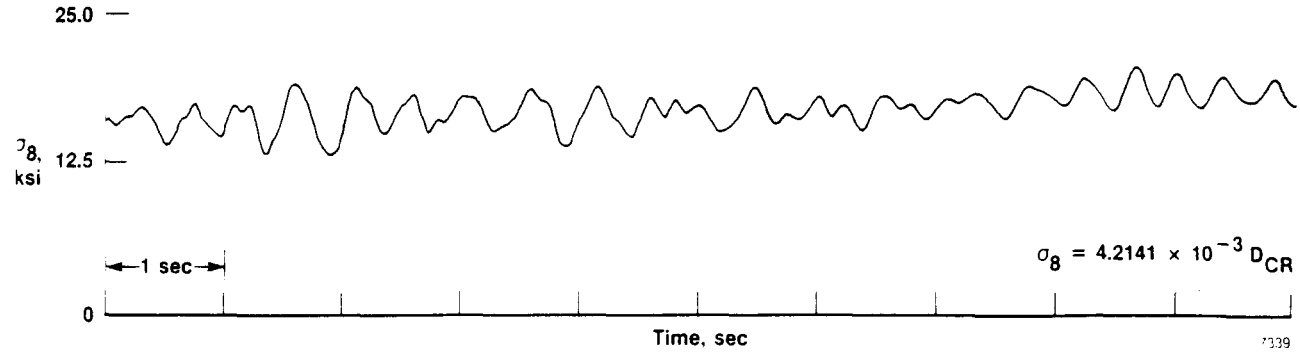

Figure 19. Stress cycles for critical stress point σ_8 at right-hand drag shaft lower support, flight 9.

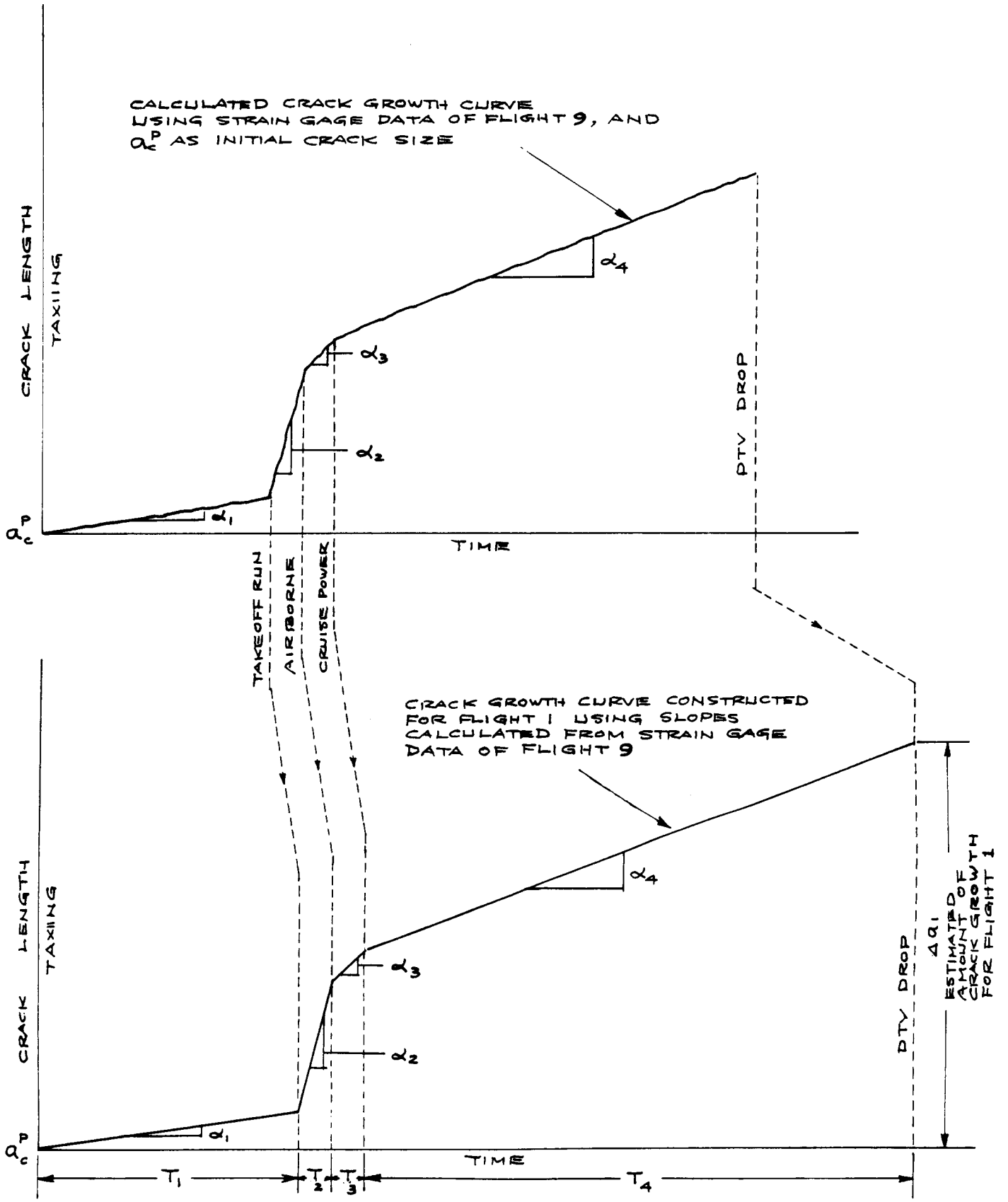

Figure 20. Construction of crack growth curve for flight 1 using slopes calculated from strain-gage data of flight 9.

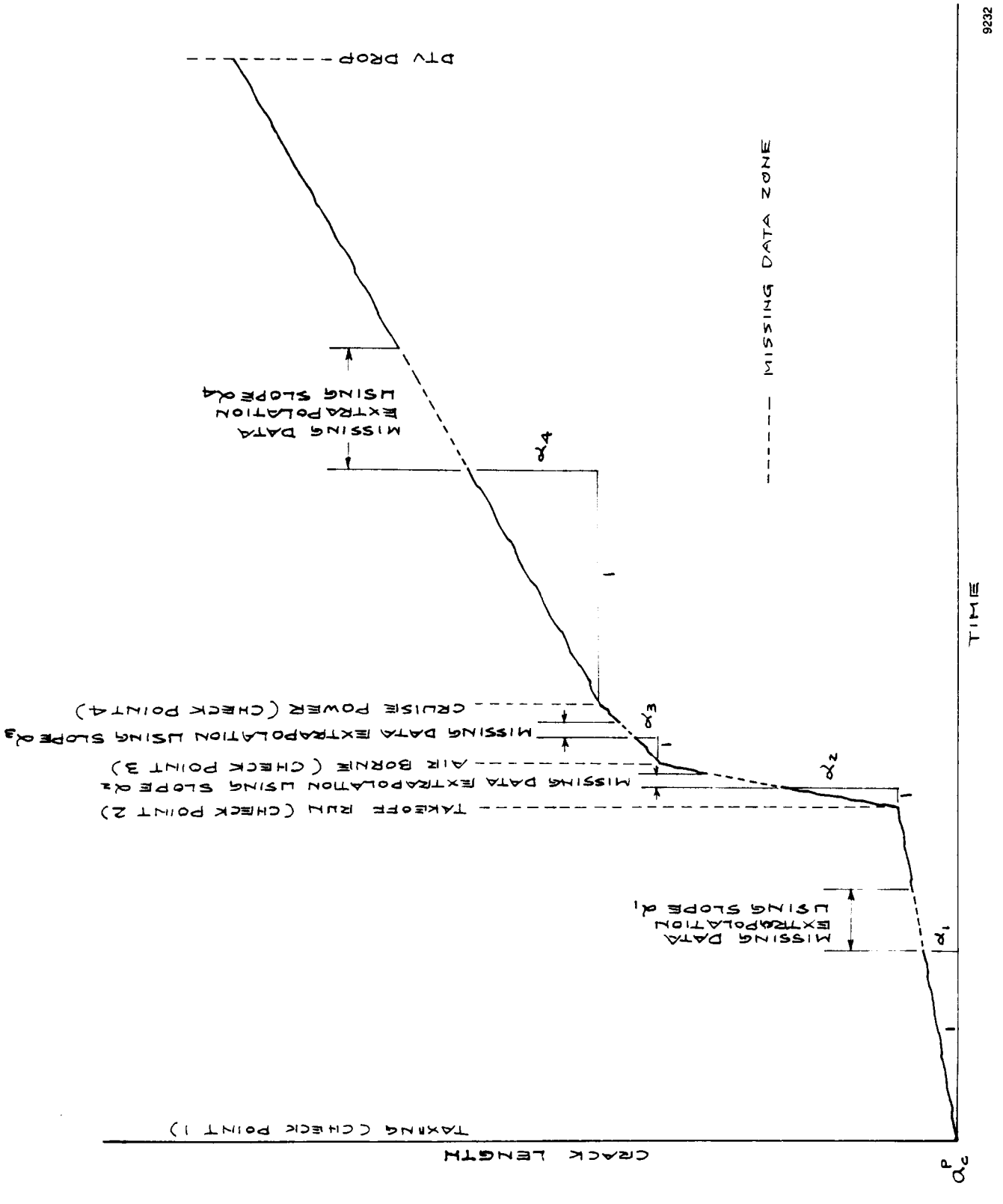

Figure 21. Extrapolation of crack growth curve for missing data zones.

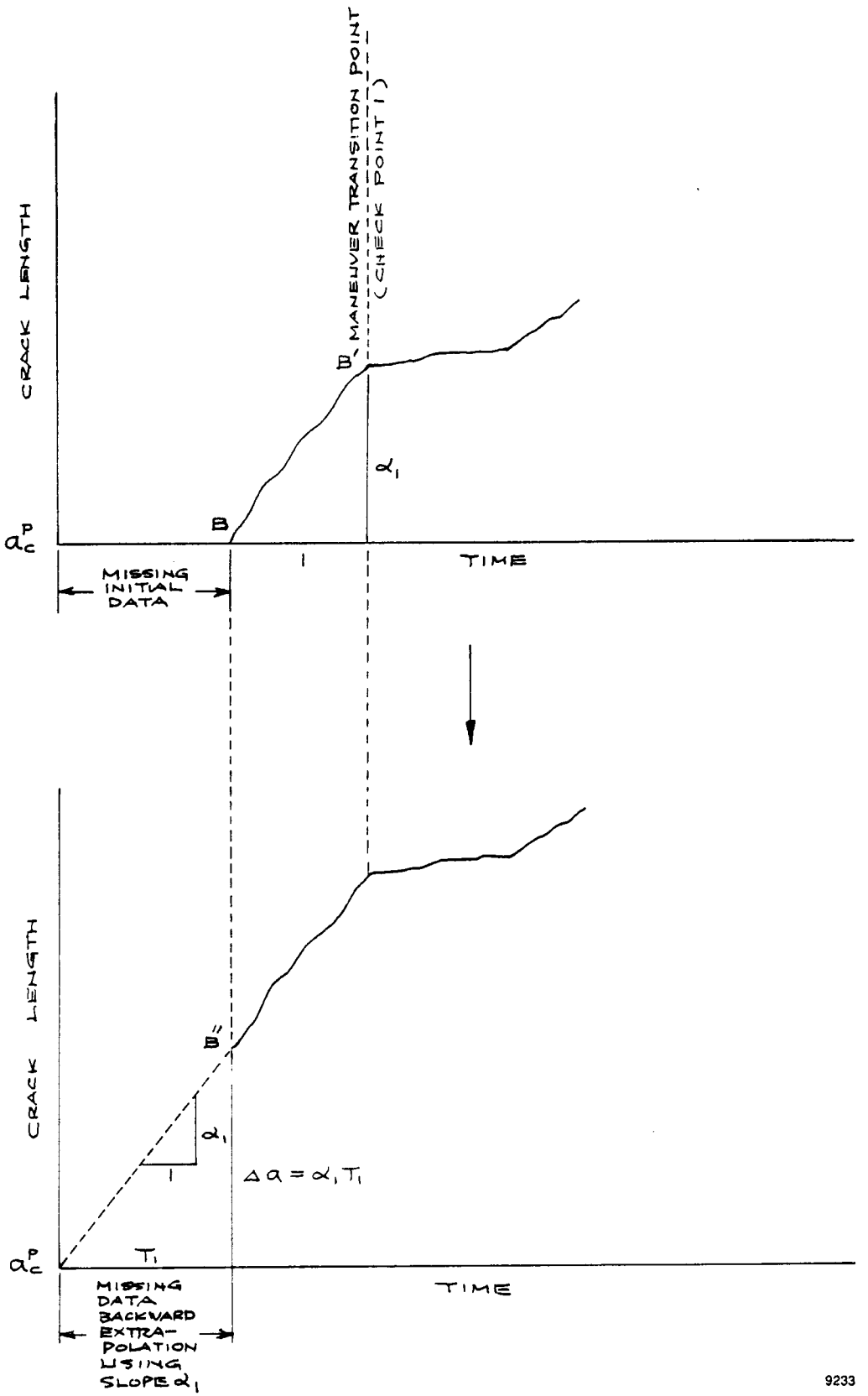

Figure 22. Backward extrapolation to construct crack growth curve for initial region of missing data.

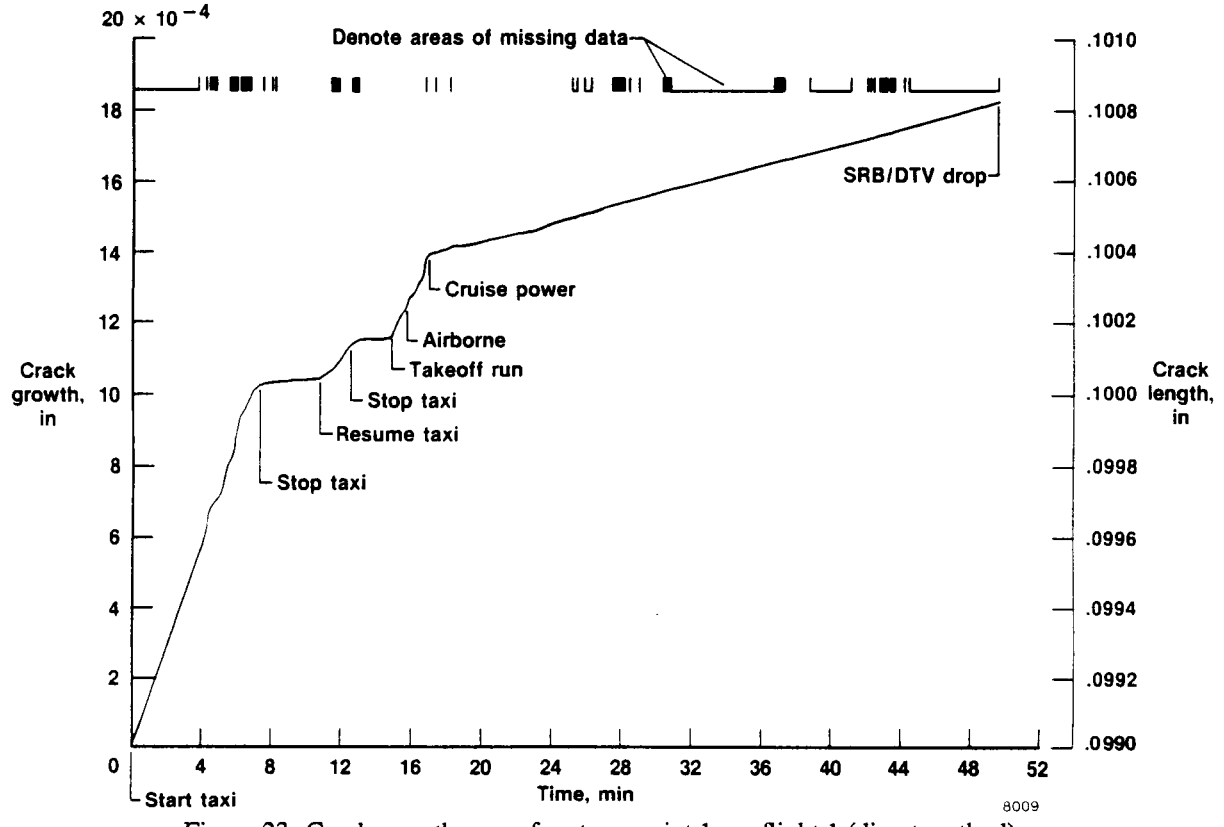

Figure 23. Crack growth curve for stress point 1 σ_1, flight 1 (direct method).

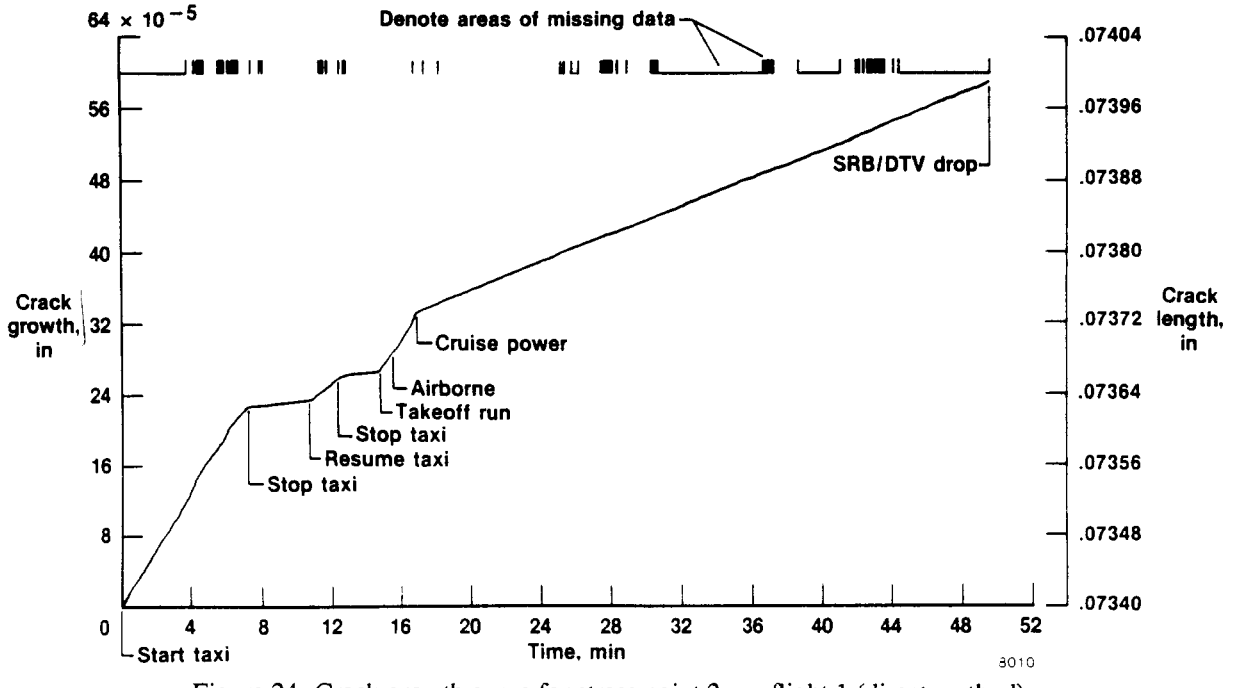

Figure 24. Crack growth curve for stress point 2 σ_2, flight 1 (direct method).

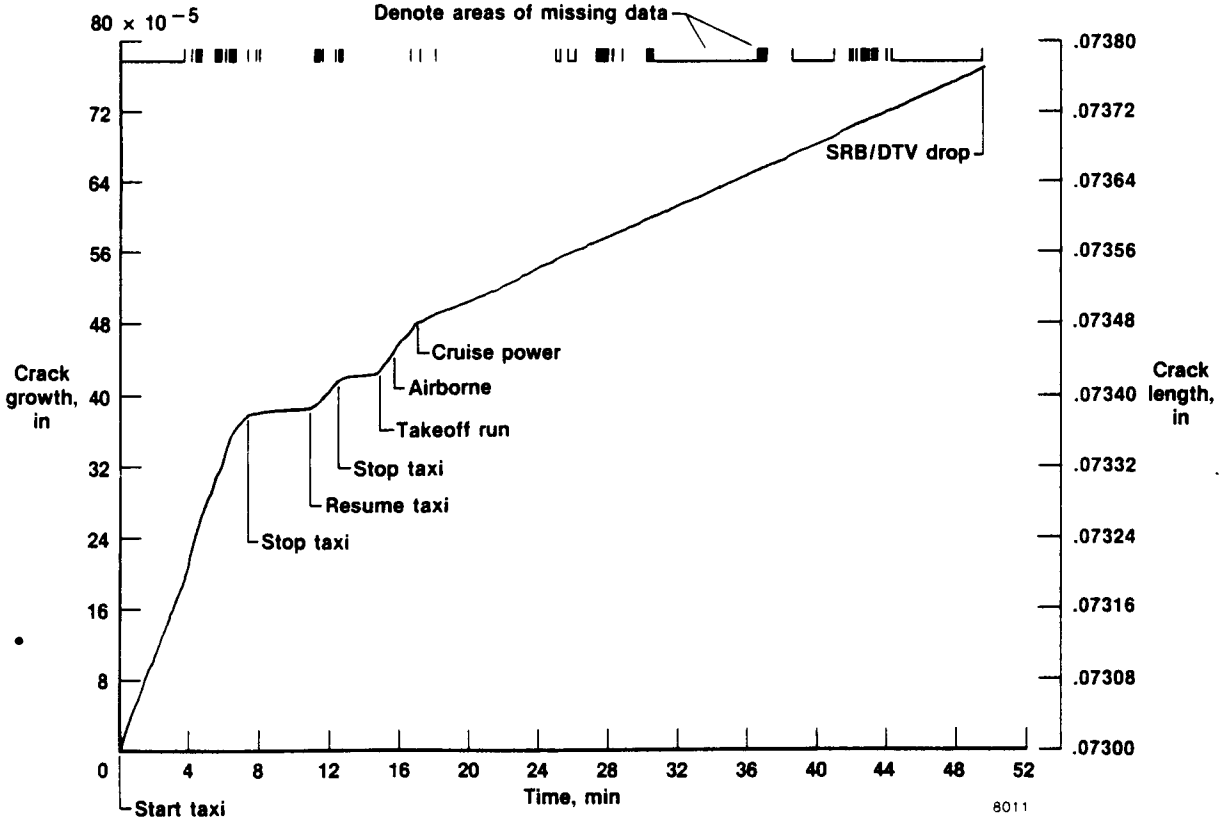

Figure 25. Crack growth curve for stress point 3 σ_3, flight 1 (direct method).

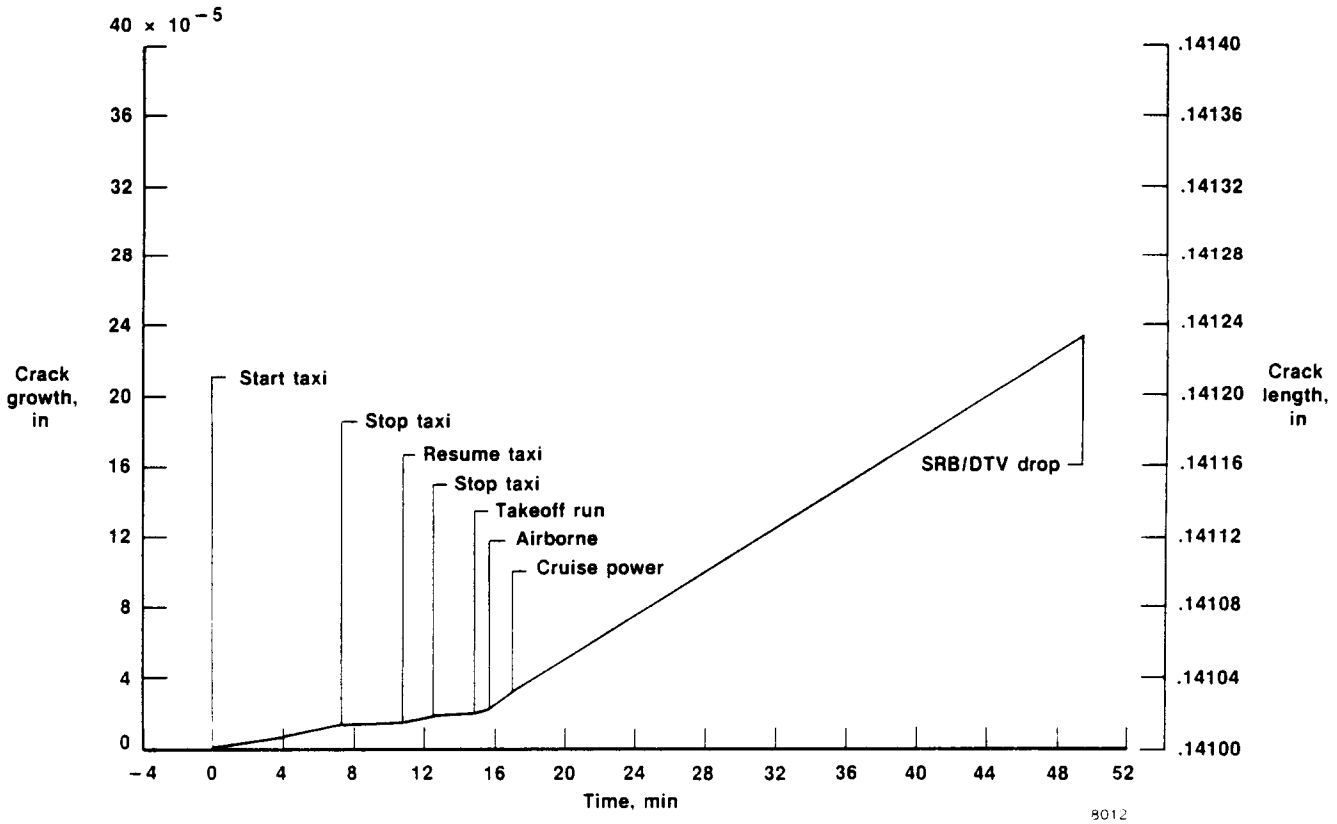

Figure 26. Crack growth curve for stress point 4 σ_4, flight 1 (indirect method).

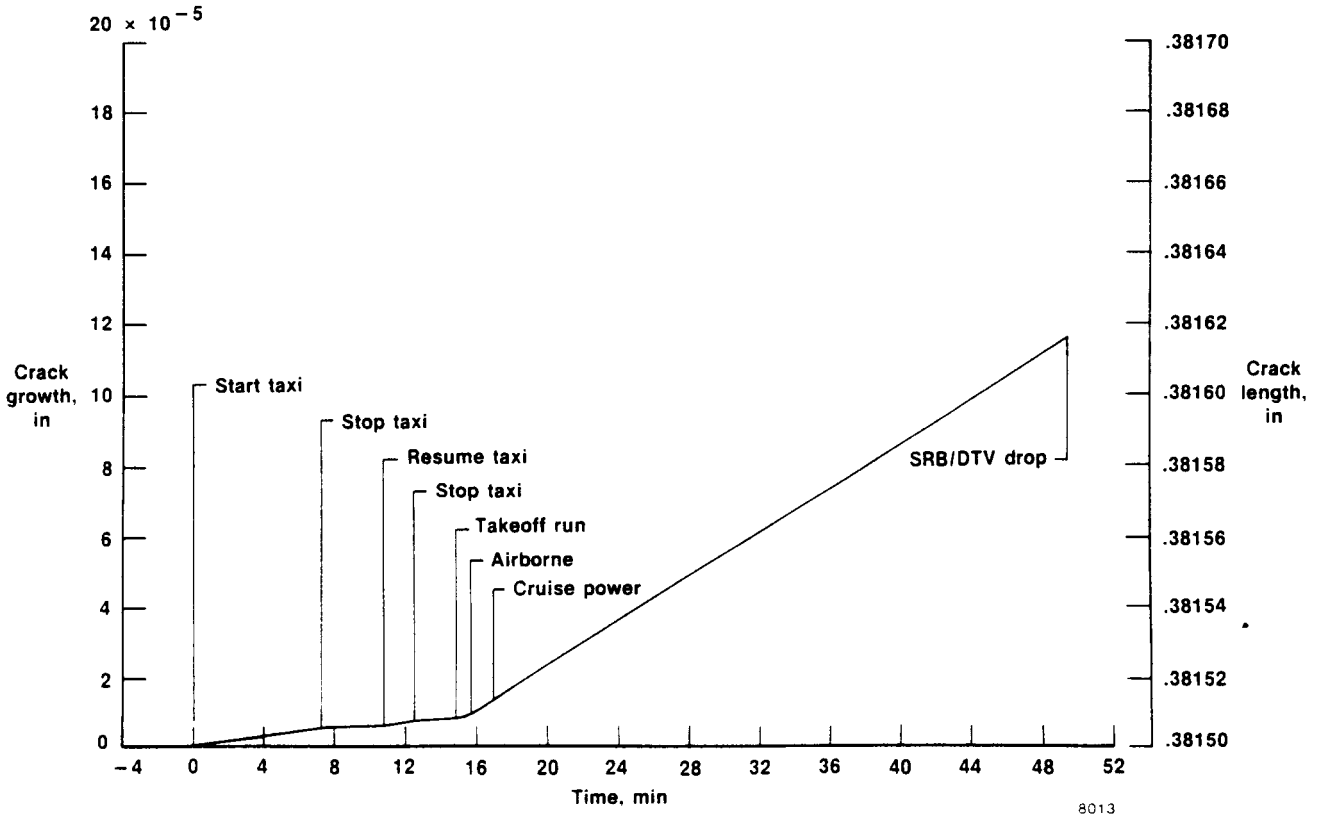

Figure 27. Crack growth curve for stress point 5 σ_5, flight 1 (indirect method).

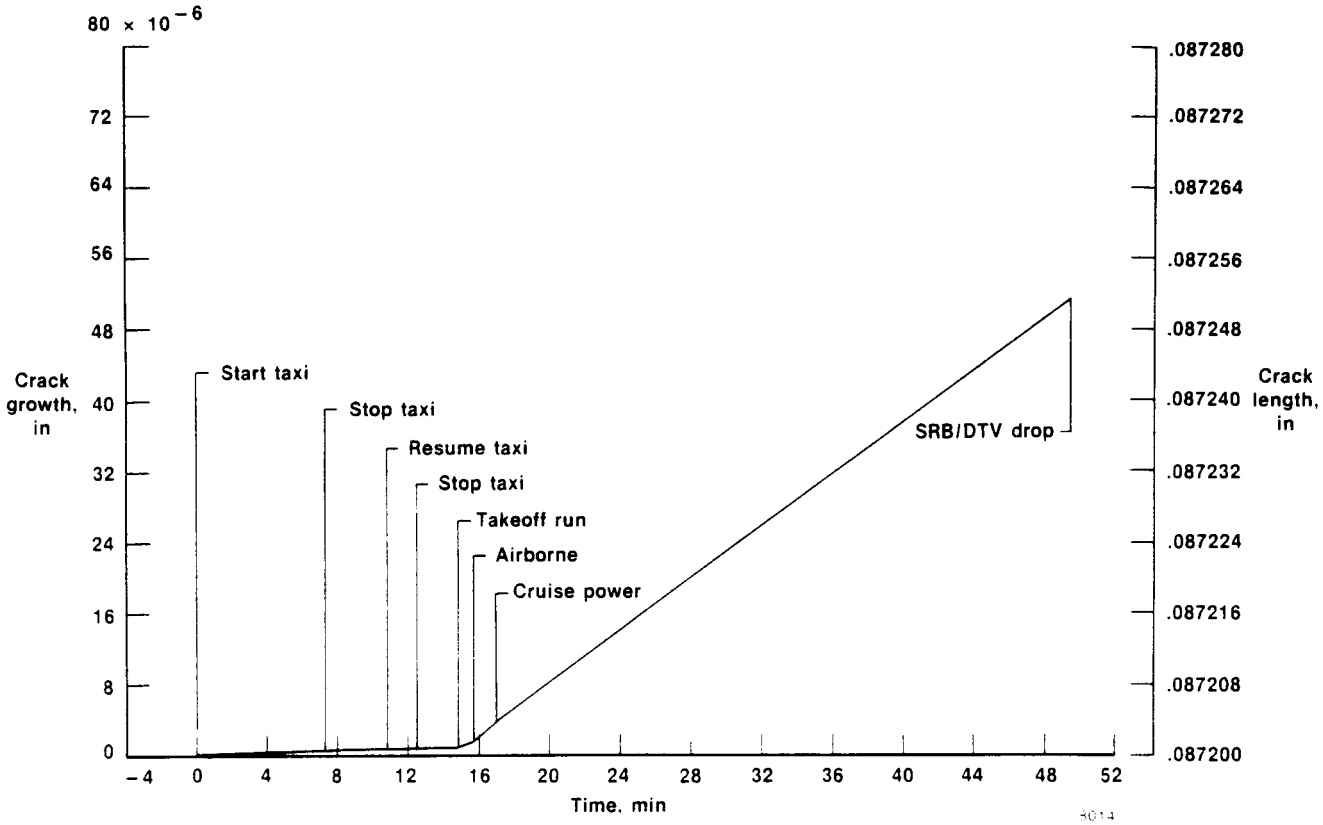

Figure 28. Crack growth curve for stress point 6 σ_6, flight 1 (indirect method).

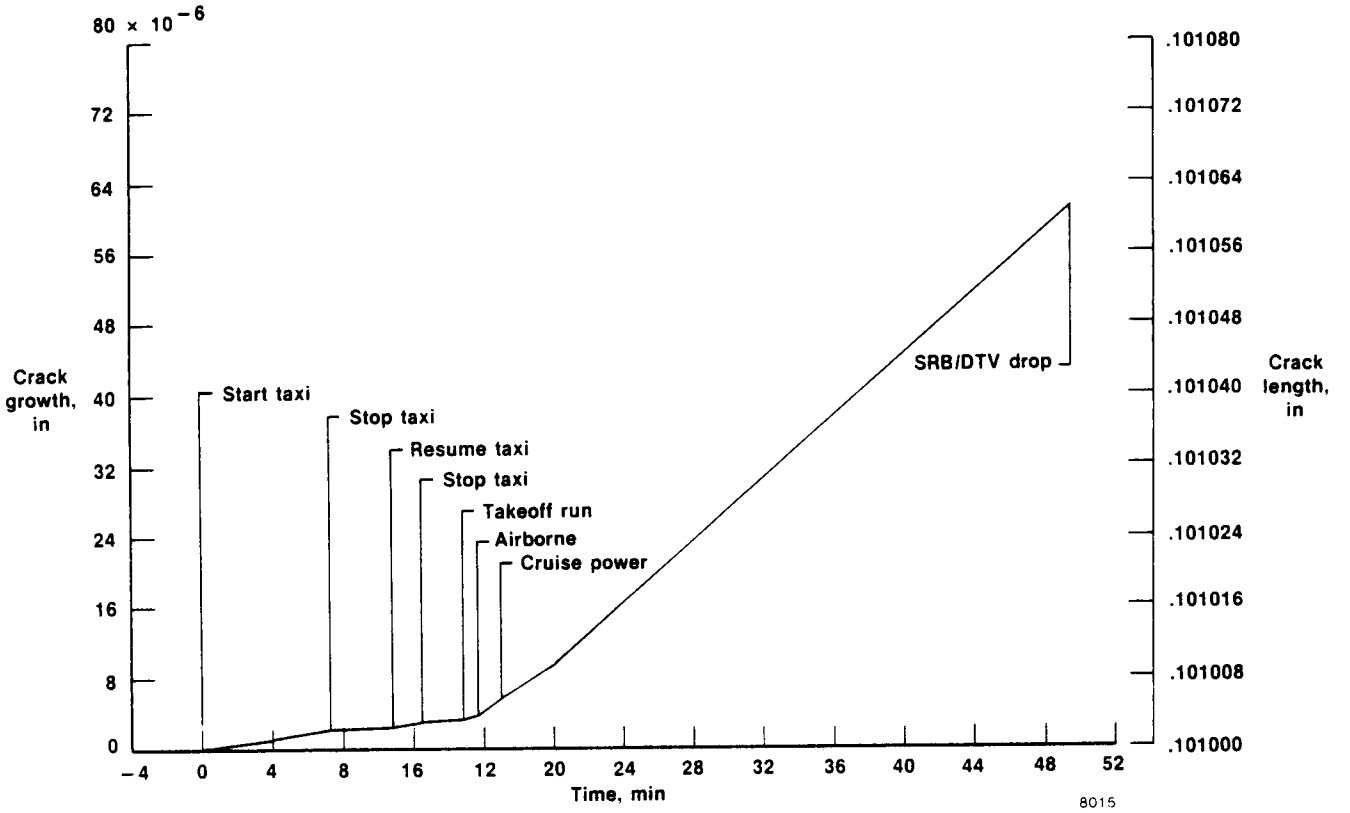

Figure 29. Crack growth curve for stress point 7 σ_7, flight 1 (indirect method).

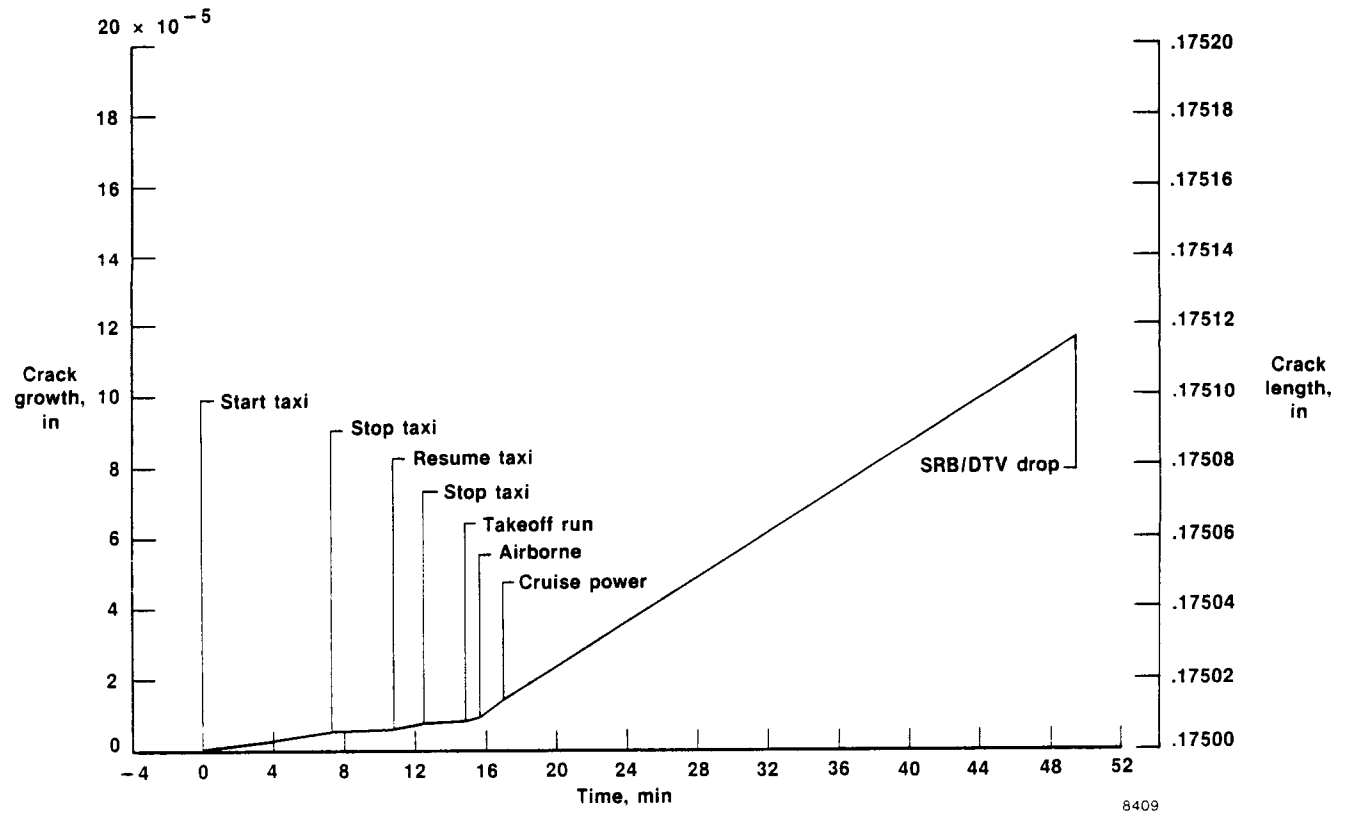

Figure 30. Crack growth curve for stress point 8 σ_8, flight 1 (indirect method).

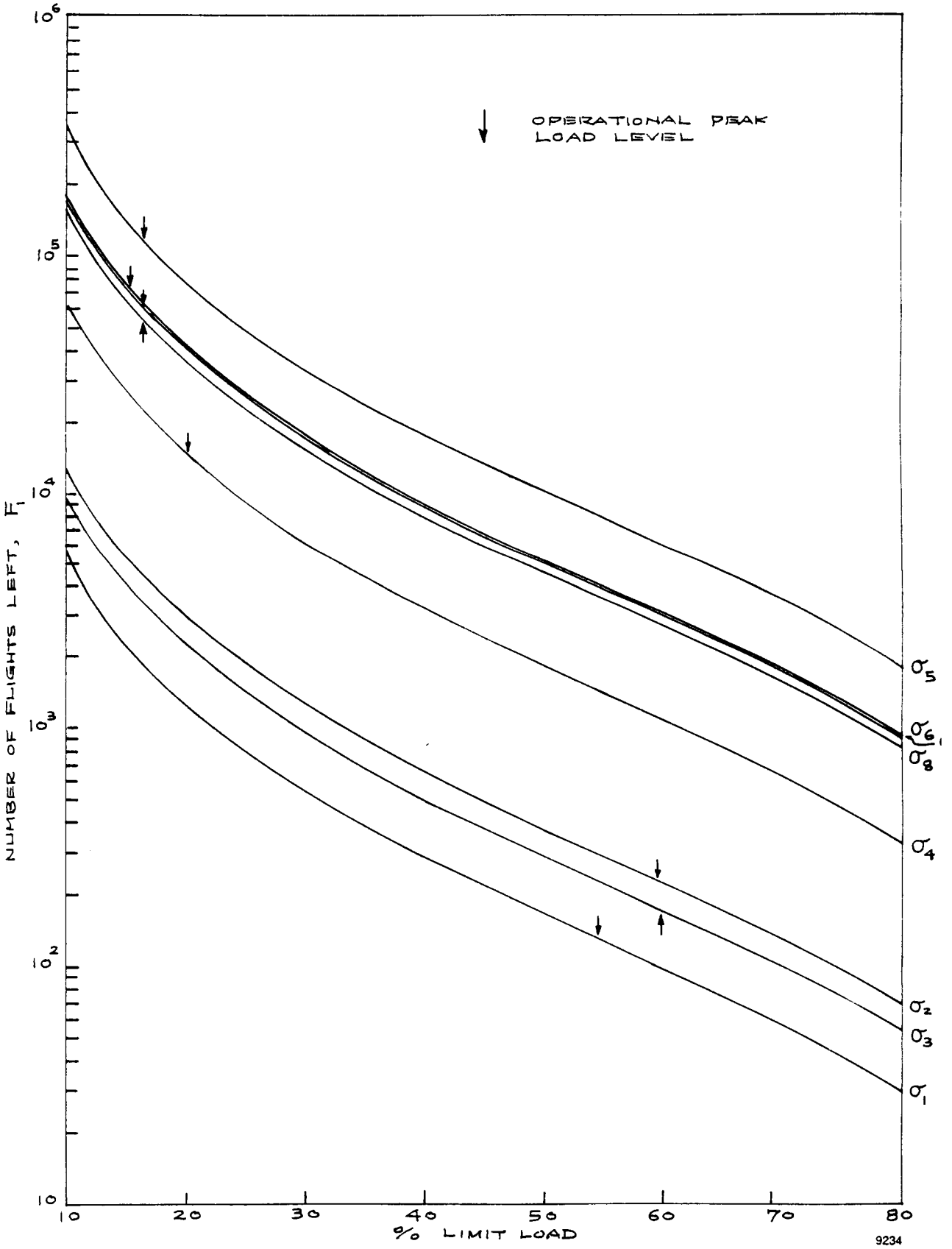

Figure 31. Number of flights left as a function of limit load, flight 1.

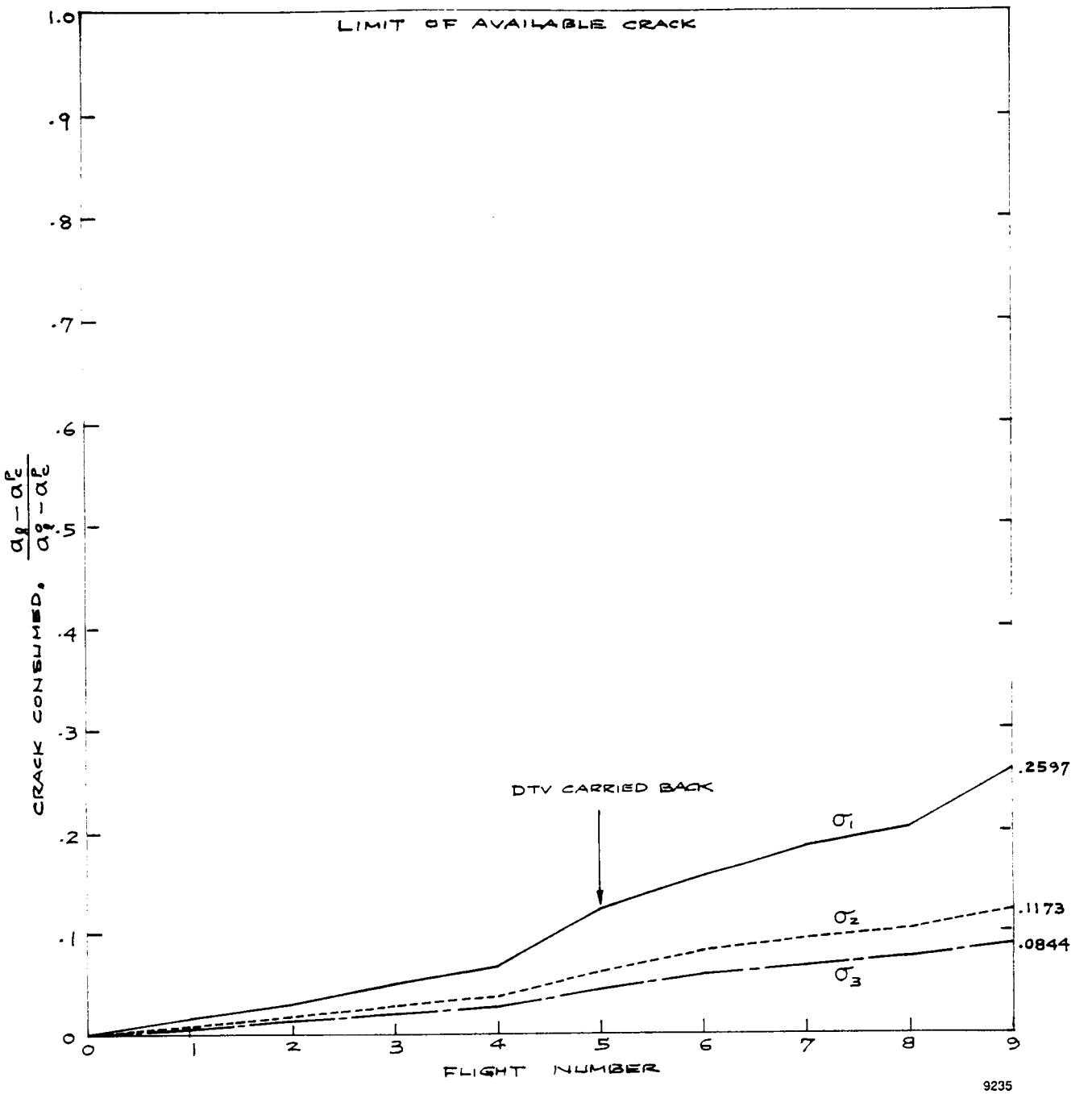

Figure 32. Portion of available cracks consumed during SRB–DTV flight tests plotted for front hook and two rear hooks.

APPENDIX A
EQUATIONS FOR B-52 PYLON HOOK LOADS

The following equations for the B-52 pylon hook loads (forces acting on hooks) were derived in accordance with the dimensions and the reference system shown in figures A-1 to A-3. All the inertia forces and moments are written in terms of inertia load factors at the SRB–DTV center of gravity (η_x, η_y, η_z, $\dot{p}$, $\dot{q}$, $\dot{r}$), respectively, where

$$\eta_x \equiv -\frac{\ddot{x}}{g}, \quad \eta_y \equiv -\frac{\ddot{y}}{g}, \quad \eta_z \equiv -\frac{\ddot{z}}{g} \tag{A-1}$$

$$\dot{p} \equiv -\frac{\ddot{\theta}x}{g}, \quad \dot{q} \equiv -\frac{\ddot{\theta}y}{g}, \quad \dot{r} \equiv -\frac{\ddot{\theta}z}{g} \tag{A-2}$$

1. Front hook vertical load V_A (positive downward)
   Considering the moment about line $CL - CR$ (see fig. A-1),

$$V_A = \frac{1}{211.0}\{9.85(-W\eta_x + P_x) + 60.8\,W(1+\eta_z) + [I_P g + W(60.8^2 + 9.85^2)]\dot{q} - P_z\bar{x} - M_y\} \tag{A-3}$$

   where W is the SRB–DTV weight; P_x aerodynamic drag force, and P_z aerodynamic lift force acting on the SRB–DTV; I_P SRB–DTV pitching moment of inertia; g gravitational acceleration; $\bar{x}$ location of aerodynamic center of pressure on x axis for SRB–DTV; and M_y aerodynamic pitching moment on SRB–DTV.

2. Front side load S_A (positive inboard)
   Considering the moment about point 0 (see fig. A-2),

$$S_A = \frac{1}{220.29}\{60.8\,W\eta_y - [I_Y g + W(60.8)^2]\dot{r} - P_y\bar{x} - M_z\} \tag{A-4}$$

   where 220.9 is the effective moment arm (defined in North American Aviation, Inc., 1963); I_Y the SRB–DTV yawing moment of inertia; P_y, aerodynamic sideforce acting on the SRB–DTV; and M_z aerodynamic yawing moment acting on the SRB–DTV.

3. Left rear hook vertical load V_{BL} (positive downward)
   Considering the moment about the line passing through point BR and parallel to the x axis (see fig. A-3),

$$V_{BL} = \frac{1}{52.874}\{26.437[W(1+\eta_z) - V_A - P_z] - 9.85(W\eta_y - P_y) - 16.3125\,S_A - [I_R g + W(26.437^2 + 12.163^2)]\dot{p}\} \tag{A-5}$$

   where I_R is the SRB–DTV rolling moment of inertia.

4. Right rear hook vertical load V_{BR} (positive downward)
   Considering the forces in the z direction (see fig. A-3),

$$V_{BR} = W(1+\eta_z) - V_{BL} - V_A - P_z \tag{A-6}$$

5. Rear side load S_{CL} (positive inboard)
   Considering the forces in the y direction (see fig. A-2),

$$S_{CL} = W\eta_y - P_y - S_A \tag{A-7}$$

6. Left drag load D_{CL} (positive rearward)
Considering the moment about the line passing through point 0 and parallel to the z axis (see fig. A-2),

$$D_{CL} = \frac{1}{1484.475}\{60.8 W\eta_y - [I_{Yg} + W(60.8)^2]\dot{r} - P_y\bar{x} - M_z\} + \frac{1}{2}(-W\eta_x + P_x) \quad \text{(A-8)}$$

where the effective moment arm 1484.475 is defined in North American Aviation, Inc. (1963).

7. Right drag load D_{CR} (positive rearward)
Considering the forces in the x direction (see fig. A-2),

$$D_{CR} = -W\eta_x + P_x - D_{CL} \quad \text{(A-9)}$$

The aerodynamic forces and moments appearing in equations (A-3) to (A-9) may be calculated from the following equations (Quade (1977), configuration 1):

$$P_x = 5.019840 \times 10^3 \bar{q} \quad \text{(A-10)}$$

$$P_y = (1.59264 - 0.521165\beta) \times 10^3 \bar{q} \quad \text{(A-11)}$$

$$P_z = (-0.220320 + 0.378778\alpha_{FUS}) \times 10^3 \bar{q} \quad \text{(A-12)}$$

$$M_y = -(3.385053 + 0.477254\alpha_{FUS}) \times 10^5 \bar{q} \quad \text{(A-13)}$$

$$M_z = (-2.085160 + 0.636736\beta) \times 10^5 \bar{q} \quad \text{(A-14)}$$

where $\bar{q}$ is dynamic pressure (lb/in.^{2}), α_{FUS} fuselage angle of attack, and β yaw angle.

For the SRB–DTV,

$$W = 48{,}143 \text{ lb} \quad \text{(A-15)}$$

$$I_{Pg} = 1.4591 \times 10^9 \text{ lb-in.}^2 \approx I_{Yg} \quad \text{(A-16)}$$

$$I_{Rg} = 4.5537 \times 10^7 \text{ lb-in.}^2 \quad \text{(A-17)}$$

Using these numerical values, the hook load equations may be written as

$$V_A = -2247.434\eta_x + 13872.485(1 + \eta_z) + 7.780750 \times 10^6 \dot{q} + 0.046682 P_x - 0.288152 P_z - 0.004739 M_y \quad \text{(A-18)}$$

$$S_A = 13287.261\eta_y - 7.431309 \times 10^6 \dot{r} - 0.275996 P_y - 0.004539 M_z \quad \text{(A-19)}$$

$$V_{BL} = 1123.717\eta_x - 13067.992\eta_y + 17135.258(1 + \eta_z) - 1.632632 \times 10^6 \dot{p} - 3.890375 \times 10^6 \dot{q} + 2.292681 \times 10^6 \dot{r} - 0.023341 P_x + 0.271448 P_y - 0.355924 P_z + 0.002370 M_y - 0.001400 M_z \quad \text{(A-20)}$$

$$V_{BR} = 1123.717\eta_x + 13067.992\eta_y + 17135.258(1 + \eta_z) + 1.632632 \times 10^6 \dot{p} - 3.890375 \times 10^6 \dot{q} - 2.292681 \times 10^6 \dot{r} - 0.023341 P_x - 0.271448 P_y - 0.355924 P_z + 0.002370 M_y + 0.001400 M_z \quad \text{(A-21)}$$

$$S_{CL} = 34855.739\eta_y - 7.431309 \times 10^6 \dot{r} - 0.724004 P_y + 0.004539 M_z \quad \text{(A-22)}$$

$$D_{CL} = -24071.50\eta_x + 1971.804\eta_y - 1.102792 \times 10^6 \dot{r} + 0.5 P_x - 0.040957 P_y - 0.000674 M_z \quad \text{(A-23)}$$

$$D_{CR} = -24071.50\eta_x - 1971.804\eta_y + 1.102792 \times 10^6 \dot{r} + 0.5 P_x + 0.040957 P_y + 0.000674 M_z \quad \text{(A-24)}$$

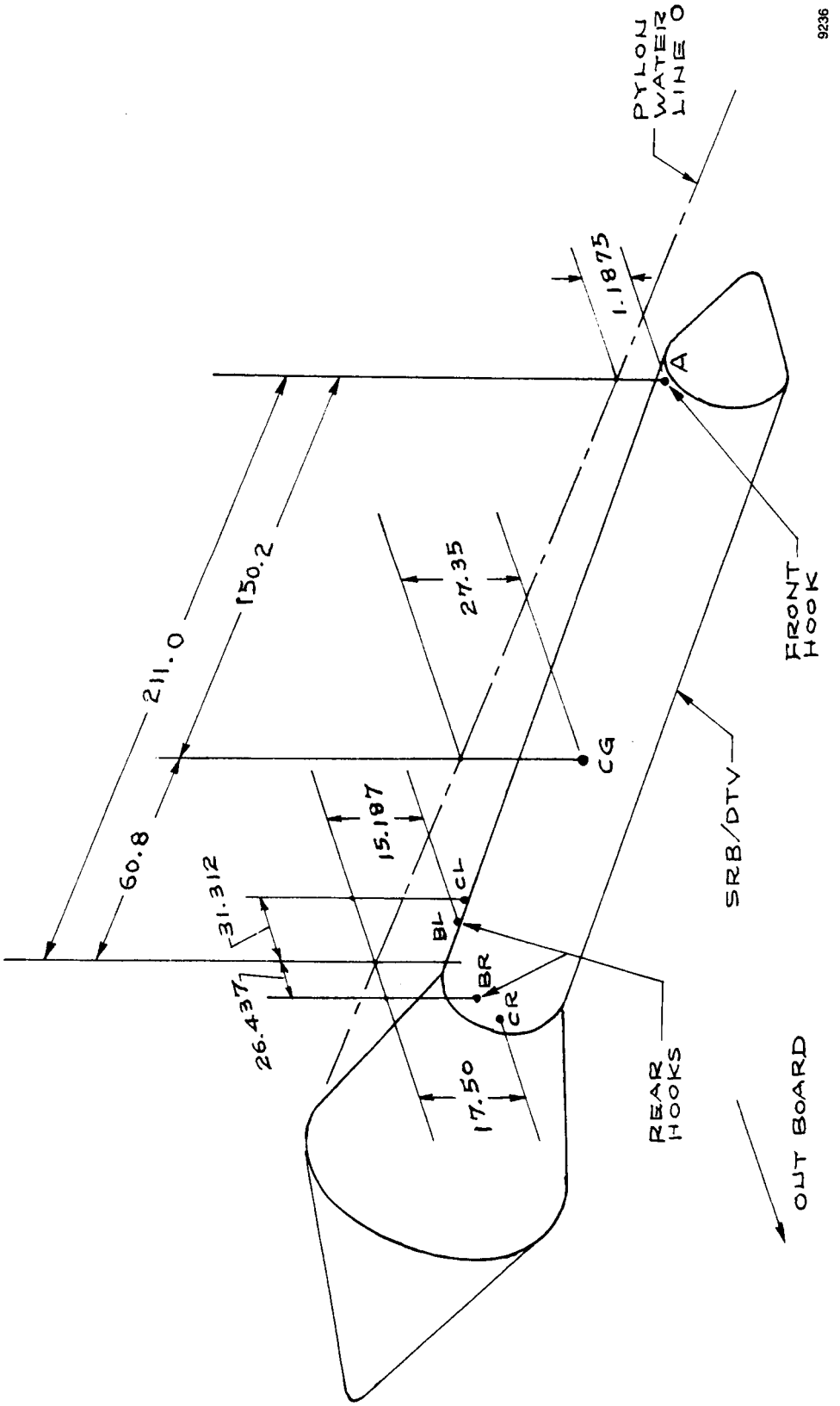

Figure A-1. Location of SRB–DTV and B-52 pylon front and rear hooks. Dimensions in inches.

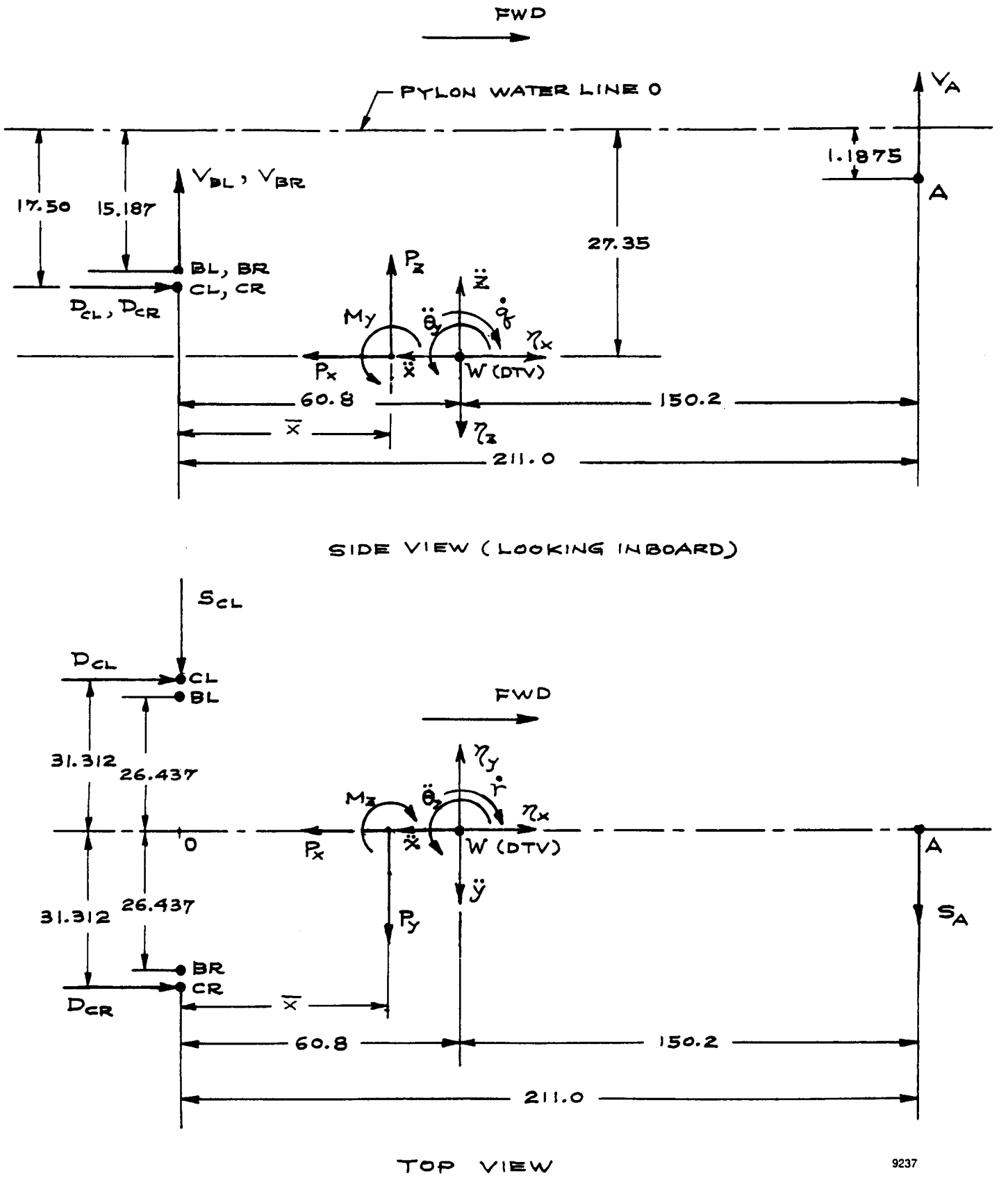

Figure A-2. B-52 pylon hook loads at SRB–DTV attach points. Dimensions in inches.

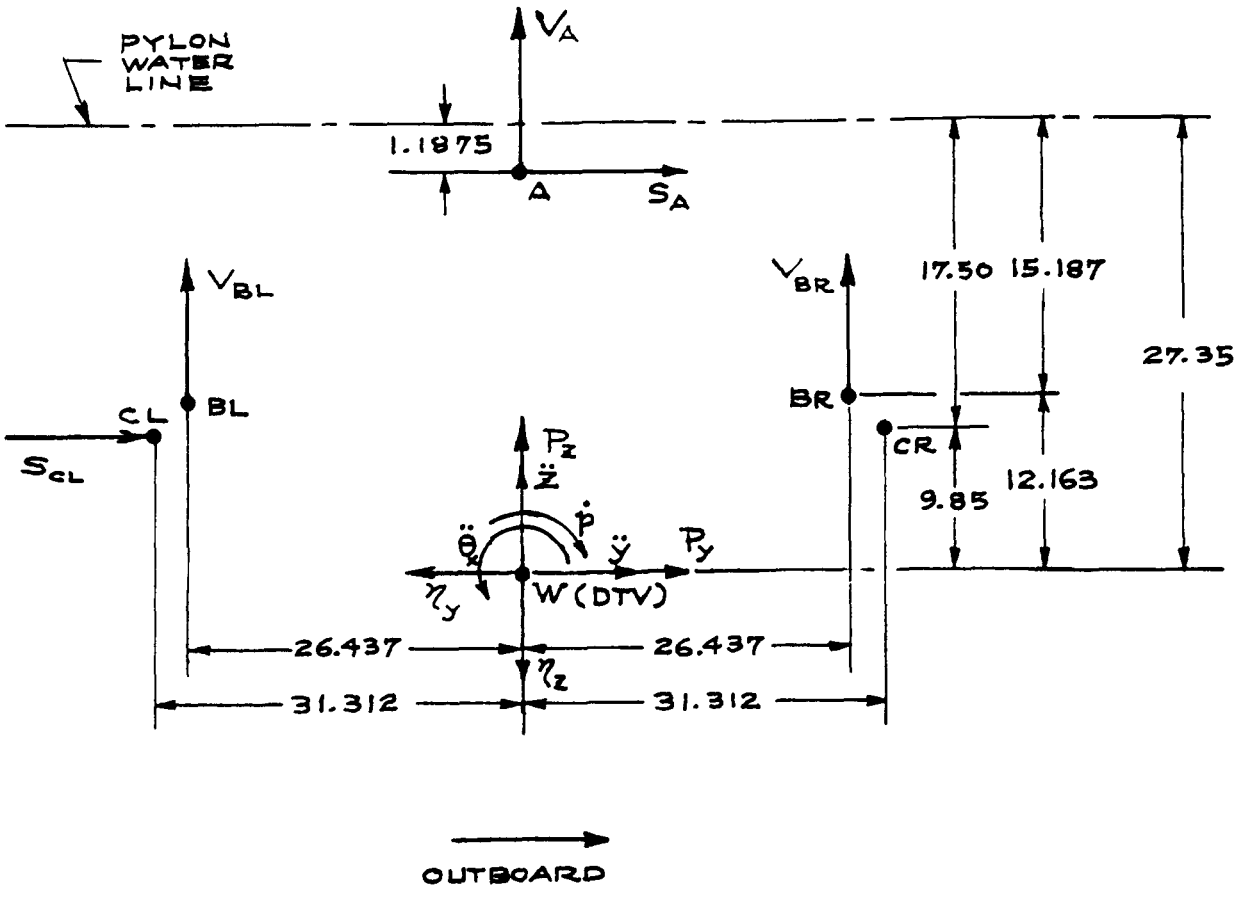

Figure A-3. B-52 pylon hook loads at SRB–DTV attach points. Dimensions in inches.

APPENDIX B
PYLON LOADS AT B-52 WING ATTACHMENT POINTS AND THE ASSOCIATED STRESS POINTS

The pylon is attached through bolts to the B-52 wing at four points (designated 1 to 4) as shown in figures 2 and B-1. The pylon vertical loads V_j (j = 1 to 4), pylon side loads S_j, (j = 1 to 4), and pylon drag loads D_3 and D_4 are expressed in terms of the hook loads and the pylon accelerations. After the pylon loads are calculated in terms of the proof load combinations given in table 2, the stress levels at the four attachment points are examined to see whether those stress points are critical in the pylon fatigue analysis.

For Case 1 of Quade (1977) (that is, 1/3 of AK_5 is carried by bolts 1 and 2), the pylon loads may be written as

$$V_1 = -0.53115150\,K_1 - 0.05045848\,K_2 - 0.18451742\,K_3 + 0.00118936\,K_4 - 0.01006607\,K_5 - 0.00363813\,K_6 \quad \text{(B-1)}$$

$$V_2 = -0.53115150\,K_1 - 0.0564432\,K_2 + 0.21055295\,K_3 - 0.00152446\,K_4 + 0.01462529\,K_5 - 0.00363813\,K_6 \quad \text{(B-2)}$$

$$V_3 = 0.02946747\,K_1 + 0.01234619\,K_2 - 0.02494134\,K_3 + 0.00163321\,K_4 - 0.02899156\,K_5 + 0.00344146\,K_6 \quad \text{(B-3)}$$

$$V_4 = 0.03233554\,K_1 + 0.05375659\,K_2 - 0.00109420\,K_3 - 0.00129812\,K_4 + 0.02443235\,K_5 + 0.00383481\,K_6 \quad \text{(B-4)}$$

$$S_1 = -0.04681422\,K_2 - 0.53124658\,K_3 + 0.00364924\,K_4 \quad \text{(B-5)}$$

$$S_2 = -0.04681422\,K_2 - 0.53124658\,K_3 + 0.00364924\,K_4 \quad \text{(B-6)}$$

$$S_3 = 0.04681422\,K_2 + 0.03124658\,K_3 - 0.00364924\,K_4 \quad \text{(B-7)}$$

$$S_4 = 0.04681422\,K_2 + 0.03124658\,K_3 - 0.00364924\,K_4$$

$$D_3 = D_4 = -0.500000\,K_2 \quad \text{(B-8)}$$

where K_j (j = 1 to 6) are functions of hook loads and pylon accelerations:

$$K_1 \equiv V_A + V_{BL} + V_{BR} + V_{CL} + V_{CR} - 1170\,\bar{\eta}_z \quad \text{(B-9)}$$

$$K_2 \equiv D_{CL} + D_{CR} - 1170\,\bar{\eta}_x \quad \text{(B-10)}$$

$$K_3 \equiv S_A + S_{CL} + 1170\,\bar{\eta}_y \quad \text{(B-11)}$$

$$K_4 \equiv -78.5\,S_A + 132.5\,S_{CL} + 1170\,\bar{\eta}_y \times 53.239 - 1170\,\bar{\eta}_x \times 13.5 + 44.812\,D_{CR} - 17.812\,D_{CL} \quad \text{(B-12)}$$

$$K_5 \equiv 25.32475\,S_A + 1170\,\bar{\eta}_y \times 9.13725 + 41.63725\,S_{CL} + 26.437(V_{BL} - V_{BR}) + 31.312(V_{CL} - V_{CR}) \quad \text{(B-13)}$$

$$K_6 \equiv 78.5\,V_A + 1170\,\bar{\eta}_z \times 53.239 - 132.5(V_{BL} + V_{BR} + V_{CL} + V_{CR}) + 1170\,\bar{\eta}_x \times 13.793 - 46.293(D_{CL} + D_{CR}) \quad \text{(B-14)}$$

where V_{CL} and V_{CR} are respectively the left and right drag shaft vertical loads and $\bar{\eta}_x$, $\bar{\eta}_y$, and $\bar{\eta}_z$ are respectively the nondimensional pylon center-of-gravity accelerations in the x, y, and z directions (see fig. B-1).

Substituting equations (B-9) to (B-14) into equations (B-1) to (B-4), the four pylon vertical loads V_j (j = 1 to 4) may be expressed as

$$V_1 = -0.816745\,V_A - 0.532803\,S_A - 0.315216\,V_{BL} + 0.096777\,D_{CL} - 0.446051\,S_{CL} + 0.217017\,V_{BR} + 0.171259\,D_{CR} - 18.460970\,\bar{\eta}_x - 249.412739\,\bar{\eta}_y + 394.829484\,\bar{\eta}_z \quad \text{(B-15)}$$

$$V_2 = -0.816745\,V_A + 0.70060487\,S_A + 0.33754952\,V_{BL} + 0.13913043\,D_{CL} + 0.61751886\,S_{CL} - 0.43574806\,V_{BR} + 31.4059356\,\bar{\eta}_x - 4.96397070\,\bar{\eta}_y + 394.829487\,\bar{\eta}_z - 0.46432619\,D_{CR} \quad \text{(B-16)}$$

$$V_3 = 0.29962208\,V_A - 0.88735234\,S_A - 1.19297585\,V_{BL} + 0.33992389\,V_{BR} - 1.015669845\,S_{CL} - 0.17605610\,D_{CL} - 0.07378191\,D_{CR} + 15.29603010\,\bar{\eta}_x - 237.3859800\,\bar{\eta}_y + 179.8935723\,\bar{\eta}_z \quad \text{(B-17)}$$

$$V_4 = 0.33386813\,V_A + 0.71955138\,S_A + 0.17064125\,V_{BL} - 1.12119483\,V_{BR} + 0.84420077\,S_{CL} - 0.10064616\,D_{CL} - 0.18193931\,D_{CR} - 21.5135856\,\bar{\eta}_x + 179.0564256\,\bar{\eta}_y + 200.4513147\,\bar{\eta}_z \quad \text{(B-18)}$$

Now, based on various combinations of the proof hook loads given in table 2, the magnitudes of V_j (j = 1 to 4) induced by the proof loads will be examined. For the proof tests, $\bar{\eta}_x = \bar{\eta}_y = \bar{\eta}_z = 0$ since the proof tests are static in nature.

Maneuver 1.

—For maneuver 1, table 2 gives

$$V_A = 35{,}019 \text{ lb}, \; V_{BL} = 29{,}708 \text{ lb}, \; V_{BR} = 31{,}437 \text{ lb}$$

$$S_A = 1684 \text{ lb}, \; S_{CL} = 5369 \text{ lb}$$

$$D_{CL} = 25{,}660 \text{ lb}, \; D_{CR} = 26{,}113 \text{ lb}$$

Using those values, equations (B-15) to (B-18) yield

$$V_1 = -27{,}165 \text{ lb} \quad \text{(B-19)}$$

$$V_2 = -24{,}544 \text{ lb} \quad \text{(B-20)}$$

$$V_3 = -21{,}943 \text{ lb} \quad \text{(B-21)}$$

$$V_4 = -20{,}246 \text{ lb} \quad \text{(B-22)}$$

Maneuver 2.

—For maneuver 2, table 2 gives

$$V_A = 35{,}603 \text{ lb}, \; V_{BL} = 36{,}754 \text{ lb}, \; V_{BR} = 36{,}088 \text{ lb}$$

$$S_A = S_{CL} = D_{CL} = D_{CR} = 0$$

Using those values, equations (B-15) to (B-18) yield

$$V_1 = -32{,}832 \text{ lb (maximum for } V_1) \quad \text{(B-23)}$$

$$V_2 = -32{,}398 \text{ lb} \quad \text{(B-24)}$$

$$V_3 = -20{,}912 \text{ lb} \quad \text{(B-25)}$$

$$V_4 = -22{,}303 \text{ lb} \quad \text{(B-26)}$$

Maneuver 3.

—For maneuver 3, table 2 gives

$$V_A = 27{,}416 \text{ lb}, \; V_{BL} = 32{,}859 \text{ lb}, \; V_{BR} = 42{,}756 \text{ lb}$$

$$S_A = 3995 \text{ lb}, \; S_{CL} = -10{,}099 \text{ lb}, \; D_{CL} = D_{CR} = 0$$

Using those values, equations (B-15) to (B-18) yield

$$V_1 = -21{,}095 \text{ lb} \tag{B-27}$$

$$V_2 = -33{,}369 \text{ lb} \tag{B-28}$$

$$V_3 = -9739 \text{ lb} \tag{B-29}$$

$$V_4 = -38{,}828 \text{ lb (maximum for } V_4) \tag{B-30}$$

Maneuver 4.

—For maneuver 4, table 2 gives

$$V_A = 27{,}415 \text{ lb}, \; V_{BL} = 42{,}871 \text{ lb}, \; V_{BR} = 32{,}744 \text{ lb}$$

$$S_A = 3995 \text{ lb}, \; S_{CL} = 10{,}099 \text{ lb}$$

$$D_{CL} = D_{CR} = 0$$

Using those values, equations (B-15) to (B-18) yield

$$V_1 = -30{,}973 \text{ lb} \tag{B-31}$$

$$V_2 = -13{,}712 \text{ lb} \tag{B-32}$$

$$V_3 = -45{,}602 \text{ lb (maximum for } V_3) \tag{B-33}$$

$$V_4 = -8844 \text{ lb} \tag{B-34}$$

Maneuver 5.

—For maneuver 5, table 2 gives

$$V_A = 29{,}728 \text{ lb}, \; V_{BL} = 31{,}806 \text{ lb}, \; V_{BR} = 30{,}991 \text{ lb}$$

$$S_A = 0, \; S_{CL} = -8210 \text{ lb}$$

$$D_{CL} = 32{,}080 \text{ lb}, \; D_{CR} = 30{,}060 \text{ lb}$$

Using those values, equations (B-15) to (B-18) yield

$$V_1 = -20{,}229 \text{ lb} \tag{B-35}$$

$$V_2 = -41{,}634 \text{ lb (maximum for } V_2) \tag{B-36}$$

$$V_3 = -18{,}029 \text{ lb} \tag{B-37}$$

$$V_4 = -35{,}023 \text{ lb} \tag{B-38}$$

In the preceding equations, the negative signs in front of V_j (j = 1 to 4) denote that the pylon reaction forces V_j are pointing downward, giving tension to the attachment bolts.

Stress Points

The four stress points σ_{V1}, σ_{V2}, σ_{V3}, and σ_{V4} are selected at the surfaces of four attachment bolts 1, 2, 3, and 4, respectively (fig. B-1). In the calculations of the initial fictitious surface crack sizes at the stress points, the peak absolute values of V_j (j = 1 to 4) will be used. They are (see eqs. (B-23), (B-36), (B-33), and (B-30))

$$V_1 = 32{,}832 \text{ lb} \tag{B-39}$$

$$V_2 = 41{,}634 \text{ lb} \tag{B-40}$$

$$V_3 = 45{,}602 \text{ lb} \tag{B-41}$$

$$V_4 = 38{,}828 \text{ lb} \tag{B-42}$$

The four attachment bolts each have a diameter of 1 in., and the cross-sectional area of each attachment bolt is $A_B = \pi(0.5)^2 = 0.785$ in.^{2} Thus, the stresses σ_{V1} to σ_{V4} may be calculated as

$$\sigma_{V1} = \frac{V_1}{A_B} = \frac{32{,}832}{0.785} = 41.824 \text{ ksi} \tag{B-43}$$

$$\sigma_{V2} = \frac{V_2}{A_B} = \frac{41{,}634}{0.785} = 53.037 \text{ ksi} \tag{B-44}$$

$$\sigma_{V3} = \frac{V_3}{A_B} = \frac{45{,}602}{0.785} = 58.092 \text{ ksi} \tag{B-45}$$

$$\sigma_{V4} = \frac{V_4}{A_B} = \frac{38{,}828}{0.785} = 49.462 \text{ ksi} \tag{B-46}$$

The four attachment bolts are NAS636AH 90 type bolts made of 4340 steel and heat treated for 180 to 200-ksi tensile strength. From table 1, the critical stress intensity factor K_I for the four attachment bolts will be $K_I = 105 \text{ ksi}\sqrt{\text{in.}}$ Taking $Q = 1.45$ (since $0 < \sigma_\infty/\sigma_y < 0.6$), $M_K = 1$, $A = 1.12$, the initial fictitious surface crack sizes a^p_{V1}, a^p_{V2}, a^p_{V3}, and a^p_{V4} associated with the four stress points σ_{V1}, σ_{V2}, σ_{V3}, and σ_{V4} may be calculated from equation (1) as

$$a^p_{V1} = \frac{Q}{\pi}\left(\frac{K_I}{AM_K\sigma^p_{V1}}\right)^2 = \frac{1.45}{\pi}\left(\frac{105}{1.12 \times 1 \times 41.824}\right)^2 = 2.319 \text{ in.} \tag{B-47}$$

$$a^p_{V2} = \frac{Q}{\pi}\left(\frac{K_I}{AM_K\sigma^p_{V2}}\right)^2 = \frac{1.45}{\pi}\left(\frac{105}{1.12 \times 1 \times 53.037}\right)^2 = 1.442 \text{ in.} \tag{B-48}$$

$$a^p_{V3} = \frac{Q}{\pi}\left(\frac{K_I}{AM_K\sigma^p_{V3}}\right)^2 = \frac{1.45}{\pi}\left(\frac{105}{1.12 \times 1 \times 58.092}\right)^2 = 1.202 \text{ in.} \tag{B-49}$$

$$a^p_{V4} = \frac{Q}{\pi}\left(\frac{K_I}{AM_K\sigma^p_{V4}}\right)^2 = \frac{1.45}{\pi}\left(\frac{105}{1.12 \times 1 \times 49.462}\right)^2 = 1.658 \text{ in.} \tag{B-50}$$

Those crack sizes are much greater than the diameter of the attachment bolts (1 in.) because the stress levels σ^p_{V1} to σ^p_{V4} are relatively low. Thus, the four attachment bolts are not critical and will not be used in the pylon fatigue analysis.

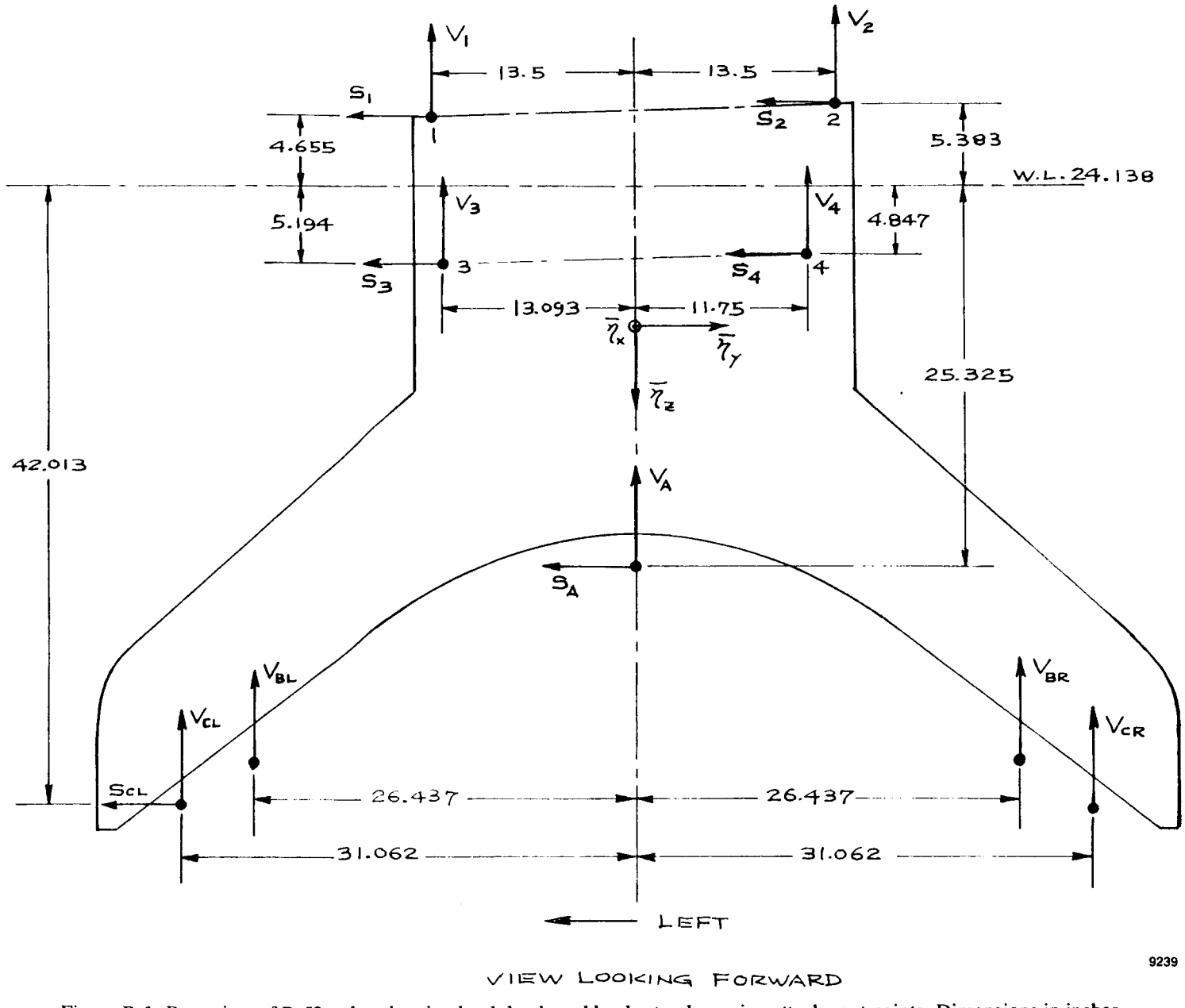

Figure B-1. Rear view of B-52 pylon showing hook loads and loads at pylon–wing attachment points. Dimensions in inches.

APPENDIX C
COMPUTER PROGRAMS USED IN THE CALCULATIONS OF σ_i AND CRACK GROWTH

Crack Growth Calculation Overview

Background.

A method of testing various vehicles at NASA is to carry the test specimen aloft under the wing of a B-52 carrier aircraft and release it to descend while transmitting measurements to ground based receivers. One such item is the SRB–DTV, which is used to develop improved parachute designs. While under the B-52 wing the specimen is supported by three hooks (one forward and two aft) and several sway braces and drag pins, all parts of a pylon structure. To determine the life expectancy of these parts, the stresses at the critical locations of each are computed from the accelerometers and strain gages on the payload. These stresses are then used to compute a theoretical crack length increase during taxi, takeoff, and flight up to the point of payload release.

Problems.

Certain problems must be taken into account when calculating crack growth.

1. Physical placement of the strain gages and the accelerometers is on the test specimen, not on the pylon, and they are separated by some distance and through flexible structures from the stress sites on the pylon. Rotation and translation calculations are therefore required to compute the stress at the desired location.

2. Vibration, especially in the accelerometer data, creates many false peaks that must be removed by heavy filtering.

3. Data loss occurs from various causes, but the greatest losses are believed to be caused by interference by parts of the B-52 aircraft when they come between the antenna on the payload and the ground based radio receivers. One loss occurs at the beginning of most flights between engine start and when the aircraft has taxied to a point out of the "radio shadow" of the rooftop antenna. Losses of 0.1 sec or more are compensated for by extrapolation.

4. Data file size is such that a full flight cannot be processed in the computer at one time. Flight durations are approximately 45 min (or more), the sampling rate is 1000 samples/sec and 68 parameters are recorded, creating more than 183 million computer words, not counting ancillary information such as parameter descriptions, calibrations, and tables of dropouts. Processing the flight tape requires breaking the flight into several files (a minimum of two and a maximum of seven have been used to date).

Procedure.

General purpose programs: A series of general-purpose programs use calibration, configuration, and setup files to convert the raw pulse code modulation (PCM) data into a flight database (FLIDAB) file in engineering units (fig. C-1). All these standard processes are shown as one in figure C-2 in the block labeled PROGDAB PROGRAMS.

Special purpose programs: Five special-purpose programs were specifically written to calculate and display crack growth. Because of the developmental nature of the programming requirements, some of the special programs are loaded from cards and compiled for each pass.

1. SRBHOOK uses the general-purpose DABIR subroutine to extract the required data channels and then applies translation, rotation, and moment arm transformations and low-pass filtering to determine the stress at each of the desired locations. Input to SRBHOOK controls the part of the flight file attached and is used to eliminate large areas of data losses. Each of the attached segments is put into a separate file, identified as SIGMA files in figure C-2.
2. The THIN program attaches the SIGMA files one at a time and recatalogs them after reducing the number of data points and interpolating missing data sections.
3. CONCAT attaches all the THIN files for a particular flight and concatenates them into a single file.
4. CCLAMP then performs the crack length calculations and computes the number of flights remaining on each part. Two files are created: One file contains the crack length for each site at specified time intervals during the flight, the other file is a list of start and stop times for each segment of the flight where data were filled in by extrapolation. These are identified as CRACK LENGTH and DROPOUTLIST files in figure C-2.
5. Plots are created by CPLOT, which utilizes the CRACK LENGTH and DROPOUTLIST files to show the progression of the cracks at periodic intervals during the flight and to identify extrapolated sections.

File naming convention: A seven-character file name is used in which each character provides significant information. A typical file name, S0705T3, would indicate S series, flight 07 (first since modification of critical parts), 0 suffix created by the THIN program, and third segment of the flight.

1. The first character indicates a computation series. All data for this report were generated in the S series.
2. The second and third characters constitute a two-digit flight-number code. The flight numbers used in this report are obtained by subtracting 6 from this number (the total number since this series of flights started).
3. The fourth character is zero for most flights but is used as a suffix when two operations have the same flight number (for example, flights 11 and 11A).
4. The fifth character indicates the filter cutoff frequency to identify files produced as a result of experimentation with other frequencies.
5. The sixth and seventh characters identify the program that generated the file, as in the following tabulation:

Sn	SRBHOOK
Tn	THIN
CX	CONCAT
CL	CCLAMP cracklengths
DL	CCLAMP dropout list

6. The seventh character is used by SRBHOOK and THIN to identify the section of the flight represented (that is, 1 denote the first part, 2 the second part, . . . , A the 10th, B the 11th, and so on).

Program running time: The following estimated program running times on the CDC Cyber 170-730 (Control Data Corp., Minneapolis, Minnesota), for each minute of flight are given in the following:

Program	Min CPU time	Min of flight
SRBHOOK	7.75	1
THIN	1.5	1
CONCAT	0.1	1
CCLAMP	3.5	1
CPLOT	— — —[a]	

[a]Running time is more dependent on the amount of annotation than on flight time. CPU time has varied between 30 and 50 sec.

SRBHOOK Program

SRBHOOK is a program used to read nine parameters from an SRB flight data base (FLIDAB), to filter these data, and then to compute several stresses σ_i, which are stored on a permanent file. This file is used to compute hook crack growth through the THIN and CCLAMP programs. The nine parameters read from the FLIDAB are

1. MO1, X-axis acceleration in g;
2. MO2, Y-axis acceleration in g;
3. MO3, Z-axis acceleration in g;
4. MO4, roll rate in deg/sec;
5. MO5, pitch rate in deg/sec;
6. MO6, yaw rate in deg/sec;
7. M56, forward hook load in kips;
8. M67, aft hook load in kips; and
9. M69, aft hook load in kips.

Card input to SRBHOOK is in the form of three name lists:

1. NAMELIST /SRBNAM/ NSIGMA, BREAK, IST, IET

   NSIGMA is the number of stresses σ_i to be computed (eight were computed so far),

   BREAK is break frequency (in Hertz) used with the fourth-order low-pass Butterworth filter used in SRBHOOK (a value of 5 was usually used),

   IST is requested FLIDAB start time (hr,min,sec,msec), and

   IET is requested FLIDAB end time (hr,min,sec,msec).

2. NAMELIST /TABLE1/ RA,RB,RC,RD,RE,RF

   These are seven-element arrays of coefficients used to compute seven hook loads R_i as shown in table C-1.

3. NAMELIST /TABLE2/ SK,SL,SM,SN,SP,SQ,SR

These are eight-element arrays of coefficients used to compute eight stresses σ_i as shown in table C-2.

The SRBHOOK program begins by reading the three name lists. Flight data procession system subroutines DABOP and DABIR are then called to extract the nine FLIDAB parameter values at each time point of the desired interval. The data are extracted from the FLIDAB at a rate of 1,000 samples/sec. Not all time points will be available, however, because of data transmission loss from the SRB–DTV. (Data that are not good, such as those that go beyond the calibration range or that result from a synchronization problem, will be rejected and data from the next time point will be read. Also, if MO4, MO5, or MO6 have changed more than 5 deg/sec from the previous time point or if M56, M67, or M69 have changed more than 3 kip from the previous time point, then those data will be thrown out and the next time point of data will be read.)

The data are then run through a fourth-order digital Butterworth low-pass filter whose desired break frequency is specified on the SRBNAM name list card. Subroutine COEF is used to compute coefficients for the filter. The values of PDOT, QDOT, and RDOT ($\dot{p}$, $\dot{q}$, and $\dot{r}$) in deg/sec^2-g are then computed between two consecutive time points from filtered MO4, MO5, and MO6 values; PDOT, QDOT, and RDOT are often filtered themselves. Accelerometer corrections are then applied to the filtered values of the three accelerometers (MO1, MO2, MO3) as follows:

$$\text{MO1c} = \text{MO1}/\cos(2.75 \times 0.017452)$$
$$\text{MO2c} = \text{MO2} - 149.12\,\text{RDT}$$
$$\text{MO3c} = [\text{MO3} - 149.12\,\text{PDOT} - 2.0\,\text{QDOT}]/\cos(2.75 \times 0.017452)$$

The seven hook loads R_i are then computed as shown in table C-1. Finally, the eight stresses σ_i are computed as shown in table C-2. (Filtered M56, M67, and M69 values, however, were substituted for V_A, V_{BL}, and V_{BR} in the equation.) Time in total seconds and the eight stresses are then stored on the permanent file. Another time point of data is then processed, and the process continues until the interval has been completed.

The job card setup for running SRBHOOK is as follows:

```
Jobname, Tseconds.
USER(SRB1,FDPS)
CHARGE(45,37)
DEFINE(TAPE4=dfpfn/CT=S,M=R)
  dfpfn = pfn of data file of stresses to be created by SRBHOOK
SWITCH(3)
GETPF(LGO=SRBHOOK)
GETPF(PROCFIL/UN=CSDO)
BEGIN(TASK,, LIST, pname)
  pname = procedure name of the desired FLIDAB
7/8/9     card                          (end-of-record card)
SRB1nnn
  nnn = SRB flight number of desired FLIDAB

$SRBNAM ..................................................................... $
$TABLE1 ..................................................................... $
$TABLE2 ..................................................................... $
6/7/8/9    card                                    (end-of-input card)
```

SRBHOOK

Revised for Flights 8 and 9

As previously mentioned, during the entire SRB–DTV flight-test program there were only three channels available for recording the strain gage outputs. From flight 1 up to flight 7 the three available channels were used to measure V_A, V_{BL}, and V_{BR} (S_A, D_{CL}, D_{CR}, and S_{CL} were not measured). In the original SRBHOOK program the measured hook loads V_A, V_{BL}, and V_{BR} were used directly to compute some of the stresses. The nonmeasured hook loads S_A, D_{CL}, D_{CR}, and S_{CL}, however, were approximated using accelerometer data, and then the other stresses were computed.

For flights 8 and 9, the two channels used for measuring V_{BL} and V_{BR} were switched to measure D_{CL} and S_{CL} instead. These measured values of D_{CL} and S_{CL} were found to be significantly different from the values approximated from accelerometer data on flights 1 to 7. It was obvious that the accelerometer outputs were just too poor and unreliable to use for approximating hook loads. Therefore, it was decided to revise the SRBHOOK program for flights 8 and 9 to read only M56 (forward hook vertical load), $DSSCL$ (left rear hook side load), and $DSDCL$ (left rear hook drag load) and compute the stresses that were a function of them:

$$\sigma_1 = 7.3522\,M56$$

$$\sigma_4 = 0.9688\,(-0.054514\,DSDCL \times DSDCL + 6.3481\,DSDCL) + 0.2479\,(-0.3436\,DSSCL \times DSSCL - 9.9653\,DSSCL)$$

$$\sigma_5 = 2.18675\,DSDCL$$

$$\sigma_6 = 7.1420\,(0.9688\,DSDCL - 0.2479\,DSSCL)$$

$$\sigma_7 = 7.3055\,DSDCL$$

$$\sigma_8 = 4.2141\,DSDCL$$

A list of the revised SRBHOOK program is included in the following pages.

THIN Program

I. Functions

A. Reduces the data sampling rate from 1,000 samples/sec to any specified number per second (50 samples/sec is currently used).

B. Interpolates new values where needed.

C. Provides capability to write file header records for later identification, verification, or documentation.

D. Provides a listing of all data dropouts, their duration, first and last values, and sums of the time loss in two categories:

1. Total time loss
2. Total of time losses greater than 1 sec.

E. Echoes input control cards and file parameter identifications and comments.

F. Lists any requested amount of data from the input file.

G. Lists any requested amount of data as they go to the output file.

II. Program organization

A. After declarations and initialization, the control cards are read and written out to the printer.

B. The header cards are then read, written on TAPE3, and printed. The page headings are written to the print files.

C. To separate data for the three listings (input from TAPE4, output to TAPE3, and dropouts), three discrete print files are created: (1) the default printer for INPUT, (2) TAPE6 for output, and (3) TAPE7 for the dropout list. Appropriate headers are written on the three files at this point.

D. Because of the requirement to have two sets of data in memory whenever interpolation is required, the processing is done with two nearly identical sections of code working in a flip-flop mode and a special first data record section to initialize the first locations.

E. In each of these sections TX (time expected) is compared with T. In this record T stands for the time found on the last data record read in and may be either T1 or T2, depending on which section is processing the record. When TX is greater than T, another record is read and tested. If TX is equal to T, the record associated with T is written to the output tape and TX is increased by DTX (the desired delta time between output records). When TX is less than T, new values are interpolated for each parameter at each value of TX + N $\times$ DTX that occurs between T and $T - 1$. The value TX is then incremented by DTX. During this procedure tests are being made to determine whether the input or output records, or both, are to be printed and when the limit time or end of file has been reached.

F. On end of file or time limit, appropriate comments are written to the print files along with the final values and the summations.

III. Input

A. TAPE4 (created by the SRBHOOK program)

B. Control cards (NAMELIST format)

```
$CCDS             Identifies the group
NPARMS            Integer number of parameters on file
NCRDSP            Integer number of identification lines per parameter
NCMTS             Integer number of comment lines
NSKIP             Integer number of unused parameters
TSTART            Real time (sec.)  to start processing
TSTOP             Real time (sec.)  to stop processing
DTX               Real time (sec.)  between output data parameters
PTLIM             Real limit time for printing input data
PNLIM             Integer limit count for printing input data
NDLIM             Integer limit count for printing output data
NSIGMA            Integer number of parameters on file
$END              Group termination
Parameter 1 ID    1 - NCRDSP identifying a parameter
Parameter 2 ID    1 - NCRDSP identifying a parameter
          :
         NPARMS
Comments          1 - NCMTS comment cards
```

IV. Output

A. FILE (TAPE3)

1. Header format

Record	Column	Mnemonic	Type	Description
1	1 to 80	TITLE	Character	– – –
2	1 to 10	NCHANS	Integer	Number of data parameters
2	11 to 20	NCRDSP	Integer	Number of lines/parameter
2	21 to 30	NCMTS	Integer	Number of comment lines
3	1 to 80	CARD	Character	NCHANS sets of NCRDSP lines each describing the data channels
⋮				
2+NCRDS × NCHANS				
3+NCRDS × NCHANS				
⋮				
2+NCRDS × NCHANS +NCMTS				
	1 to 80	CARD	Character	Comments

2. Data format

Record	Heading
1	TIME
2	SIGMA 1
3	SIGMA 2
⋮	⋮
9	SIGMA 8

B. LISTING

1. Echo of the card input data
2. Header records from TAPE9
3. First PNLIM points
4. Last record from TAPE4
5. Last record output to TAPE3
6. Postmortem dump of all variables
7. First NDLIM points going to TAPE3
8. TIME and sigmas spanning data dropouts
9. Sum of all dropout periods
10. Sum of dropout periods greater than 1 sec

V. Job setup

```
THIN,T10000.                    Job name and time estimate
USER(user name,user ID)
CHARGE(charge numbers)
MAP,ON.                         Optional
FTN5(ET,LO,DB=PMD)              Compile with cross
                                references
NOEXIT.                         Prevents abort on forced
                                dump
ATTACH(TAPE4=input file         Gets input file
name)
LGO.                            Starts program operation
REPPF(TAPE3= output file        Names and catalogs the
name)                           output
NOEXIT.                         Prevents an error condition
                                from aborting the following
                                commands
REWIND,TAPE6,TAPE7.             Commands to move the
COPYCF,TAPE6,OUTPUT.            temporary output files to
COPYCF,TAPE7,OUTPUT.            the print file
7/8/9                           Separator
   PROGRAM DECK
7/8/9                           Separator
   CONTROL CARDS
   HEADER DATA CARDS
6/7/8/9                         End-of-job indicator
```

CONCAT Program

I. Functions

A. Concatenates files containing separate parts of a flight into a single file.

B. Places all the header records from the various files onto the front of the first file on the output tape.

C. Will remove any number of "bad" initial values that get through the filter algorithm during the startup process.

D. Can be made to print any distance into each of the files for verification.

II. Program organization

A. The PARAMETER statement is used to assign values to the constants which control the program's operation.

B. CHARACTER strings and REAL arrays are defined in the next group of statements.

C. The loop beginning with DO 35 reads the header records from each input file, prints them, and then writes them to the output file, TAPE10. TAPE9 is used as an intermediate transformation medium.

D. The section between DO 37 and 37 CONTINUE eliminates the first FP data values from the first file (that is, the first flight segment).

E. DO 45 through 45 CONTINUE is the main data copy algorithm and logically includes the section from statement number 62 to the end of the program.

1. In the DO 45 statement N is progressively incremented by 1 from 11 through 10 + NTS and specifies the file being read from.
2. Statements 38 through 39 read from tape unit N, increment the input and output counters (NIN and NOUT), print (if the number of inputs is within the range specified by the print control parameter NPP), and write the data out to TAPE10.
3. On sensing an end of file, processing commences at statement 62 where the last data scan is printed, followed by the title line for the next file.
4. The loop DO 64 through 64 CONTINUE reads and prints but does not save the required deletion records.
5. Statement 65 through GO TO 65 provides a fill-in for any time gaps occurring between consecutive files by copying the last data scan over and over with an incremental time value until the new time is reached.
6. Transfer then goes to the beginning to the DO 45 loop, which copies the rest of the file to TAPE10.

F. Statement numbers 51 and 52 write appropriate messages when input errors or unexpected end-of-file characters are encountered.

III. Input

A. Tape files
The file containing the first portion of the flight is assigned to TAPE11, the second segment of the flight is assigned to TAPE12, and so on, for as many as needed.

B. Program controls
Four integer parameters must be set in the program to provide the necessary processing information.

L	Number of data channels (8)
NTS	Number of files to be combined (2 to ?)
NFP	Number of the first usable data scan from each file (that is, eliminate NFP-1 scans)
NPP	Number of points to be printed from the beginning of each input file

IV. Output

A. A FILE denoted as TAPE10 is created that contains all the headers and data from the input files except those data scans specifically removed from the beginning of each input file. It also contains the "fill" data between the end of each original file and the beginning of the next.

B. A LISTING is produced containing all the header records, the first NPP scans from each input file, the last scan from each file, and notification of read errors or premature end-of-file statements detected.

V. Job setup

```
CONCAT,T10000.                  Job name and time estimate
USER(SRB1,FDPS)                 User name and user
                                identification
CHARGE(45,37)                   Charge numbers
FTN5(ET,LO,DB=PMD)              Requests a FORTRAN compile
GETPF(TAPE11=S0705T1)           Gets first part of flight
GETPF(TAPE12=S0705T2)           Gets second part of flight
GETPF(TAPE13=S0705T3)           Gets third part of flight
          :                                :
GETPF(TAPE10+N=S0705TN)         Gets Nth part of flight
LGO.                            Starts program execution
CATLIST.                        Requests listing of file
                                names
REPPF(TAPE10=S0705CX/CT=S)      Catalogs the newly created
                                file
CATLIST.                        Requests listing of file
                                names (for comparison)
7/8/9                           Separator
PROGRAM DECK
6/7/8/9                         END-OF-JOB
```

CCLAMP Program
(Compute crack length at maximum points)

I. Functions

A. Computes crack length at every maximum and minimum value detected on each of the requested parameters (DIRECT method).

B. Extrapolates crack growth each time a string of invalid or missing data points is encountered.

C. Uses data from other flights to compute crack growth (INDIRECT method).

D. Computes remaining number of flights for each part.

E. Compiles statistics on flight profile.

F. Provides results of intermediate calculations and supporting data for validity checking.

II. Method

Data scans are read from the input file and checked against the various time boundaries. If the associated time is within the limits, processing continues.

When a data field containing either a maximum or a minimum is detected on a parameter, it is held until the next extreme point in the opposite direction occurs on the same parameter. Then the maximum and minimum are passed to the CRACK subroutine. When the next extreme on the same parameter occurs, the process is repeated.

When the maximum occurs earlier in time than the minimum, the slope indicator is set to -1; in the reverse order it is $+1$.

On each subroutine call for a half-cycle calculation, the crack length multiplier is set to 0.5.

If a time lapse greater than a specified limit (0.1 sec) occurs, extrapolation is performed by extending the average slope from the previous check point.

Three types of time boundaries determine (1) the starting-stopping time, (2) segment limits for extrapolation and intermediate output, and (3) duration between plotting points.

A. Peak detection

A storage location, SIGN(J), is set aside for the sign of the slope of each parameter as it exists on the current record in memory. The value J indicates the parameter number. SIGN(J) is +1 when the slope of parameter J is positive and −1 when the slope is negative. Another set of locations, SAVL(J) is set aside to hold the previous value of each parameter J.

1. Detection of maximum occurs when the slope SIGN(J) is positive (+1) and the current value of the parameter FLIM(J) is less than the previous value SAVL(J). The value in SAVL(J) is used for calculation and is then replaced with the subsequent value in FLIM(J). The value of SIGN(J) is changed to −1 and the peak counter N(J) is incremented.
2. Detection of minimum occurs when the slope SIGN(J) is negative (−1) and the current value of the parameter FLIM(J) is greater than the previous value. The previous value SAVL(J) is used for calculation then replaced with the current value FLIM(J). The variable SIGN(J) is then set to a +1 value.

B. Subroutine CRACK is used to compute crack growth H and a new crack length CCL for each half-cycle by the following method. (Symbols in parentheses reflect mathematical variables used elsewhere in this report.)

1. $H = CR \times DELTK^{(NBAR)} \times OMR^{(SHX)} \times 0.5$ $\quad (da/dN)$

where:

CR	is the cycle ratio,	c
NBAR	is the slope of log (da/dN) as a function of log (DELTA K), and	(m)
SHX	is the strain hardening exponent.	(n)

2. $DELTK = DK1 \times (SMAX - SMIN) \times \sqrt{CCL}$ $\quad (\Delta K)$

where:

SMAX	is the current maximum,	(σ_{max})
SMIN	is the current minimum,	(σ_{min})
CCL	is the current crack length,	(a)
DK1	is a constant computed once at the beginning of the program with values that do not change during the run,	
DK1	$= \frac{CLP \times FMF \times \sqrt{PI}}{\sqrt{CSF}}$	
CLP	is the crack location parameter,	(A)
FMF	is the flaw magnification factor,	(M_k)
CSF	is the crack shape factor, and	(Q)
PI	is the constant 3.14159265359.	

3. $OMR = 1 - SMIN/SMAX$ $\quad (1 - \sigma_{min}/\sigma_{max})$

4. Several nonvalid conditions are tested for and eliminated. These occur when OMR is negative or when DELTK or SMAX is zero or less. NC(J) is incremented by one each time any of these

conditions occur on parameter J. Printing of the calculation results and many of the input values occurs when the peak count N is less than the print control variable NCTL and whenever one of these nonvalid conditions exists.

5. Some variables are passed through to the subroutine that do aid in interpreting the information being printed although they are not needed for calculations. These variables are:

   TMIN the time at which the minimum occurred,
   TMAX the time at which the maximum occurred,
   M the slope direction indicator, and
   NIM the number of the last record read prior to calculation.

   The value of L is computed to direct the print to a separate file for each parameter.

C. Timing

1. START and STOP indicate the time when processing is to start and to stop. Zero values imply that the first time and the last time (respectively) in the file are to be used for these values. If the start time is earlier or the stop time is later, or both, than any file data, the crack length for each sigma is extrapolated appropriately.
2. End-of-segment (EOS) times force the printing of intermediate results and provide reference points from which extrapolation occurs.
3. Delta time (DELT) is an incrementing value for the TTIM, which forces the output of crack lengths to the plotting file.

D. Extrapolation

Although some of the short-duration data losses have little effect, others can exist for several seconds, and required compensation must be made for missing information.

Extrapolation with respect to time is performed based on the average growth rate from the previous checkpoint. Checkpoints may be specified each time the type of flight activity changes, such as start taxi, stop taxi, resume taxi, begin takeoff run, airborne, or reduce to cruise power. The default start of interpolation occurs when more than five consecutive second-derivative values are less than epsilon (EPSL) (currently 0.1×10^{-5}) on the specified data channel NOTC (currently channel number 1) (see fig. 21).

"Back" extrapolation is performed at the start of some flights when the first recorded data occur after the first motion of the aircraft is recorded in the flight log. Back extrapolation is a linear extrapolation back to the start from the first checkpoint through the first recorded data point (see fig. 22).

III. Program organization

A. Main program

Initial coding was written to permit a variable number of parameters (σs), but as development progressed, the number of σs was frozen at eight. In the interests of time and efficiency, some code (primarily print statements) was written for the fixed number.

1. After declarations and initialization, the control cards are read and written out to the printer. Additional initialization is performed in the block containing statements 1 and 2, which needs to be reset after back extrapolation. DK1, computed in this block, is the portion of the DELTK that uses variable values not changed during the flight. The temporary print files are initialized with the appropriate header information in the block terminated with statement 4.
2. TAPE4 (the file generated by CONCAT) is read for its header information, which is printed for verification, then the dropout list file header is written.
3. The first data record is read from TAPE4 by a special section of code, beginning with statement 15, which initializes the START and TTIM variables with its time value and initializes the SAVL

locations with its parameter values. This section causes the first part of the file to be bypassed when start time is later than the first times in the file, and it initializes the variables required for back extrapolation when the start time is earlier than the first time in the data file.

4. The block of code containing statements 22 and 24 is an end-of-file procedure to update the printer variable and to compute the final slopes if the indirect method is being used.
5. At statement 26, a TAPE4 read is again performed with the time going into a variable named TIME and the parameter values going into an array named FLIM. Since TIME should be greater than TTIM, the crack sizes (initial values at this point) will be printed and written to files named TAPE6, TAPE3, TAPE7, and TAPE8 for listing and for later use by the CPLOT program.
6. Just ahead of statement 28, TIME is compared with the current delta time terminator TTIM and the current end-of-segment marker (EOS). When either of these or an end-of-tape condition exists, indirect computed crack lengths CCLH are formed for those channels having a positive SLOPE value. Time and all the CCLH values (both direct and indirect) are written to plot (TAPE3) and print (TAPE6) files under control of format statements 101 and 100.
7. The statement DO 40, J = 1, NSIGMA starts a loop that analyzes each of the parameters (SIGMAS) one at a time.
8. If the SLOPE value corresponding to the current SIGMA and flight segment is a positive value, direct calculation of crack size is bypassed, and the DO control integer J is incremented. When the SLOPE value is zero or negative (a nonpermissible physical condition), calculation proceeds down through statement 40.
9. The variable SIGN is checked for slope; because it has had no chance to be changed from its initialization to zero, the tests for greater than zero and less than zero will fail, and computation will continue at the test for SIGN = 0. Here any change in amplitude of each parameter is detected and is used to establish the initial sign of the slope and either the maximum or the minimum test value for the next record.
10. After each parameter has been checked, control is transferred back to the data read statement (statement 26). When SIGN $\neq$ 0, the comparisons between FLIM and SAVL become significant. When SIGN is positive and the last data point (FLIM) is less than the previous point (SAVL), a maximum has been passed. The time and data in storage from the previous read are input to subroutine CRACK, which is called in the positive half-cycle mode. SIGN is set to a value of -1.
11. When SIGN is negative and the change in value of a parameter is positive, a minimum has been passed. SIGN is set to a +1, the data from the previous read are input to the subroutine CRACK, and it is called in the negative half-cycle mode.
12. After an initial slope direction has been established, all points not qualifying for maximum or minimum are ignored except for the test for invalid data and dropouts.
13. Because the CONCAT program filled missing data areas with linear interpolated values, these areas are detected by testing their second derivatives for values less than a very small EPSL. When the number of consecutive dropouts is greater than a specified number (NEPCS.GT.NEPS), linear extrapolation of crack size is computed by extending the slope from the last checkpoint through the last computed point. NEPS is currently set to 5, which is 0.1 Hz at the 5-cycle cutoff frequency and 50 samples/sec.
14. Transfer then goes to the top of the loop (statement DO 40) for analysis of the next parameter.
15. After each parameter has been processed (as described in paragraphs 7 to 14) control goes back to the statement labeled 26 to bring in another record from TAPE4. The input record is printed if the record count is not greater than the limit LPRINT. The current crack size computed from each data parameter is output if the new time TIME is equal to or greater than the last value TTIME. The

peak detection process is repeated for each channel as before. This process continues to the end of TAPE4 file.

16. An end of file, an exceeded STOP time, or a zero end-of-segment (EOS) value cause all the outputs to take place, and control is moved to the statement labeled 50 where summations are formed and printed. Calls to subroutine HMS convert the times from seconds to hours, minutes, and seconds.
17. One more linear interpolation is performed on the crack sizes if the last EOS time is greater than the last time in the data file.
18. Based on the peak values from this flight, the remaining number of flights is calculated for each parameter from the crack lengths.
19. Peaks from previous flights are compared, and remaining flights are calculated again based on the peak values detected on this and previous flights.
20. The MOD array is used to modify the selection of slopes that are output for use in a subsequent flight when the indirect method is required but the flight pattern (that is, starts, stops, and taxi periods) does not match the current flight.
21. An output listing of all values to be entered in the subsequent flight is produced along with a relisting of the slope values with reduced precision but in more readable format.
22. An input-selectable postmortem dump and FORMATS constitute the final statements in the main body of the CCLAMP program.

B. Subroutine CRACK

1. Initialization
   a. PARAMETER LOC size is set to 8.
   b. REAL arrays, including NBAR, which would normally be INTEGER mode, are declared to be size LOC specified in the PARAMETER statement.
   c. INTEGER arrays are declared to size LOC, FLAG is declared LOGICAL and set to FALSE.
   d. The COMMON array's order and size is declared consistent with the MAIN program's COMMON array.
   e. Output file control variable L is set to 10 plus the σ number J for which crack length is being computed.
2. Delta K (DELTAK) is computed using SMAX (the peak amplitude), CCL (the previously computed crack length for this location), and DK1 (a constant formed from input variables that do not change during the flight).
3. OMR $(1 - R)$ is computed using σ minimum and σ maximum (SMIN and SMAX).
4. The various error conditions are checked, and if any exist, the growth increment H is set to zero, the FLAG is set TRUE, the error counter for this channel is incremented, and control is transferred around any further calculations to the print output.
5. When the error conditions do not exist, H is computed and added to the total crack length.
6. Input to and results of the calculation are written to an output file (TAPEL) for later printing when any of the following conditions exist:
   a. The error FLAG is TRUE.
   b. The number of printed lines requested (NCTL) has not been exceeded.
   c. A print control request (NPL) transmitted from MAIN is turned on (that is, equals 1).

C. Subroutine HMS is a very short (three active lines) algorithm that converts time in seconds to hours, minutes, and seconds.

IV. Input

A. Time and associated stress amplitude (SIGMA) data are entered from the tape format file created by CONCAT, assigned to local file name TAPE4.

B. Constants and controls are entered from cards via the two NAMELIST groups TABLEX and TABLEC.

1. TABLEX contains the values that are most frequently changed. This group is set up as follows:

Name	Type[a]	Content
$TABLEX		
ID	C	string of 1 to 70 characters in quotes
NFLT	I	flight number
NPRT	I	number of previous flight
LOCNAM	CA	8 to 20 character strings, each in quotes
LOCNR	I	sigma numbers for nonsequential assignment
START	R	time to start process (default is start of file)
STOP	R	time to stop process (default is end of file)
DELT	R	time between crack size outputs
NSKIP	I	spurious data channels to be skipped
NSIGMA	N	number of σs (data channels)
LPRINT	I	number of input records to be printed
NCTL	I	number of calculation lines to be printed
IPMD	I	turns off the postmortem dump when IPMD = 0
NOTC	I	number of test channel
NEPS	I	dropout number threshold for interpolation
EPSL	R	epsilon, minimum permitted value of second derivative
EOS	RA	end-of-segment times (up to 10)
CCLQ	RA	calculated crack length from previous flight
SID	CA	segment identification
PKVAL	RA	peak values (for each σ) from prior flights
PKTIME	RA	time in the flight when peak occurred
NFLTPK	IA	number of the flight contributing the peak
PKFLST	RA	peak flight start time
NFLTP	I	number of flight previous
NCYO	I	third code digit in plot and listing file
IGNO	I	fourth code digit in plot and listing file
NOFNCK	I	no flight number sequence check
STARTP	R	start time for printing input data
STOPP	R	stop time for printing input data
SLOPE	RA	10 × 8 array of slopes for indirect calculations
MOD	IA	10 × 8 array to modify the slope's sequence
$END		

[a]C denotes CHARACTER, R denotes REAL, I denotes INTEGER, and A denotes ARRAY.

2. TABLEC contains values that are less frequently modified. They are all REAL each having as many entries as there are parameters (currently 8) for each item name (except the group name $TABLEC and terminator $END).

$TABLEC	
CLP	crack location parameter
FMF	flaw magnification factor
CSF	crack shape factor
CR	cycle ratio (from heat treating)
NBAR	stress intensity factor exponent
SHX	strain hardening exponent
CAPC	initial crack size from proof test
SLIM	sigma limit
$END	

V. Output

A. Printer

1. The control card input, TABLEX and TABLEC, are echoed back for verification.
2. The header records from TAPE4 are listed for their verification.
3. Crack size summaries at the end of each flight segment are printed in order of occurrence.
4. A summary of the entire flight lists flight duration, crack size growth rate, methods of calculation (direct calculation, interpolation, or indirect calculation), and number of flights remaining as determined by various criteria.
5. The next set of printed values is TABLEP, which is also the file punched out for entry into the next flight.
6. TABLED shows the values of the remaining flights test criteria.
7. The final directly printed table shows the crack growth rates for each σ for all flight segments.
8. Several additional listings may be produced or eliminated under program input and control card setup by creating and then copying intermediate files to the printer.

B. Intermediate files

1. TAPE1 is actually the print file as described in the preceding section (V.A.).
2. TAPE2 is used for temporary storage and for reformatting the header data on TAPE4.
3. TAPE3 contains the crack sizes as functions of time, used primarily for plotting.
4. TAPE5 is used to collect any error messages generated during calculations.
5. TAPE6 contains crack sizes as functions of time, the same as TAPE3 except that TAPE6, being designed for the printer, contains a title block and column headings not included on TAPE3.
6. TAPE9 contains a listing of the missing data areas (dropouts) for subsequent printing or plotting.
7. TAPE11 to TAPE18 contain the input, output, and intermediate values associated with the crack calculation subroutine CRACK. Calculations of σ_1 crack size are written to TAPE11, calculations of σ_2 are written to TAPE12, and so on.
8. TABLEP output in the form of punched cards is used to transmit final crack sizes, amplitude, and location of the highest peaks detected and crack growth rates (SLOPES) for use in the next flight.

VI. Job setup

```
      CCLAMP,T10000.                Job name and time estimate
      USER(username,Password)
      CHARGE(account number)
      MAP,ON.                       Provide a cross-reference
                                    map
      FTN5(ET,LO,DB=PMD)            Compile the source file
*     GETPF(TAPE4=filename)         Get the file to be
                                    processed
      NOEXIT.                       Recover lists up to point
                                    of failure
      LIBLOAD(SRVLIB,GETJN)
      LGO.                          Start computing
         REWIND,TAPE1,TAPE5,TAPE6,TAPE7,
      TAPE8,TAPE9,TAPE10.
         REWIND,TAPE11,TAPE12,TAPE13,TAPE14,TAPE15,TAPE16,TAPE17,TAPE18.
         COPYEI,TAPE1,TAPE99        Copy information on the
      COPYEI,TAPE6,TAPE99.          first file named to the
      COPYEI,TAPE5,TAPE99.          second file named; the
      COPYEI,TAPE9,TAPE99.          range of data copied is
      COPYEI,TAPE11,TAPE99.         from the beginning to the
      COPYEI,TAPE12,TAPE99.         end of information
      COPYEI,TAPE13,TAPE99.
      COPYEI,TAPE14,TAPE99.
      COPYEI,TAPE15,TAPE99.
      COPYEI,TAPE16,TAPE99.
      COPYEI,TAPE17,TAPE99.
      COPYEI,TAPE18,TAPE99.
         PACK,TAPE99.               Removes file separators
         COPYBF,TAPE99,OUTPUT.      OUTPUT is the print file
      REWIND,TAPE9.
*     REPPF(TAPE9=S0705DL)          Catalogs dropout lists for
                                    next program
*     REPPF(TAPE3=S0705CL)          Catalogs crack lengths for
                                    next program
      7/8/9                         Separator
      Program deck
      7/8/9                         Separator
      Control cards
      6/7/8/9                       End-of-job indicator
```

*Indicates cards to be changed from one run to the next.

CPLOT Program

I. Functions

A. Generates a tape for use by CALCOMP plotters, model 925 plotter controller, to create annotated graphs (figs. 23 to 30).

B. Draws any number of function-time curves on each sheet.

C. Creates multiple vertical and horizontal scales according to specified values or generates them automatically with calculations from data maxima and minima.

D. Can draw a series of horizontal lines with vertical end markers to indicate such things as areas of interpolated data.

E. Can draw annotations at any angle or location.

F. Can place a block of legend lines at any desired location.

G. Will write a title at the top of each page.

H. Accepts input data and control parameters from either cards or tape files in any combination.

I. Prints five levels of diagnostic messages under control of an input parameter.

II. Program organization

A. PARAMETER, TYPE SPECIFICATION, and DATA statements set some nondefault variable types, array sizes, and default values.

B. Control parameter input name lists

1. CPDATA is the primary control variable input list.
2. ZDATA is a secondary input list used only when more than one each horizontal or vertical scale are required.

C. Call to TIME subroutine entry point TIME1 establishes a reference for measuring elapsed time periodically throughout the processing so that excessively long procedures may be optimized in future runs and may provide a clue to input errors.

D. The call to PLOTS and PLOT are required by the plot subroutines to initialize and establish the origin location; the call to FACTOR sets the unit distance increment. A default size of 2 cm is used in place of the 1-in. unit assumed in the CALCOMP writeup. All subsequent uses of the word "inches" actually references a 2-cm distance and are multiplied by 2/2.54 to obtain the true size; other spacing may be specified in the first set of control cards.

E. Statements 1 to 10 store all control parameter sets on a file named TAPE1 for future recall. Messages and various levels of print echo are controlled by the IECHO parameter. TAPE5 is used for intermediate storage to permit the input to be printed exactly as entered, whereas subsequent input data displays show all the possible input parameters with their default values or carryovers from previous settings.

F. The next block of statements down through number 25 load the data onto TAPE2 so that one independent variable may be paired with several dependent variables (that is; TIME as a function of SIGMA1, TIME as a function of SIGMA2, . . . , TIME as a function of SIGMA8).

G. Statements 29 to 32 control the positioning of TAPE2 looking for a data set whose FID (identification field) matches the one specified in the data set identification parameter XYCG. When no field identification is required (that is, when only one data set is in the file) XYCG may be set to "* ".

H. The next group of statements initialize the storage locations for the minimum and maximum X and Y values. Then beginning with statement DO 37 through 37 CONTINUE, each pair of XY coordinates is read and stored in the X and Y arrays. Input values may be adjusted by subtracting a constant (XMIN or YMIN) and then multiplying by another constant (XMPF and YMPF). When the MIN values are zero and the MPF values are 1.0, the input values are unchanged as stored in X and Y arrays. If the MIN parameters are set to the code value $-9999.$, the first data point is subtracted from all others in the set. This capability permits the conversion of time in seconds from midnight to be plotted in elapsed time in minutes and crack length in inches to be shown as crack growth in microinches. The highest and lowest values of each X and Y array are saved in XHI, XLO, YHI, and YLO locations. Input is terminated in one of three ways:

1. an end of file detected on READ,
2. the value of NPTS is exceeded, or
3. the size of the X and Y arrays are exceeded (currently set at 1000 each).

I. X scale factors specified by XSF are applied unless XSF is zero, in which case a scale factor is calculated from the highest (HI) and lowest (LO) X values saved during input. CALCOMP's subroutine SCALE does the actual calculation after the values are provided.

J. Y scale factors are calculated in the same manner using YSF for the controlling parameter.

K. The Y-axis length here becomes a test value since it cannot be zero if it is to exist at all. A YLEN = 0 indicates that no axis, annotation, or titles are to be drawn on this pass.

L. A TITLE of up to 80 characters is drawn at a fixed location—10.5 "inches" up and starting 1 "inch" to the right of the Y axis. The letter height is 0.2667 "inches" (the inches in quotes are actually 2 cm).

M. A vertical (Y axis) is drawn by line 43. The default location is at the left edge of the plotting area starting at location (0.0, 0.0). YXPG and YYPG control its position and may be set to other values. The characters stored in YNAME will be written vertically at the left of the scale. NYCH may be used to specify the number of characters (up to 40) in the string when positioning is to be controlled, otherwise the character string length (calculated by statements DO 42 to 42 CONTINUE) will be calculated to center the axis annotation. YLEN specifies the length of the Y axis in "pseudo" inches (2-cm units) and may not be zero unless all scales and annotation are to be omitted. YIVAL is the annotation for the first tick mark of the axis. YSF(1) is the value increment between tick marks.

N. When the parameter NZAX is greater than zero, NZAX auxiliary axes will be drawn. Z axes can be placed anywhere at any angle but the default orientation and location is vertical, 2 cm left of the previous axis. These may be changed by setting ZANGE, ZXPG, and ZYPG. The length and the scale factor defaults, ZLEN and ZSF, are the values used for the Y axis. ZIVAL, the first tick mark annotation, default is zero. ZNAME is used to enter an axis title up to 40 characters and NZCH is used as YNCH as in the previous section.

O. The horizontal (X) axis is drawn starting at the default location of (0.0,0.0). The X-axis control parameters XNAME, NXCH, XXPG, XYPG, XLEN, XIVAL, XSF, XMIN, XMPF, and LOCX have the same function as their Y-axis counterparts.

P. Statements DO 54 through 54 CONTINUE control the generation of a LEGEND block of 1 to 20 lines, each up to 40 characters in length.

Q. Statements DO 56 through 56 CONTINUE control the generation of 20 markers that may be placed at any location and at any angle. The placement (X and Y location), size, and angle of the 40 MARK characters is by the XYSAM variable array locations 1 to 4, respectively.

R. Up to 20 vertical markers (VMARKs) are similar to the MARKs except that no angle is specified and the X location is specified in terms of the X value of the input data rather than page coordinates. XYSVM array locations 1 to 3 specify X value, Y location, and letter height, respectively.

S. Up to 20 horizontal markers (HMARKs) are similar to VMARKs except that the Y location is specified in terms of the values on the Y axis. XYSHM array locations 1 to 3 specify X location, Y value, and letter height, respectively.

T. Call to subroutine LINE produces a line plot of the pairs of data values in the X and Y arrays. The data points may be represented by centered symbols or connecting lines between points, or both. LTYPE and INTEQ control the line type and symbol selection. See CALCOMP line subroutine writeup for description of their use. Prior to calling LINE a test is made for "out of range" condition, which aborts the plot and prints a diagnostic message when the data fall more than two "inches" left or below (0.0,0.0), more than 12 "inches" high, or more than 4 "inches" past the right end of the X axis.

U. DROPOUT areas, where data were extrapolated, can be indicated on the plot. The statement IF(DOL.NE.0)THEN commences the section of code by testing for a nonzero value, which then indicates the height in pseudoinches above the X axis.

V. Plot identification and tear marks for each plot are generated by the statements in the block between lines 80 and 81 and written vertically 4 "inches" to the right of the right end of the X axis. Plot sequence, number, time, date, and JSN are computed or automatically picked up from the system. User identification may be entered as a four-character string assigned to the USER parameter.

W. The reading of a new set of primary control parameters occurs in the program after statement 81 through the GO TO 29 statement and includes the following processes:

1. Location of the new page XNEW is increased to a point 8 "inches" past the end of the X axis (XLEN), and page and plot counters are incremented.
2. Name list CPDATA is read and checked for end of file and read ERRORS.
3. The ID file FIDA is searched for, and pointer K1 is set, on a match with the current field ID(FID).
4. The ID file is again searched for, and pointer K2 is set, on a match with the data set identification parameter XYCG.
5. Comparison between K1 and K2 determines the need of a rewind to locate the data requested in the new CPDATA parameter set.
6. If the test of YLEN reveals it not to be zero, indicating an overplot, a call to PLOT reinitializes a new page.
7. Processing then returns to statement 29 (see paragraph II.G) where the new data set is searched for and loaded into the X and Y arrays.

X. Termination procedure

1. Statement 90 reports on end-of-control-parameter-sets condition.
2. Statement 95 provides notification of a tape error detected on the data file (TAPE2).
3. Statement 96 moves the pen off of the page, flushing the buffer and writing a termination file (999) on the plot tape.

III. Input

A. Data files

1. PRIMARY file format for TAPE3 is a file containing no header records having the following formatted fields repeated in each record.

Program variable name	Field size and type	Application
FID	A5	field for identification
NCD	I5	number of card (sequence number)
NFPC(1)	F10.3	independent variable, X (time)
NFPC(2)	E15.9	first dependent variable Y1 (σ_1)
⋮	⋮	⋮
NFPD(9)	E15.9	Eighth dependent variable Y8 (σ_8)

2. An optional auxiliary file, TAPE9, which may be attached and processed, contains the list of dropout areas. The format is X, 3I8,5F14.3, of which the first three integer fields and the last three floating-point fields are unused. The first two floating point fields contain the start time and the end time for a period during which extrapolation occurred. The file contains one record for each section of extrapolation during the flight.

B. Control parameters (NAMELIST format)

One or more sets of control parameters are required for each plot. The primary set is preceded by a $CPDATA field and followed by a $END field. This set of controls can provide all the specifications for a single set of data points, the X and Y axes, the annotation, and a dropout line. Secondary sets are used to specify additional axes (Z axes). Secondary sets are preceded by a $ZDATA field and followed by the standard $END field. When more than one set of data points is to be plotted on the same sheet previously generated, a new primary set of controls is used. All axes and annotation are suppressed by setting the Y-axis length parameter YLEN to 0.0. Most control parameters have default values and all are saved from one plot to the next so that only new or changed values need be entered.

Mnemonic	Type[a]	Use	Default
		General parameters	
$CPDATA	---	specifies beginning of a primary data set	---
FACTR	R	adjusts size of plot	0.7874016
NSETS	I	number of data sets	1
NFPC	I	number of fields per card (input line)	9
IECHO	I	diagnostic print control	1
LTYPE	I	type of line connecting points[c]	0
INTEQ	I	plotting symbol[c]	0
XYCG	5CH	data set identification	Blank
NZAX	I	number of additional (Z) axes	0
DOL	R	dropout line, "inches" from X-axis	0
DATA	4CH	input file source TAPE or CARD	CARD
USER	4CH	computer user identification	Blank
ANOT	40CH	annotation to go at end of plot	Blank
NPTS	I	number of points to be plotted (0 = all)	0
XL	R	left margin spacing, "inches"	4.0
XT	R	not implemented	4.0
$END	---	specifies end of each data set	---

Mnemonic	Type[a]	Use	Default
		Annotation parameters	
TITLE	80CH	graph title	Blank
LEGEND(1)	40CH	legend line 1	Blank
⋮	⋮	⋮	⋮
LEGEND(20)	40CH	legend line 20	Blank
LEGSYM(1)	I	legend 1, first char symbol indicator[c]	0
⋮	⋮	⋮	⋮
LEGSYM(20)	I	legend 20, first char symbol indicator	0
NLEGS	I	number of legend lines	0
XYSLEG(1)	R	X location of first legend	0.0
XYSLEG(2)	R	Y location of first legend	0.0
XYSLEG(3)	R	size of legend letters	0.0
NHM	I	number of horizontal markers	0
HMARK(1)	40CH	horizontal annotation marker 1	Blank
⋮	⋮	⋮	⋮
HMARK(20)	40CH	horizontal annotation marker 20	Blank
XYSHM(1,1)	R	X location of first horizontal marker	0.0
XYSHM(2,1)	R	Y value of first horizontal marker	0.0
XYSHM(3,1)	R	size (letter height) of first horizontal marker	0.0
XYSHM(1,2)	R	X location of second horizontal marker	0.0
⋮	⋮	⋮	⋮
XYSHM(3,20)	R	size of 20th horizontal marker	0.0
NVM	I	number of vertical markers	0
VMARK(1)	40CH	vertical annotation marker 1	Blank
⋮	⋮	⋮	⋮
VMARK(20)	40CH	vertical annotation marker 20	Blank
XYSVM(1,1)	R	X value of first vertical marker	0.0
XYSVM(2,1)	R	Y location of first vertical marker	0.0
XYSVM(3,1)	R	size of first vertical marker	0.0
XYSVM(1,2)	R	X value of second vertical marker	0.0
⋮	⋮	⋮	⋮
XYSVM(3,20)	R	size of 20th vertical marker	0.0
NAM	I	number of annotation markers	0
MARK(1)	40CH	annotation marker, any angle	Blank
⋮	⋮	⋮	⋮
MARK(20)	40CH	annotation marker, any angle	Blank
XYSAM(1,1)	R	X location of first any-angle marker	0.0
XYSAM(2,1)	R	Y location of first any-angle marker	0.0
XYSAM(3,1)	R	size of first any-angle marker	0.0
XYSAM(4,1)	R	angle of first any-angle marker	0.0
XYSAM(1,2)	R	X location of second any-angle marker	0.0
⋮	⋮	⋮	⋮
XYSAM(4,20)	R	angle of 20th any-angle marker	0.0

Mnemonic	Type[a]	Use	Default
		Horizontal axis parameters	
XNAME	40CH	X-axis title	Blank
NXCH	I	number of X axis title characters	N
XXPG	R	X-axis X starting location on page	0.0
XYPG	R	X-axis Y starting location on page	0.0
XLEN	R	X-axis length	0.0
XIVAL	R	X-axis initial value	0.0
XSF	R	X-axis value between tick marks	0.0
XMIN	R	X-axis minimum value (offset)	0.0
XMPF	R	X data multiplication factor	1.0
LOCX	I	location of field with X data	1
		Vertical axis parameters	
YNAME	40CH	Y-axis title	Blank
NYCH	I	number of Y-axis title characters	N
YXPG	R	Y-axis X starting location on page	0.00
YYPG	R	Y-axis Y starting location on page	0.00
YLEN	R	Y-axis length	10.00
YIVAL	R	Y-axis initial value	0.00
YSF	R	Y-axis value between tick marks	0.00
YMIN	R	Y-axis minimum value (offset)	0.00
YMPF	R	Y data multiplication factor	1.00
LOCY	I	location of field with Y data	2
		Auxiliary (Z) axis parameters	
$ZDATA	---	specifies start of secondary data set	---
ZNAME	40CH	Z-axis title	Blank
NZCH	I	number of Z-axis title characters	N
ZXPG	R	Z-axis X starting location on page	1.00
ZYPG	R	Z-axis Y starting location on page	0.00
ZANGL	R	Z-axis angle	90.0
ZLEN	R	Z-axis length	YLEN
ZIVAL	R	Z-axis initial value	0.00
ZSF	R	Z-axis value between tick marks	YSF

[a]Type codes

---	no values are associated with these control words
I	integer data, numeric values without decimal points
R	real data, numeric values, must have a decimal point
CH	CHARACTER data, a string of characters bracketed by single quote marks. The preceding numbers indicate the maximum size of the character string.

[b]Default codes

N	value is determined from actual length of string
Blank	initial contents are all blank characters
YLEN	initial value is taken from previous YLEN setting
YSF	initial value is taken from the previous YSF setting

[c]Refer to CalComp user's manual (California Computer Products, Inc., 1976) for description of line types and plotting symbols.

IV. Job setup

```
   CPLOT,T10000.                    Job name and time estimate
   USER (SRB1,FDPS)                 User name and user ID
   CHARGE(45,37)                    Charge numbers
   FTN5(ET,LO,PL)                   Requests FORTRAN compile
*  GETPF(TAPE3=S0705CL/UN=SRB1)     Gets primary data file
*  GETPF(TAPE9=S0705DL/UN=SRB1)     Gets secondary data file (dropout list)
   GETPF(PENLIB/UN=LIBRARY)         Gets the plot subroutines
   LIBLOAD(SRVLIB,GETJN)            Gets a system subroutine
   LDSET(LIB=PENLIB,PRESET=ZERO)    Initializes memory locations to zero
   LOAD(LGO)                        Loads the FORTRAN object file
   EXECUTE                          Starts the program execution
   GETPF(PROCFIL/UN=CSDO)           Gets plot procedure file
   BEGIN(PROCFIL/UN=CSDO)           Starts plot output procedure
   BEGIN,WRITAPE,,PL,,,TAPE4,TIME+,.
   ENDIF(DOTHIS)
   7/8/9                            Separator
   PROGRAM DECK
   7/8/9                            Separator
   CONTROL CARDS
   6/7/8/9                          Job termination card
```

*Indicates cards to be changed from one run to the next.

Table C-1. Coefficients of hook load equation for hook loads $R_i = R_{a_i}\,\eta_x + R_{b_i}\,\eta_y + R_{C_i}\,\eta_z + R_{d_i}\,\dot{p} + R_{e_i}\,\dot{q} + R_{f_i}\,\dot{r}$.

R_i, lb hookload	R_{a_i}, lb	R_{b_i}, lb	R_{C_i}, lb	R_{d_i}, lb/in.	R_{e_i}, lb/in.	R_{f_i}, lb/in.
Front hook vertical load V_A	−2247.434	0	13872.485	0	7.780750×10^6	0
Front hook side load S_A	0	13287.261	0	0	0	-7.431309×10^6
Rear hook vertical load left V_{BL}	1123.717	−13067.992	17135.258	-1.632632×10^6	-3.890375×10^6	2.292681×10^6
Rear hook side load S_{CL}	0	34855.739	0	0	0	-7.431309×10^6
Rear hook vertical load right V_{BR}	1123.717	13067.992	17135.258	1.632632×10^6	-3.890375×10^6	-2.292681×10^6
Rear hook drag load left D_{CL}	−24071.50	1971.804	0	0	0	-1.102792×10^6
Rear hook drag load right D_{CR}	−24071.50	−1971.804	0	0	0	1.102792×10^6

Table C-2. Coefficients of stress equation for stresses

$\sigma_i = S_{k_i}\,V_A + S_{\ell_i}\,S_A + S_{m_i}\,V_{BL} + S_{n_i}\,D_{CL} + S_{p_i}\,S_{CL} + S_{q_i}\,V_{BR} + S_{r_i}\,D_{CR} + S_i[0.9688\,DCL - 0.2479\,S_{CL}]$

Stress point σ_i, ksi	Location	S_{k_i}, ksi/lb	S_{ℓ_i}, ksi/lb	S_{m_i}, ksi/lb	S_{n_i}, ksi/lb
σ_1	Front hook	7.3522×10^{-3}	0	0	0
σ_2	Left rear hook	0	0	5.8442×10^{-3}	0
σ_3	Right rear hook	0	0	0	0
σ_4	Shaft—left sway brace	0	0	0	0
σ_5	Shaft—right sway brace	0	0	0	0
σ_6	Left drag pin	0	0	0	0
σ_7	Right drag pin	0	0	0	0
σ_8	Right drag shaft support lower	0	0	0	0
Stress point σ_i, ksi	Location	S_{p_i}, ksi/lb	S_{q_i}, ksi/lb	S_{r_i}, ksi/lb	S_i, ksi/lb
σ_1	Front hook	0	0	0	0
σ_2	Left rear hook	0	0	0	0
σ_3	Right rear hook	0	5.8442×10^{-3}	0	0
σ_4	Shaft—left sway brace	0	0	0	4.7559×10^{-3}
σ_5	Shaft—right sway brace	0	0	2.18675×10^{-3}	0
σ_6	Left drag pin	0	0	0	7.1420×10^{-3}
σ_7	Right drag pin	0	0	7.3055×10^{-3}	0
σ_8	Right drag shaft support lower	0	0	4.2141×10^{-3}	0

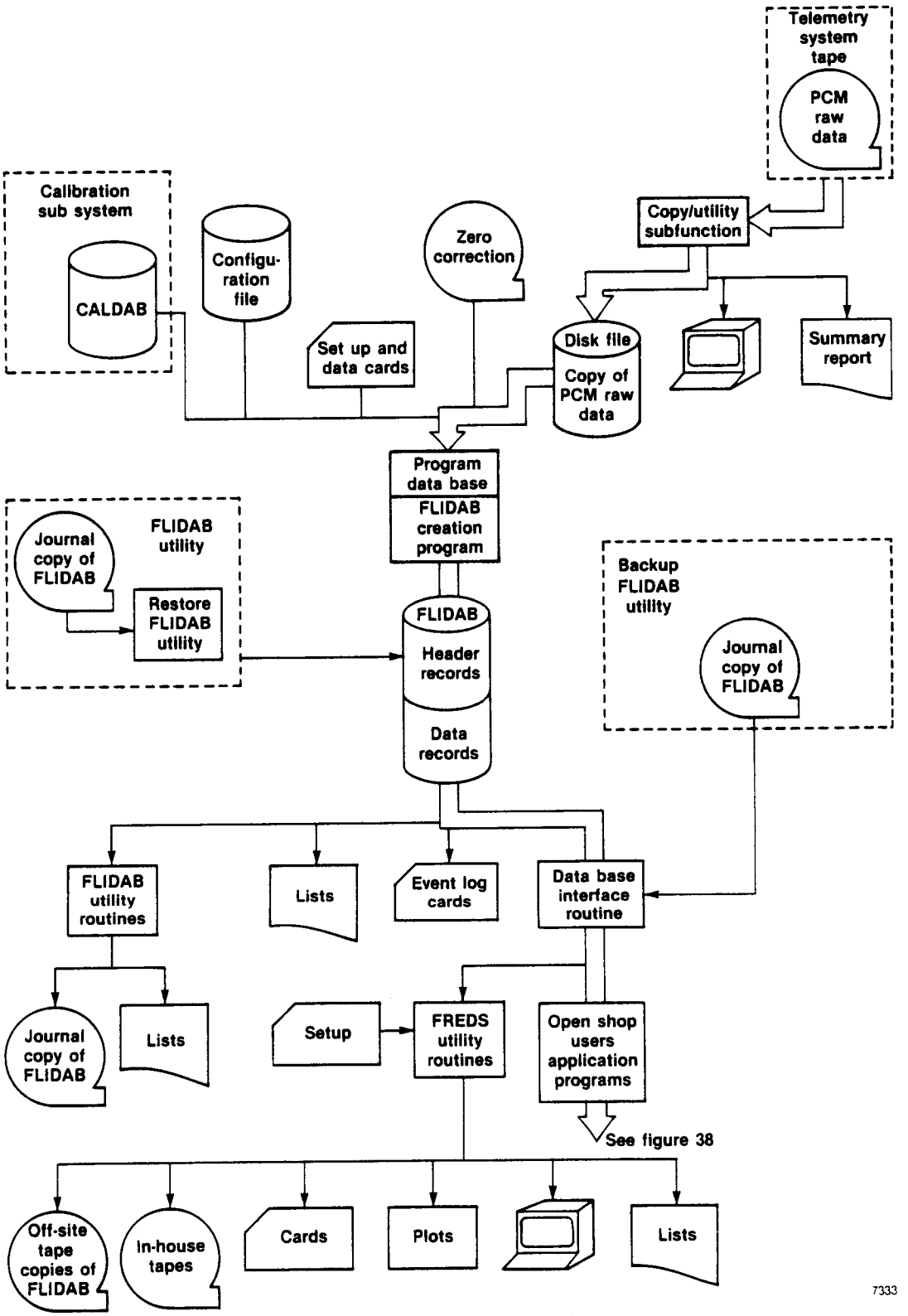

Figure C-1. FREDS overview.

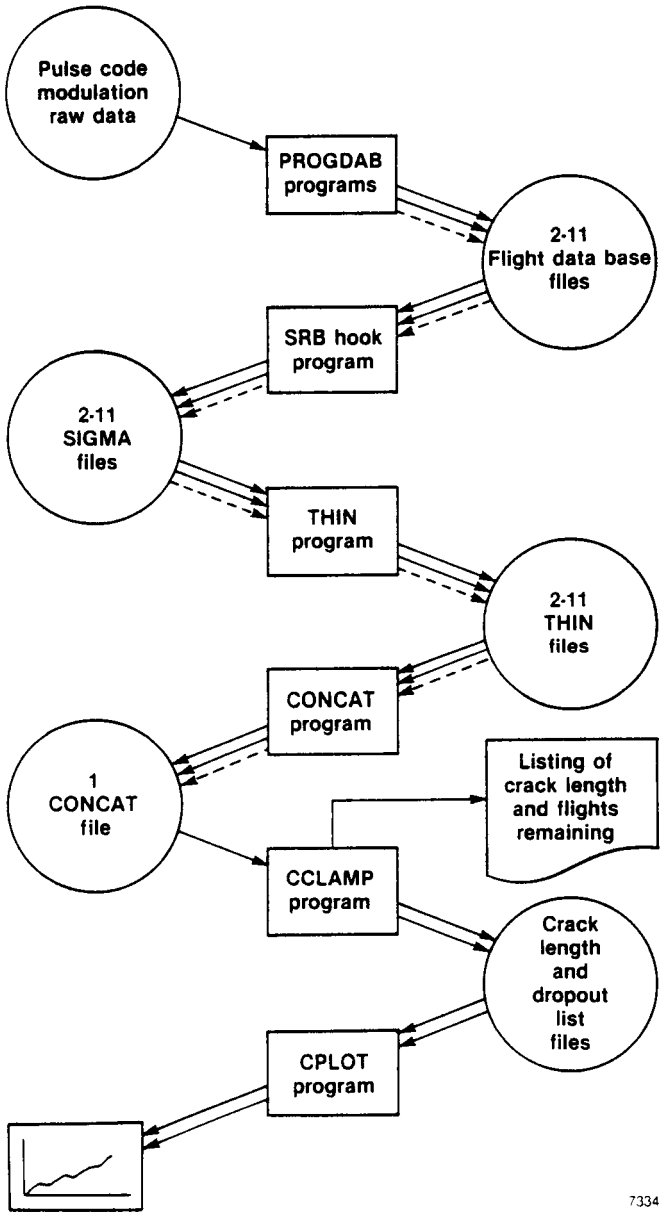

Figure C-2. Crack length calculation.

REFERENCES

Ko, W.L., and L.S. Schuster, *Stress Analyses of B-52 Pylon Hooks*, NASA TM-84924, 1985.

Forman, R.G., V.E. Kearney, and R.M. Engle, "Numerical Analysis of Crack Propagation in Cyclic Loaded Structures," *J. Basic Engng., Trans. ASME-D*, vol. 89, 1967, p. 459.

Walker, E.K., "The Effect of Stress Ratio During Crack Propagation and Fatigue for 2024-T3 and 7075-T6 Aluminum," *Effects of Environments and Complex Load History on Fatigue Life, ASTM-STP*, vol. 462, 1970, p. 1.

Schijve, J., "Four Lectures on Fatigue Crack Growth," *Engng. Fracture Mech.*, vol. II, 1979, pp. 167–221.

Starkey, W.L., and S.M. Marco, "Effects of Complex Stress Time Cycles on the Fatigue Properties of Metals," *Trans. ASME*, Aug. 1957, pp. 1329–1336.

Incarbone, C., "Fatigue Research on Specific Design Problems," *Fatigue of Aircraft Structures*, Proc. Symposium on Fatigue of Aircraft Structures, Paris, May 16–18, 1961, MacMillan, New York, 1963, pp. 209–217.

Smith, S.H., "Fatigue Crack Growth Under Axial Narrow and Broad Band Random Loading," *Acoustic Fatigue in Aerospace Structures*, Syracuse University Press, New York, 1965, p. 331.

Structural Analysis for the Modified B-52A Pylon for Advanced X-15A-2 Airplane Suspension, TFD63-876, North American Aviation, Inc., Nov. 1963.

Quade, D.A., *Load and Dynamic Assessment of B-52-008 Carrier Aircraft for Configuration 1 and 2 Space Shuttle Solid Rocket Booster Decelerator System Drop Test Vehicles, Volume IV, Pylon Load Data Method 2*, D3-11220-1, The Boeing Company, 1977.

CalComp Software Reference Manual, California Computer Products, Inc., Anaheim, California, Oct. 1976.

NASA National Aeronautics and Space Administration

Report Documentation Page

1. Report No.	2. Government Accession No.	3. Recipient's Catalog No.
NASA TM-88277		

4. Title and Subtitle

Application of Fracture Mechanics and Half-Cycle Method to the Prediction of Fatigue Life of B-52 Aircraft Pylon Components

5. Report Date
September 1989

6. Performing Organization Code

7. Author(s)
W.L. Ko, A.L. Carter, W.W. Totton, and J.M. Ficke

8. Performing Organization Report No.
H-1383

10. Work Unit No.
RTOP 505-43-31

9. Performing Organization Name and Address
NASA Ames Research Center
Dryden Flight Research Facility
P.O. Box 273
Edwards, CA 93523-5000

11. Contract or Grant No.

13. Type of Report and Period Covered
Technical Memorandum

12. Sponsoring Agency Name and Address
National Aeronautics and Space Administration
Washington, DC 20546

14. Sponsoring Agency Code

15. Supplementary Notes

16. Abstract

Stress intensity levels at various parts of the NASA B-52 carrier aircraft pylon were examined for the case when the pylon store was the space shuttle solid rocket booster drop test vehicle. Eight critical stress points were selected for the pylon fatigue analysis. Using fracture mechanics and the half-cycle theory (directly or indirectly) for the calculations of fatigue-crack growth, the remaining fatigue life (number of flights left) was estimated for each critical part. It was found that the two rear hooks had relatively short fatigue life and that the front hook had the shortest fatigue life of all the parts analyzed. The rest of the pylon parts were found to be noncritical because of their extremely long fatigue life associated with the low operational stress levels.

17. Key Words (Suggested by Author(s))
B-52 pylon hooks
Fatigue life
Fracture mechanics
Half-cycle method

18. Distribution Statement
Unclassified — Unlimited
Subject category 39

19. Security Classif. (of this report)	20. Security Classif. (of this page)	21. No. of pages	22. Price
Unclassified	Unclassified	80	A05